FACULTY OF MATHEMATICS, PHYSICS AND INFORMATICS
COMENIUS UNIVERSITY
BRATISLAVA

Department of Nuclear Physics and Biophysics

# Synthesis and properties of neutron deficient isotopes of elements around Z=100

Thesis

Mgr. Stanislav Antalic

**Supervisors:**
Prof. Štefan Šáro
Dr. Fritz Peter Heßberger

**Bratislava 2005**

# Abstract

In the presented Thesis work the results of spectroscopic studies of $^{246}$Md,$^{247}$Md, $^{254}$Lr and $^{255}$Lr decay chains are given. These isotopes were produced using heavy ion induced fusion reactions of $^{40}$Ar + $^{209}$Bi and $^{48}$Ca + $^{209}$Bi as a part of the long term project aimed to study spectroscopy properties of superheavy elements. The experiments were performed at velocity filter SHIP, placed at the central beam line of the UNILAC accelerator at GSI Darmstadt in Germany.

The work also gives a basic overview of research in the region of superheavy elements, description of the used experimental setup and shows the usual analysis methods used in spectroscopic studies in the region of elements around Z $\approx$ 100. The results were obtained using $\alpha$, $\alpha$ - $\gamma$ spectroscopy methods and recoil - $\alpha$, $\alpha$ - $\alpha$ correlations search.

Although these isotopes have been known for a longer time, no detailed spectroscopy investigation were performed so far and only rough information was known. Beside the improved precision of known data, this work gives a new information about the decay properties of these isotopes. This give us the possibility to build a decay schemes for mentioned decay chains.

# Acknowledgements

I would like to cordially thank to my supervisor, Prof. Štefan Šáro, for his continuous help, support and interest in this work.

The special gratitude goes to Dr. Fritz Peter Heßberger for all his valuable advices, suggestions and patient guidance during last few years.

I am deeply indebted to Prof. Sigurd Hofmann for the help, consultations and for giving me the chance to periodically visit Darmstadt and to work at GSI over the past few years.

I am very grateful to the Dr. Dieter Ackermann and Dr. Andrei N. Andreyev for many fruitful discussions and their help.

Many thanks go to my colleagues at the department especially to Dr. Peter Cagarda, Branislav Streicher, Ivan Brida and Martin Venhart for many enthusiastic discussions and for helping me to solve everyday problems.

Finally, I want to thank my parents for their continuous encouragement and especially my wife Janka for her love, patience and support.

# Contents


**1 Introduction** **9**

**2 Stability and production of heavy and superheavy elements** **13**
2.1 Spontaneous fission lifetime . . . . . 13
2.2 Alpha decay lifetime . . . . . 15
2.3 Cross-section for reactions of synthesis . . . . . 16

**3 Identification of heavy and superheavy elements** **19**
3.1 Separation . . . . . 19
3.2 SHIP . . . . . 20
3.3 Detectors . . . . . 22
3.4 Calibrations . . . . . 25
3.5 Electronic system . . . . . 27
3.6 Data acquisition . . . . . 29
3.7 Time and position correlation method . . . . . 29

**4 Physical background** **32**
4.1 Alpha decay . . . . . 32
4.2 Gamma Ray Decay . . . . . 36
4.3 Internal conversion . . . . . 38

**5 Experiments** **39**
5.1 Reaction $^{40}$Ar + $^{209}$Bi . . . . . 39
5.2 Reaction $^{48}$Ca + $^{209}$Bi . . . . . 41
5.3 Calibrations . . . . . 42

**6 Results and Discussion** **45**
6.1 Reaction $^{40}$Ar + $^{209}$Bi . . . . . 45
6.1.1 Decay chain of $^{247}$Md . . . . . 45
6.1.2 Decay chain of $^{246}$Md . . . . . 54
6.2 Reaction $^{48}$Ca + $^{209}$Bi . . . . . 68
6.2.1 Decay chain of $^{255}$Lr . . . . . 68
6.2.2 Decay chain of $^{254}$Lr . . . . . 77

**7 Conclusion and Outlook** **82**

**Appendices** **87**

**A Reaction $^{40}$Ar + $^{208}$Pb** **87**

**Zhrnutie** **90**

**Bibliography** **93**

# Chapter 1

# Introduction

At present some 2700 various isotopes are known, but theory predicts more than 6000 isotopes with a lifetime longer than 1 microsecond. Until now the information about new elements with proton number up to 116 was published but the theoreticians predict the possibility for production of elements with proton number more then 120.

The research of transuranium elements started in the year 1940. In the beginning these elements were produced by neutron capture reactions and subsequent beta decays (1940 - Np, 1944 - Am) or using a reaction with deuterium (1940 - Pu). For heavier elements reactions with accelerated $^{4}$He nuclei were used (1944 - Cm, 1949 - Bk, 1950 - Cf, 1955 - Md). Some elements were identified in the radioactive debris from the first thermonuclear bomb explosion (1952 - Es and Fm). [Web]

Possibilities of these methods were exhausted by a synthesis of mendelevium and it was necessary to use a reactions with heavier projectiles what was contingent by development of new and more powerful accelerators. Transuranium elements from nobelium up to the bohrium were produced using fusion reaction with boron, carbon, nitrogen and neon beams. [Web]

The next step in this field was achieved at GSI Darmstadt with reaction using lead and bismuth targets and medium heavy projectiles $^{54}$Cr, $^{58}$Fe, $^{70}$Zn. During the years 1981 - 1996 the elements bohrium [Mun81a], hassium [Mun84], meitnerium [Mun82], darmstadtium [Hof95a], roentgenium [Hof95b, Hof01] and 112 [Hof96, Hof01] were synthesized. In recent years the synthesis of new neutron rich isotopes of element 112 and a synthesis of new elements 114 and 116 in JINR Dubna using the plutonium and curium targets were reported [Oga99a, Oga99b, Oga99c, Oga00a, Oga00b, Oga01a, Oga01b, Oga02]. The last published results announced the syntheses of the elements 115 and 113 using reaction with $^{243}$Am target in JINR Dubna [Oga04] and synthesis of element 113 in reaction with $^{209}$Bi in RIKEN (Japan) [Mor04].

Because of the low production rate, in the order of few atoms per week due to a low fusion cross-section, it was necessary to significantly improve the detection and identification technique as well to achieve these results. Presently the most

reliable technique for the identification and study of new superheavy elements[1] and for spectroscopy study of transuranium elements is the indirect identification via the reconstruction of their decay chains created by alpha particles emitted during the decay of the fusion product and its daughter products. This topic will be discussed in detail in the chapter 3.

Theory predicts the existence of an "island of stability" for superheavy elements, located around the closed shell, was developed in the early 60s. Based on the work of Strutinsky [Str67, Str68] the area, where the lifetime of these nuclei was expected to be million of years, should exists around the isotope with magic neutron number N=184 and magic proton number N=114. These results were later corrected and the lifetime estimations were decreased [Smo97], [Rut97], [Ben01]. Also the situation with closed proton and neutron shells - so-called magic numbers - is not clear. While the prediction for the neutron magic number remains the same (N=184), the predictions for the proton magic number differ considerably - from Z=114 to Z=126. This topic will be discussed in more detail in chapter 2.

The basic nuclear properties of superheavy elements such as nuclei deformation, decay modes, masses and lifetimes are very often unknown and the theoretical calculations are unable to give us satisfactory precise prediction. For a retrieval of these information which can help to improve theory and enhance the prediction power a long, patient and systematic research is necessary. These experiments are very often at the limits of possibility for current experimental technique. However, significant experimental and analytical improvements enables us to make more detailed spectroscopy studies for the elements up to the Hassium.

In the introductory chapters a brief description of the experimental techniques and overview of the superheavy elements physics is given. The basic methods of superheavy nuclei identification and the limitation of current experimental conditions will be described as well.

After that the particular results of reactions of our interest performed at the velocity filter SHIP will be presented. The main task is the study of the spectroscopic properties for various isotopes from berkelium up to the lawrencium. These isotopes have been known for a longer time, but for most of them only some basic decay properties were measured due to low production rates. As will be shown later some decay properties extracted from the data in the past are inaccurate and need to be corrected. Accuracy of some data will be improved. A more detailed physical interpretation of measured data will be given too. The work is a part of a long-term project aimed to detailed study of the superheavy elements performed at SHIP.

The first reaction - $^{40}$Ar + $^{209}$Bi - was chosen to study the isotopes $^{246}$Md [Nin96] and $^{247}$Md [Mun81b] and their daughter products as well. Because of small statistics of data, which was collected in previous experiments, only some rough information was obtained. In the mentioned experiment unexpected high fission branch for $^{246}$Md was observed with a possible explanation of electron capture

[1] In this work under the term "superheavy elements" will be considered the elements around Z=100 and heavier.

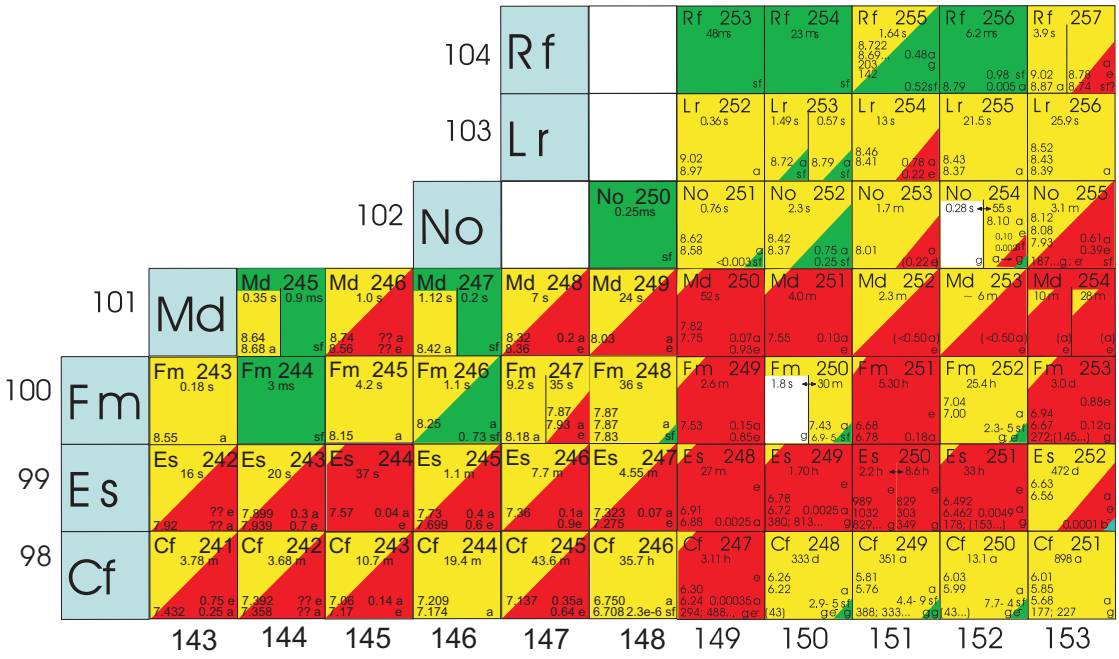


Figure 1.1: Excerpt from chart of nuclei, Z=98-105 and N=146-153 showing the area of interest - the isotopes $^{246}$Md, $^{247}$Md, $^{254}$Lr, $^{255}$Lr and their decay products products.

delayed fission (ECDF) having a branching ration of $b_{ECDF}$ = 6.5 %. In the case of $^{247}$Md published data is also uncertain and need to be improved. This isotope was observed in the year 1981 [Mun81b] when five events with a mean energy of $E_\alpha$ = 8428 ± 25 keV were reported and four of them were correlated to $^{243}$Es. More detailed information was obtained in the year 1993 when the previously known alpha activity was confirmed and two fission events at the beam energy of $E_{lab}$ = 4.78 AMeV were observed. These fissions were preliminary attributed to an isomeric state of $^{247}$Md.

The second reaction - $^{48}$Ca + $^{209}$Bi - was chosen for the study of $^{254}$Lr, $^{255}$Lr and their daughter products $^{250}$Md and $^{251}$Md. The isotopes $^{254}$Lr and $^{250}$Md were reported for the first time in the work of *G. Münzenberg et al.* [Mun81a] but first spectroscopy results were published in work of *F.P. Heßberger et al.* [Hes85]. Some spectroscopic information about $^{255}$Lr and $^{251}$Md is already known for a longer time [EsK71], [Dru70], however detailed spectroscopic analysis are missing until now. Some recent measurements show a broad energy distribution for the $\alpha$ decay of $^{254}$Lr indicating a strong influence of energy summing with conversion electrons.

Presently a more detailed spectroscopy information on decay properties of these isotopes, mentioned above, can be obtained. By means of $\alpha$, $\alpha$ - $\gamma$ spectroscopy in combination with the $\alpha$ - $\alpha$, recoil - $\alpha$, $\alpha$ - $\alpha$ - $\gamma$ correlation search, not only a detailed study of decay properties but also an assignments of spins and parities

(however very often only tentative) for the ground states and low-energy excited states can be obtained. These results deliver valuable information on the nuclear structure of the mentioned nuclei and their decay products. A confrontation with existing theoretical calculation therefore creates a basis for further development of theoretical predictions of still unknown superheavy nuclei.

# Chapter 2

# Stability and production of heavy and superheavy elements

One of the most significant questions in superheavy elements research is the one about their stability. What can be the heaviest synthesized nuclei? Is there any "island of stability" for superheavy nuclei? Where are the proton and neutron magic numbers for superheavy elements? What are the decay modes of these nuclei? What is the life-time of these nuclei? How can they be synthesized? In the next section these questions will be discussed along with the possibilities of the superheavy element production from the point of view of their lifetime and reaction cross-section.

## 2.1 Spontaneous fission lifetime

It is well known that spontaneous fission lifetime for heavy elements beyond uranium dramatically decreases with increasing proton number. This tendency can be shown on the spontaneous fission partial half-lives. In figure 2.1 the experimental spontaneous fission half-lives are shown in dependence on the fissility parameter $x$ for various transuranium isotopes together with half-live predictions based on the liquid drop model.

Fissility parameter $x$ for these nuclei is calculated with following parametrization based on a liquid drop model [MyS66]:

$$x = \frac{(Z^2/A)}{(Z^2/A)_{crit}} \tag{2.1}$$

$$(Z^2/A)_{crit} = 50.883\left(1 - 1.7826[(A-2Z)/A]^2\right) \tag{2.2}$$

According to liquid drop model already for the Fermium ($Z$=100) the fission half-lives are below the limit of present experimental technique (around few microseconds) as can be seen in figure 2.1. The real decrease of the half-lives for superheavy elements is much slower as is predicted. For example the measured

half-lives for Fermium are about several orders of magnitude above the experimental limit and around 10-20 orders above liquid drop model half-lives.

It is nice example that the life of the superheavy elements does not depend only on macroscopic parameters (e.g. mass, proton number, deformation) but there is an important influence of microscopic parameters (e.g. shell correction). The liquid drop model is not applicable for the transuranium elements, in case of spontaneous fission lifetime calculations. These elements are able to survive because of small, few MeV, shell correction. In addition it should be mentioned that the spontaneous fission of the isotopes with odd neutron or proton number is hindered because of the existence of unpaired nucleon can cause an effective increase of the fission barrier. The spontaneous fission lifetime is then around 2-7 orders of magnitude longer compare to the fission lifetime of even-even isotopes.

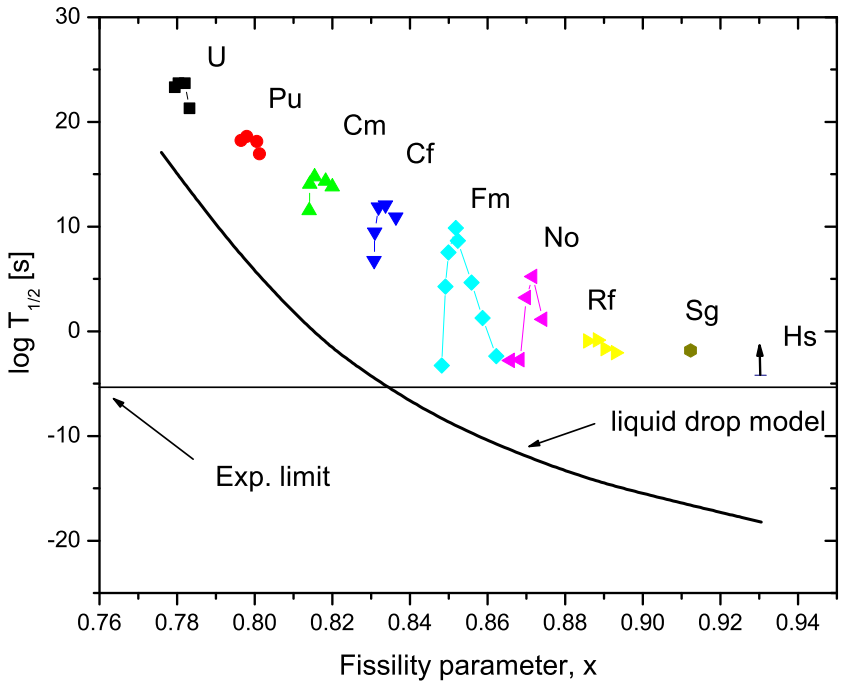


Figure 2.1: Spontaneous fission partial half-lives of doubly even isotopes in dependence on the fissility parameter $x$ (see equation 2.1). Each mark represents various isotopes of the same element. The solid line shows the tendency of the fission half-lives as predicted by the liquid drop model.

## 2.2 Alpha decay lifetime

As it was shown in previous section the measured spontaneous fission half-lives indicate the stabilization effect of shell structure for superheavy elements. One can see from the measured data that alpha decay is the main decay mode for most of the isotopes in transfermium region. The important question is what is the tendency of $\alpha$ decay lifetime. Is there a stabilization effect due to the closed shells too?

The theory is able to reproduce the measured energies and half-lives in quite good agreement with the experiment but can we expect such a good agreement also for a predicted, and until now unknown, isotopes?

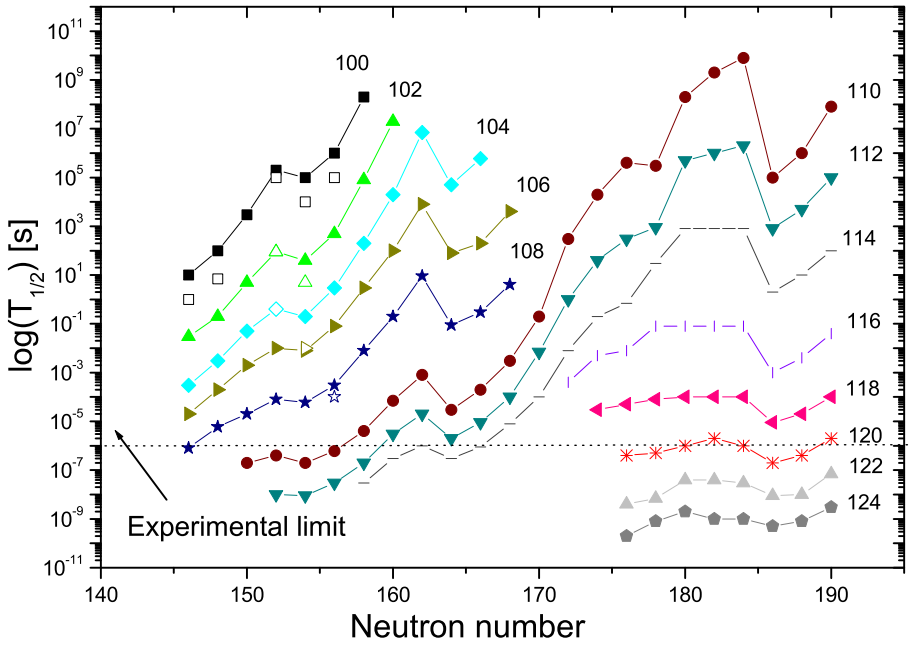


Figure 2.2: Calculated and experimental $\alpha$ decay half-lives for a different isotopes of superheavy elements with $Z = 100$ - 120 as a function of neutron number $N$. The open symbols mark the experimental values. Solid symbols mark the calculated values [Smo97].

One of the theoretical results [Smo97] for heavy and superheavy elements half-lives is shown in figure 2.2. The stabilization effect of magic neutron number $N = 184$ - the next neutron magic number after $N$=126 - is clearly visible. Weaker, but still visible, is the influence of the deformed neutron shell at $N$=162. According to these results the element 120 should be the heaviest element above the present experimental limits for lifetime of produced nucleus - $T_{lim} \approx 1$ $\mu$s. With this decay half-life it is still possible to separate, detect and identify synthesized nucleus. Due

to the effect of an unpaired nucleon the $\alpha$-decay half-lives for odd-odd isotopes of the element 121 may be comparable or even higher than those calculated for even-even isotopes of the element 120. Therefore the element 121 may be the heaviest one which may be detected if it will be successfully synthesized [Smo97].

Using other models one can get different results which should be also discussed. According to the results of *Cwiok et al.* [Cwi96] the lifetimes above the experimental limit of $\approx 1$ $\mu$s may be also present for isotopes of elements up to the Z=126. Similar result can be found for example in the work of *K. Rutz et al.* [Rut97] and *M. Bender* [Ben01]. It is also possible that the shell effect will not only have influence for one element or a small area around the center of the island of stability but influences a larger area, however, with a smaller effect.

At this place it should be mentioned that all experiments on the synthesis of superheavy elements are carried out in the neutron deficient region on the border of the area of enhanced stability because of non-existence of suitable neutron rich combination of projectile and target.[1]

## 2.3 Cross-section for reactions of synthesis

Very important and one of the limiting factors of heavy and superheavy elements production is the exponential decrease of reaction cross-section. Reaction with complete fusion can be classified by dependence on the excitation energy of compound nucleus. This energy is given by equation:

$$E^* = Q + \frac{M}{M+m} E_p \tag{2.3}$$

where $Q = (M + m - M_{CN})c^2$ is the Q-value of reaction, $E_p$ is the beam energy in laboratory system and $M$, $m$ and $M_{CN}$ are the masses of the target, projectile a compound nuclei, respectively. For the fusion reaction with excitation energy less than 50 MeV the main de-excitation process is the evaporation of neutrons. Each neutron takes away $\approx 10$ MeV of energy. As was already mentioned the complete fusion reaction can be divided into two groups [2].

1. The reaction using heavier target (e.g. uranium, plutonium) - is a reaction with typical excitation energy of 30-50 MeV and in the process of de-excitation 3 - 6 neutrons are evaporated. For this reaction usually a light projectile and a transuranium target is used. This type of reaction was successfully used for the synthesis of new elements with proton numbers from 101 to 106 and probably also for the synthesis of elements 113 - 116, which were not confirmed yet by independent measurement.

[1] This problem may be partially solved in the future by using the neutron rich radioactive beams

[2] Before the reaction for superheavy element production were usually divided into a hot fusion and cold fusion reaction. But from physical point of view is better to divide them according to the reaction symmetry or according to the mass of target nuclei, what is used also in this work.

2. The reaction using lighter target (e.g. lead, bismuth) - is the reaction with a typical excitation energy up to 20 MeV when only a few, up to three, neutrons are evaporated. In this kind of reaction usually the lead or bismuth targets are used for SHE production. Using this method the elements 107 - 112 were observed.

In figure 2.3 the comparison of the cross-section as a function of proton number is shown [3]. There is a typical exponential decrease for the reactions with lead and bismuth targets but no indication of any significant decreasing tendency for the reactions with uranium and transuranium targets.

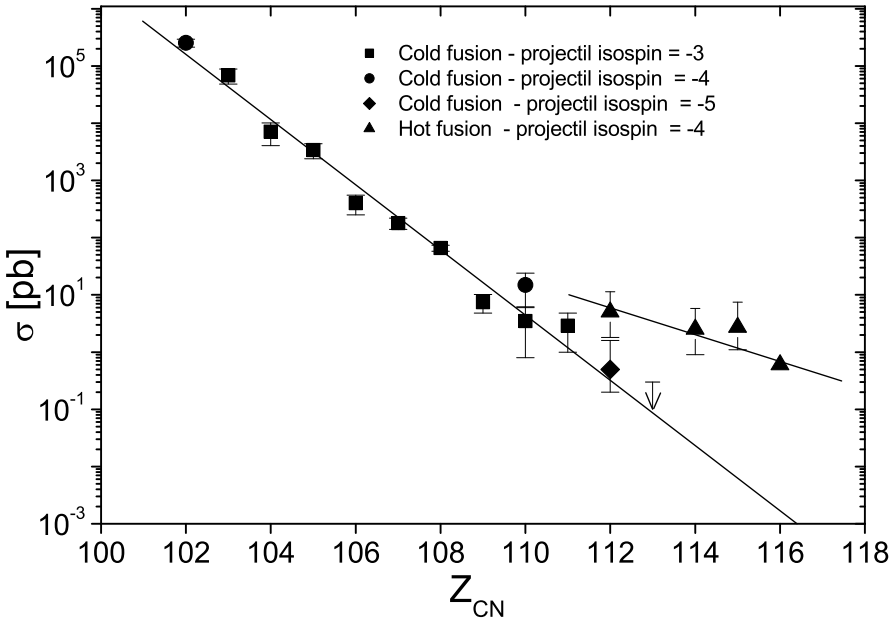


Figure 2.3: Comparison of the cross-sections $\sigma$ for the production of superheavy elements as a function of compound nucleus proton number $Z_{CN}$ using cold fusion and hot fusion reactions.

For the synthesis of the element 111 - Roentgenium - the measured cross-section in the reaction of $^{64}$Ni + $^{209}$Bi at the beam energy of $E_{beam}$ = 320 MeV (14.1 MeV of the excitation energy) was $\sigma = 2.9^{+1.9}_{-1.3}$ pb. For the $^{277}$112 produced in the reaction of $^{70}$Zn + $^{208}$Pb at beam energy of $E_{beam}$ = 343.8 MeV (10.1 MeV of the excitation energy) the measured cross-section was $\sigma = 0.4^{+0.9}_{-0.3}$ pb and $\sigma = 0.5^{+1.1}_{-0.4}$ pb at the beam energy of $E_{beam}$ = 346.1 MeV (12 MeV of excitation energy) [Hof02]. For the element 113 only the cross-section limit was obtained. In two experiments with

[3] on this figure the maximum measured cross-section for this isotope is used

the mean beam energy of $E_{beam}$ = 351 MeV (12.02 MeV of excitation energy) no event was detected at SHIP and the limit of $\sigma < 0.3$ pb was achieved [Hof04]. The positive result in case of element 113 synthesis was recently reported from RIKEN where a decay chain was detected using a reaction of $^{70}$Zn + $^{209}$Bi. The cross-section was evaluated to the value of $\sigma = 55^{+150}_{-45}$ fb, half-life to the value of $T_{1/2}$ = 344 $\mu$s and measured $\alpha$ decay energy was $E_\alpha$ = 10.03 ± MeV [Mor04].

According to the experiments with synthesis of new elements using $^{48}$Ca induced reaction in Dubna, the elements from 112 up to the 116 show no significant difference and decrease of cross-section (see figure 2.3). The presented values for the cross-section are from $\sigma$ = 0.6 pb (for the element 116) [Oga00b] up to the $\sigma = 5^{+6.3}_{-3.2}$ pb (for the element 112) [Oga99c]. The maximum measured cross-section for the isotope $^{287}$114 is $\sigma = 2.5^{+3.3}_{-1.6}$ pb [Oga99a] and for other isotopes of this elements ($^{289}$114 a $^{288}$114) $\sigma$ = 2.5 pb [Oga99b, Oga00a] as well. The last reported results with a synthesis of the element 115 gives for the isotope $^{288}$115 ($E_{beam}$ = 248 MeV) the value $\sigma = 2.7^{+4.8}_{-1.6}$ and for the isotope $^{287}$115 ($E_{beam}$ = 253 MeV) the value $\sigma = 0.9^{+3.2}_{-0.8}$ pb [Oga04].

The evaluation of the reaction cross-section is a crucial point in the experiment preparation. Especially in spectroscopy experiment one needs to estimate the reaction yield and the possible contribution of un-wanted reaction products. There are several computer codes which can be used for cross-section evaluation - for example ALICE [Pla77], [Pla78], JULIAN/PACE [Hil76], [Gav80], HIVAP [ReS81], [ReS92]. For all analyzed reactions discussed in this work the theoretical excitation functions were estimated and compared to the measured values. These calculations were done using computer code HIVAP developed by *W. Reisdorf* [ReS81], [ReS92]. Because of large number of semi-empirical parameters used by this code only rough values of the cross-sections can be estimated and the difference between the measured and calculated values can for some reactions reach up to one order of magnitude[4].

[4]It should be mentioned here that the results of other codes are not in better agreement with experimental results

# Chapter 3

# Identification of heavy and superheavy elements

## 3.1 Separation

As it was mentioned already in the previous chapter experiments on the investigation of superheavy elements have to be laid out to be sensitive to very low cross-sections and very short decay half-lives. These factors determine a high requirement on precise and reliable methods of reaction products identification. Crucial is the ability to separate very fast the expected reaction products from the primary beam and from a background created mainly by scattered ions of primary beam and unwanted products of transfer reactions.

The first transfermium products were separated using a gas transport systems (helium jets), when the reaction products were stopped in the gas (usually helium) and after that they were carried through a thin capillary to the detector system which detected the emitted alpha particles or fission fragments. The efficiency of this method was relatively low and the transport time was quite long - up to several seconds.

Another successfully used separation method was the mechanical separation. In this case the reaction products were implanted to a rotating wheel or band and afterwards they were transported to the detector system. Disadvantage of this method was the contamination and activation of the catcher material by the target-like products and long transport time.

Presently the main method used for separation is the one utilizing in-flight separators. The reaction products are picked up from the beam and directed to the detector system using electric and magnetic fields. Such separators can be divided into two groups:

a. Wien filters and energy separators are using specific kinematic properties for products of complete fusion reaction, which have different energy and velocity compare to the projectiles or transfer reaction products. This method is used for example at separators SHIP (Separator for Heavy Ion reaction

Products) [Mun79] in GSI Darmstadt and VASSILISSA [Yer97] in JINR Dubna.

b. Gas filled separators use different magnetic rigidity for the reaction products flying in the magnetic field filled with a gas (usually Helium). The typical pressure for this gas is around 1 mbar. To this category belong for example the RITU (Recoil Ion Transport Unit) in Jyväskulä (Finland) [Lei95], DGFRS (Dubna Gas Filled Recoil Separator) in JINR Dubna (Russia), GARIS (GAs-filled RecoIl Separator) in Riken (Japan) or BGS (Berkeley Gas-filled Separator) in Berkeley (USA).

The main advantages of in-flight separators are:

a. *The short separation time* in the order of a few microseconds, that allows to study the isotopes with a half-live in the order of 1 microsecond.

b. *High background suppression* gives the possibility to study reaction products with a very low cross-section in the order of 1 pb when the production rate is around 1 atom per month.

c. *Low energy scattering* enables us the possibility to do at least some rough mass measurement, using measured value for kinetic energy of the implanted nucleus and its velocity. In dependence on experimental conditions it is possible, at least approximately, to distinguish the transfer reaction products, the scattered projectiles and complete fusion reaction products.

The detail properties and construction of the vacuum in flight separator SHIP will be explained in more detail in the following section.

## 3.2 SHIP

SHIP is placed at the central beam line of the UNILAC - UNIversal Linear ACcelerator - at GSI Darmstadt in Germany. This accelerator is able to deliver beam for all stable elements up to the Uranium with a relatively high intensities (3.0 p$\mu$A for $^{40}Ar^{8+}$, 1.2 p$\mu$A for $^{58}Fe^{8+}$ and 0.4 p$\mu$A for $^{82}Se^{12+}$)[1] and energies up to the 20 AMeV. The relative accuracy of the beam energy is $\pm$ 0.003 AMeV and the absolute energies are accurate to $\pm$ 0.01 AMeV. This accuracy is sufficient for measuring narrow excitation functions with a width of only few MeV as it is in case of 1n and 2n emission channels in the reactions on the production of heaviest elements (Z>100) using Pb and Bi targets. [Hof00]

The velocity filter SHIP [Mun79] was designed to give a high yield of heavy ions reaction products, especially for the products from complete fusion reactions. The separator accepts ions in a velocity interval of $\pm$ 5% and a charge state of the products up to $\pm$ 10% around the mean value.

[1] 1 p$\mu$A = 6.24 x $10^{12}$ particles/s

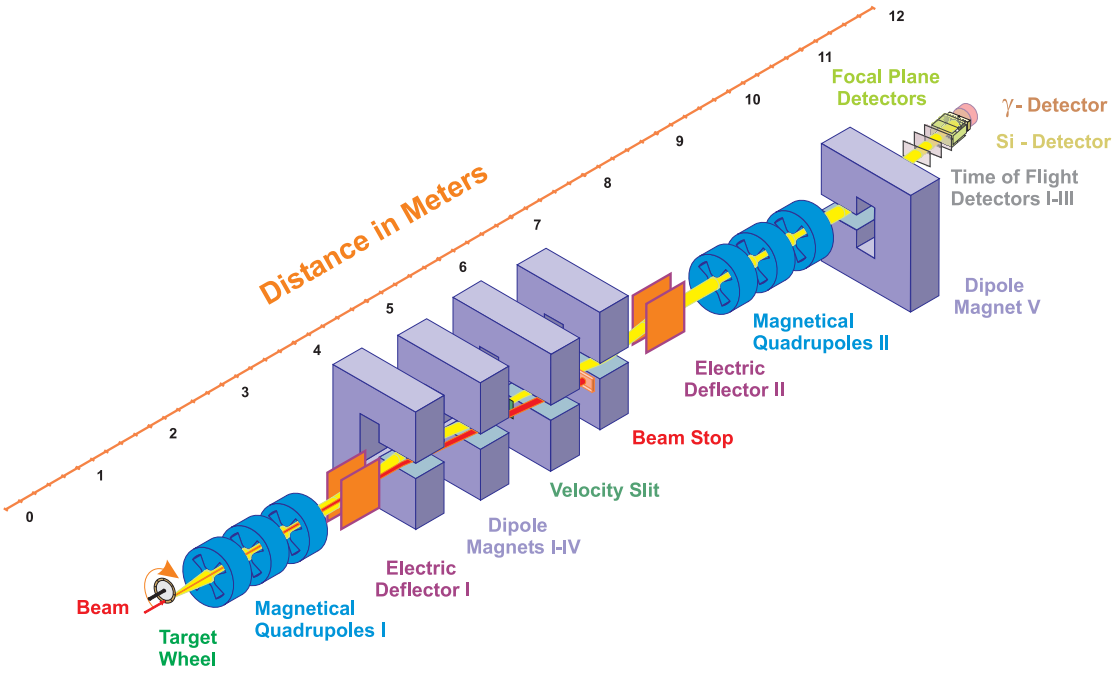


Figure 3.1: Velocity filter SHIP. The length of SHIP from target to detector is 11 m. The flight time of reaction products is $\sim$ 2 $\mu$s. Detector system is schematically shown in figure 3.2 .

For synthesis of heavy and superheavy elements usually lead or bismuth target with thicknesses around 450 $\mu g/cm^2$ are used. The target material is evaporated on a thin carbon foil with a thickness of $\sim$ 40 $\mu g/cm^2$ and it is covered with $\sim$ 10 $\mu g/cm^2$ carbon foil to reduce the radiation damage of the target and increase its emissivity.

For SHIP experiments two target types - fixed and rotating - are employed. Fixed targets usually have a diameter of 15 or 20 mm and are mounted on a target ladder which can be moved in and out of the beam. Because the melting point of lead and bismuth is relatively low (327.5 °C for the lead and 271.3 ° C for the bismuth) the rotating target wheel is used to increase an irradiated area and spread out the deposited energy. For the rotating mode eight circular ring sector targets (110 x 23 $mm^2$) are mounted on a wheel of 310 mm diameter that rotates synchronously to the beam macrostructure with a rotation speed of 1125 rpm (frequency 18.75 Hz) [Fol95]. The typical beam macrostructure is $\sim$ 5.5 ms pulse and $\sim$ 14.5 ms pause[2]. The same target is irradiated after three cycles of the target wheel with a typical time of $\approx$ 160 $\mu$s.

A movable carbon stripper foil with a thickness of 40 - 60 $\mu g/cm^2$ is mounted behind the target. This foil is used for charge equilibration of the reaction products and striping of the electrons.

[2]In the experiments the pulsed length is usually from 4 ms (limit for $^{238}$U) up to the 6 ms.

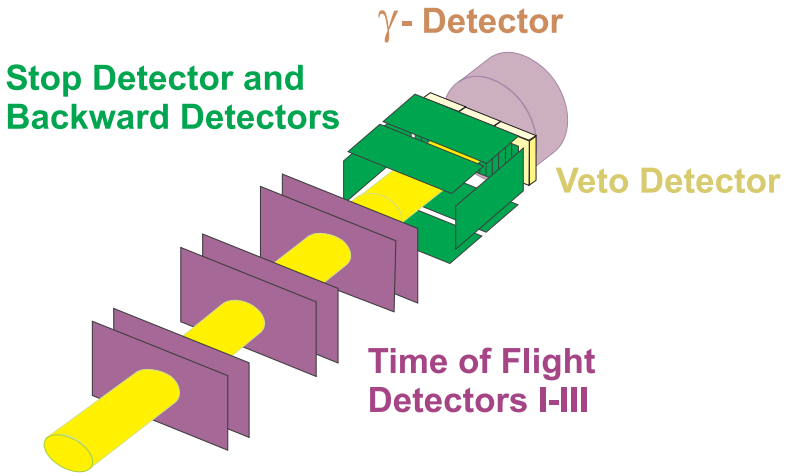


Figure 3.2: Assembly of detectors for identification of heavy elements, composed of large-area secondary-electron time-of-flight detectors, position-sensitive silicon strip detectors (detector to stop the ions and backward detectors), veto detector and germanium detectors for detection of $\gamma$ rays (see text for more details).

The separator itself is a combination of two velocity filters with separated deflecting electric and magnetic fields. One triplet of the quadrupole magnets is collecting the recoiling products which are usually intermediately focused in the plane of the velocity slit. The second quadrupole triplet, placed behind the separator, focuses the separated recoils on the silicon detector. Behind the filter an additional dipole magnet is placed which provides an additional 7.5 ° deflection. Using this additional magnet it is possible to reduce the background created by projectiles with a low charge state which have a high rigidity. Total background suppression of the separator over the whole energy spectrum is $10^{10}$ - $10^{11}$.

## 3.3 Detectors

The detector system used for the identification of the reaction products at SHIP consists of a time-of-flight system (TOF), seven 16-strip silicon detectors (one detector to stop the ions and six backward detectors), veto detector and gamma detector (see figure 3.2).

The TOF system consists of three detectors. One serves usually as a start detector and the other two as stop detectors. The efficiency of TOF system is around 99.8 %. Therefore in anti-coincidence with the silicon detector very clean decay spectra can be obtained. The time resolution is $\approx$ 700 ps and transparency is 100 %. The TOF detector is based on the registration of secondary electrons produced by ionizing particles crossing a thin carbon foil mounted perpendicular to the direction of the detected ions.

Each detector is supplied with two self-supported carbon foils with an active

area of 55 $cm^2$ and thickness around 30 $\mu g/cm^2$ [Sar96]. Between these foils a high voltage of 4 kV for accelerating emitted secondary electrons is used. Afterwards these electrons are deflected by a magnetic field to the surface of microchannel electron multiplier plates (MCP). The time pulse is derived from the anode of the MCP detector unit.

Active area of the silicon strip detectors is 35x80 $mm^2$. Each strip is 5 mm wide and the position sensitivity in the vertical direction is around 150 $\mu$m (FWHM) for $\alpha$ decay what results in an equivalency with a system of 3700 single detectors with the area of 5x0.15 mm. Because of pulse height defect the position resolution of the recoils is worse and a position uncertainty at least 0.5 mm should be considered. An energy resolution is 14 keV[3] for an external $^{241}$Am $\alpha$ source [Hof00]. For implanted nuclei are measured summed energies of the alpha particle energy and part of the recoil energy[4] and the energy resolution is worse. Even worse is the resolution of summed spectrum taken from all strips because of non-ideal calibration for different strips. The typical alpha energy resolution in experiment is usually around 20 keV.

A six wafers of multi-strip silicon detector are placed around the area in front of the stop detector. These can measure the escaping $\alpha$ particles or fission fragments. They cover around 80% of $2\pi$ hemisphere. The energy resolution obtained by summing the energy-loss signal from the stop detector and the signal from the backward detector around 60 keV for escaping $\alpha$ particles is achievable. All silicon detectors are cooled to a temperature of -10 °C.

An another silicon detector - the Veto detector - is placed behind the stop detector. The task of this detector is to reject, in coincidence with stop detector, the signals coming from the particles which pass through the stop detector and are not recognized by the TOF system (mainly high energy protons).

The germanium 'clover' detector consist of four crystals measuring the X-rays and $\gamma$-rays. This signal can be taken and proceeded to the data analysis as a separated event or as a signal in coincidence with an $\alpha$ decay, using coincidence time of 4 $\mu$s. The registration of $\alpha$ - $\gamma$ coincidences or search for a short-living ER - $\gamma$ or $\alpha$ - $\gamma$ coincidences is an useful tool to study excited levels in daughter nuclei. The registration probability for $\alpha$ - $\gamma$ coincidences is 14 % in the energy region of 100 - 300 keV [Hes04].

The position sensitivity and multi-strip detection system allows us to check in the on-line and/or off-line analysis the position distribution of the reaction products and to make the correction for separator setting (mainly for last dipole magnet) if necessary. In figure 3.3 a typical example for the distribution of the events in anti-coincidence with TOF system across the focal plane is shown. Using the same plot without anti-TOF condition the distribution of the low-energy background events can be checked. For reduction of this background in some experiments aluminum or mylar degrader foils is placed in front of the stop detector. The thickness of this foils can be varied in step of 0.5 $\mu$m up to the several $\mu$m.

[3] All resolutions in this work are given as FWHM of particular peak.

[4] Around 60 - 65 % of the recoil energy is not detected due to the PHD

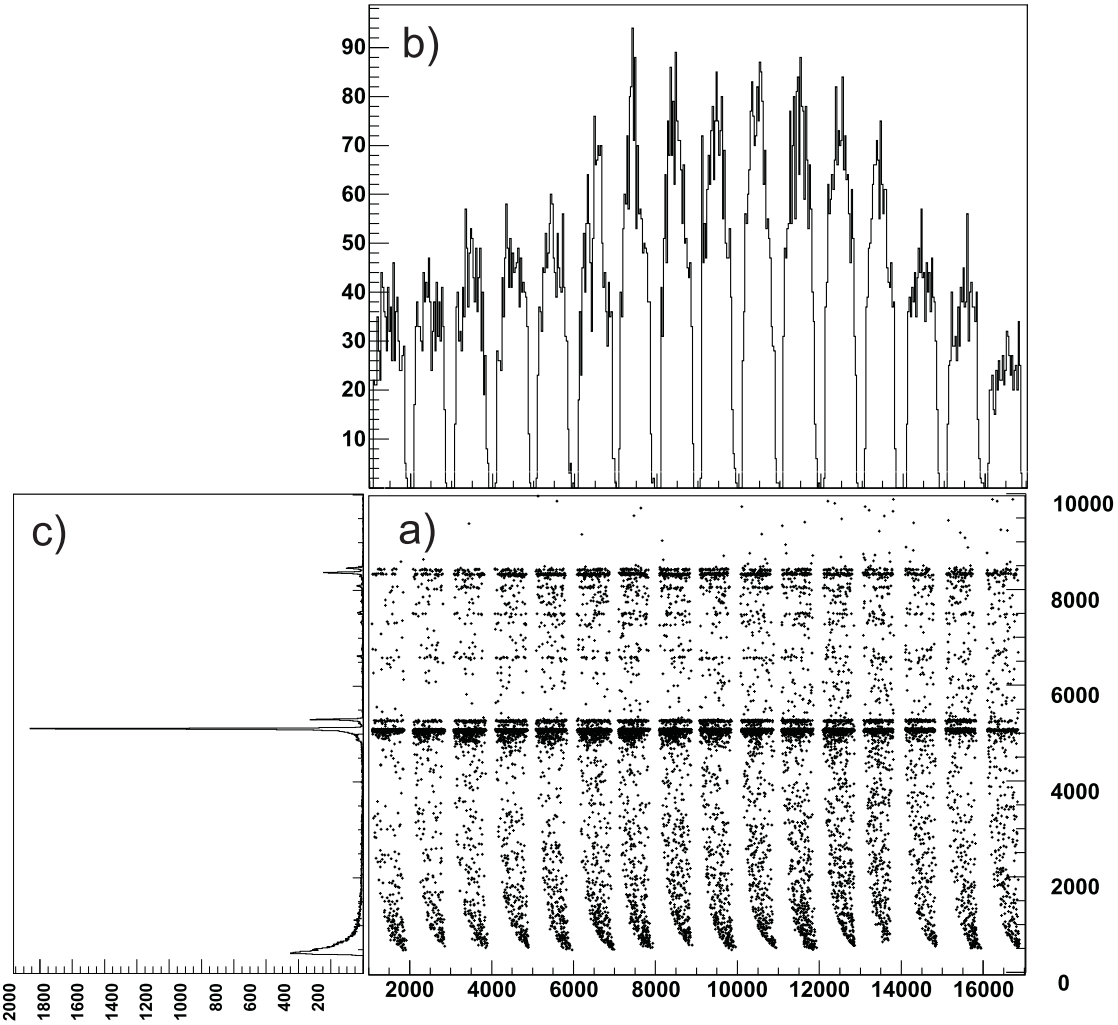


Figure 3.3: Position distribution vs. energy of events in anti-coincidence with TOF system (mainly the $\alpha$ decays) measured in the reaction of $^{48}$Ca + $^{209}$Bi at beam energy of $E_{beam}$ = 4.69 AMeV. The position in the parts a) and b) on the X axis is calculated as 1000*(strip number) + (position in strip). At the upper part the position histogram is shown, at the left part the energy histogram is placed. One can see the well centered distribution of the events with the energy 8.4 MeV which are attributed to the decay of $^{255}$Lr. The intensive group of events with the energy 5.11 MeV (slightly shifted to the left side) comes from the decay of $^{208}$Po coming mainly from previous irradiations.

In addition wedge-shape degrader foil can be used for reduction of asymmetric low energy background. Except of the background suppression in some experiments the degrader foils can be used also for energy shift of the recoils to the low energy branch.

## 3.4 Calibrations

An essential part of the analysis is the calibration. The calibrations used in the analysis of presented experimental data are described in following section. Altogether six calibrations are applied. Some of them are correlated and should be performed in certain order and they are described in the same order as they are applied in the calibration process.

a. *The energy-position calibration* is necessary because of the so-called ballistic effect. The measured signals are position dependent what leads to a worse energy resolution. The applied correction is used for every strip separately and calculated by fitting the position dependence of a reference energy from a known emitter using polynomial function of 2nd order.

$$\Delta E = (E_{meas} - E_{ref}) = a \times position^2 + b \times position + c \qquad (3.1)$$

where the a,b and c are fitting parameters of the calibration function.

b. *Alpha energy calibration* should be done as an internal calibration from the alpha emitters decaying directly inside the detector. This has to be done because the alpha signal is summed with a fraction of the recoil energy. The recoil energy is usually around $E_{rec} \approx 150$ keV and more than half of this energy is lost because of the pulse height defect. Disadvantage for external alpha source, besides of the lack of recoil effect, is the energy loss in the death layer for all strips, what leads to additional uncertainties. The external source is usually used only for rough calibration during the tuning of the electronics. For this calibration a mixture $\alpha$ source ($^{239}$Pu+$^{241}$Am+$^{244}$Cm) is used. The calibration reactions used in the experiments presented in this work will be described and discussed later.

   During the calibration one needs to take into the account possible effects which can cause the shift of the measured alpha energy. For instance the decay into the excited state can create a shift to higher energies because of summing with possible created conversion electrons and such a lines should not be used for the calibration. Additional source of an energy shift is the pile-up effect for the decays with a half-live in the order of several tens of microseconds. As was already mentioned compare to the external source the alpha energy is summed with the the recoil energy. Due to a pulse height defect only part of this energy - usually around 35 - 40 % - is registered. For illustration the typical values for some isotopes [Hes04] are shown in table 3.1.

c. *Calibration of backward detectors* is usually done from the test reaction, however for rough setting also an external $\alpha$ source may be used. For calibration events with coincidence signal from the stop detector and backward detector

| **Isotope** | $\mathbf{E}_{\alpha}$ **[keV]** | $\mathbf{E}_{rec}$ **[keV]** | $\mathbf{E}_{rec-reg}$ **[keV]** |
|---|---|---|---|
| $^{251}$No | 8610 | 139.4 | 49 |
| $^{216}$Th | 7923 | 149.5 | 52 |
| $^{214}$Ra | 7130 | 135.8 | 48 |
| $^{217}$Th | 8250 | 173.7 | 61 |
| $^{212}$Rn | 6260 | 120.4 | 42 |

Table 3.1: Some examples of the recoil energies $E_{rec}$ and their registered part, $E_{rec-reg}$, that a summed with alpha energies [Hes04].

are used. The summed energy from both detectors must be in the predefined energy window around well separated peak. Because the alpha particle goes through death layers of both detectors the energy resolution is worse than energy resolution for the stop detector and has a value from 60 keV to 100 keV.

d. *The position calibration* between the positions in high and low energy branch should be done because of different amplification in these branches. High energy branch usually covers the energy range from 18 MeV up to few hundreds of MeV and is necessary for reactions where expected reaction products have kinetic energy in this energy range or where the products with a fission activity are produced.

   This calibration is done by linear fitting of the positions from the high energy branch as the function of positions from the low energy branch.

$$high\ energy\ position = a \times low\ energy\ position + b \tag{3.2}$$

   where $a$ and $b$ are fitting parameters.

   These positions are taken from events where identical positions in both branches are expected. This condition is usually fulfilled by two types of the events.

   (a) Positions can be taken from events in the part of energy spectra which is covered by both of the energy branches.

   (b) The second possibility is of using the reaction with a very short half-life for products when the position of the high energy recoil is compared to the positions of subsequent alpha decay. From this difference can be evaluated the shift of the positions in both branches of acquisition system (high energy and low energy branch).

e. *The calibration of the $\gamma$ detector* at the experiments on SHIP is performed using $^{152}$Eu and $^{133}$Ba. These sources give us the possibility to calibrate a wide range of gamma energies, from several ten keV up to the 1.5 MeV. The energy uncertainty of summed spectra from all four detector clovers is usually better than 1 keV.

f. *Calibration for high energy branch* is usually more complicated due to the presence of pulse height defect (PHD) and lack of suitable mono-energetic sources. Rough calibration can be done with the known maximum energy of projectiles and using of $^{252}$Cf source of fission fragments. It is necessary to keep in mind that for light projectiles with typical energies around 200 - 300 MeV the PHD is around 1-2 % and for fission fragments of $^{252}$Cf it is around 5-15 % [Wil71].

## 3.5 Electronic system

Electronic system of stop and backward detectors is schematically drawn in fig. 3.4. Two position signals (top and bottom) for each individual strip are summed after the preamplification to obtain the energy signal. Shaping-time constants are 0.3 $\mu$s and 2.0 $\mu$s for the position and energy signals, respectively. All signals are converted in fast analog-to-digital converters (3.5 $\mu$s conversion time) and buffered in 128-word FIFO (first in first out) buffers in each channel. Before conversion, the signals from the silicon detector are split into two branches. For the first - low energy - branch the amplification factor of 10 is used. With this branch a processed signals with the energy up to $\approx$ 16 MeV and this branch is optimized for detection of $\alpha$ decays. The second - high energy - branch has no amplification (factor of 1 is used). With this branch signals up to $\approx$ 300 MeV are process. In this branch mainly the spontaneous fission and recoil implantation events are detected. The same branching is applied on the backward detectors but since they have galvanically connected stripes, they provide only the energy signals.

The time is measured with the accuracy of 1 $\mu$s using 1 MHz clock increasing the contents of a 15 bit scaler. The scaler is reset at the end of each 20 ms macro-pulse period. Two other scalers register the number of macro-pulses and overflows. The additional scaler counting with a period of 160 ms (period of three cycles of the target wheel - typical time between two irradiations of the same target elements - see section 3.1) and step of 10 $\mu$s is also present. This scaler is not used for the time evaluation usually but may serve as backup counter. Beam currents are monitored by a scaler which is connected to a current digitizer.

An additional electronic circuit, allows fast switching-off the beam when an implanted residue with defined energy and time-of-flight values is detected. The beam-off time window is set in the way that expected subsequent $\alpha$ decay(s) fall into it. If it happens, the beam-out period can be prolonged up to the expected measurable end of the decay chain. Described setup is usually used when the

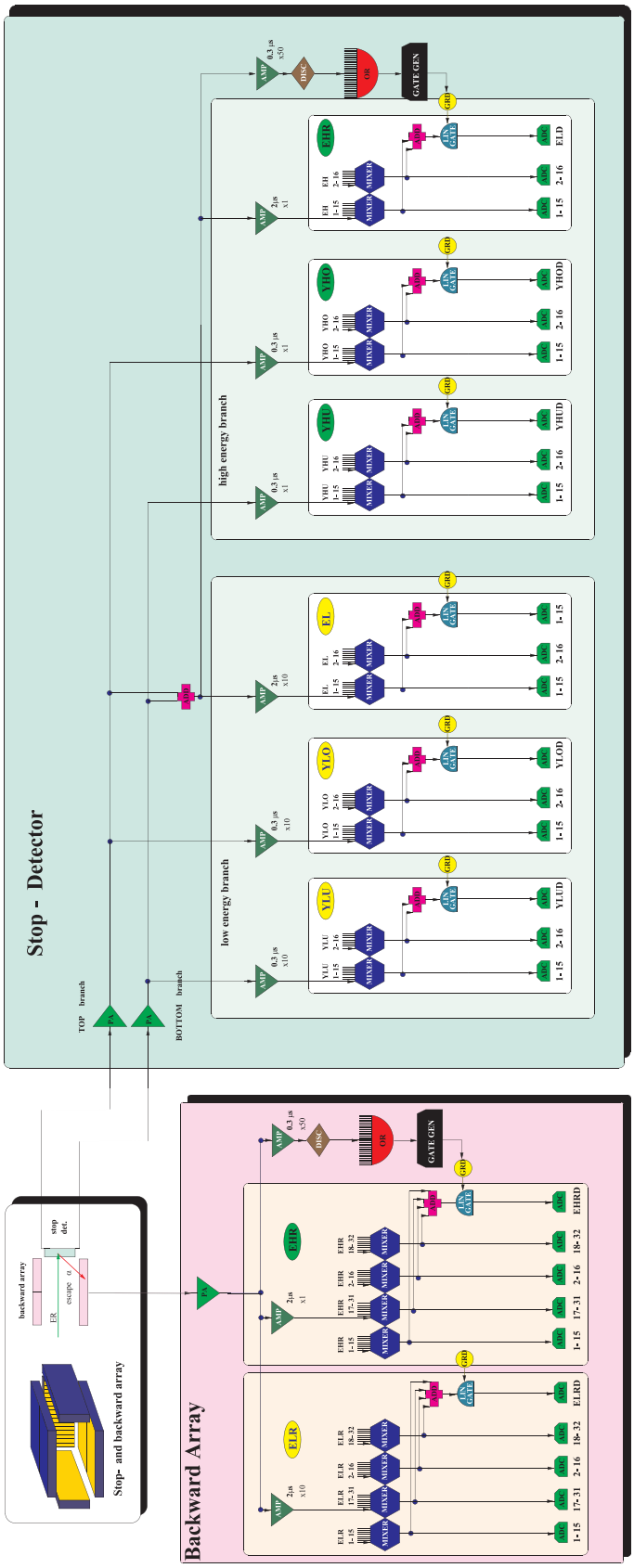


Figure 3.4: A schematic drawing of the electronic system of stop and backward detectors on SHIP.

rapid decay, within time of several ten $\mu$s, is expected[5] and was successfully used for example in the identification of the new isotope $^{270}$110 [Hof01].

## 3.6 Data acquisition

In the experiment altogether 40 parameters are read out from the CAMAC crates using the Multi-Branch acquisition system (MBS) developed at the GSI running on PowerPC board (CES RIO2). These values, stored in the events, are simultaneously analyzed by on-line analysis and written to the large capacity magnetic tapes. The online analysis is performed using GOOSY (GSI on-line off-line data processing) [GOO] and using GO4 (GSI Object Oriented On-line Off-line system) [GO4] with implemented analysis part GO4SHIP developed by the SHIP group. The GO4 is an analysis system based on ROOT [ROOT] with the specific requirements of the low and medium energy nuclear and atomic physics experiments implemented as extensions. For the off-line data analysis presented in this work only the GO4 was used. The analysis part of the program was modified for each experimental run, to match the individual settings and changes necessary for each experiment. One of the most important parts of the analysis program is the correlation search which will be described in the following section.

## 3.7 Time and position correlation method

The position sensitivity of silicon strip detectors gives us the possibility to use time and position correlation method. For elements with a very low production rate this method represents a very strong tool for their identification. The principle is to search for the relationship between subsequent alpha decays coming from the same position in a chosen time window which can be assigned to a decay of the desired reaction products and their daughter nuclei.

The method is described schematically in figure 3.5. Beginning from time $t_{ER}$ around the position $x_{ER}$ of the detected candidate with expected parameters suitable for the proper reaction products (mainly TOF value, energy, pulse bit) are searched the signals of its decay or of its daughter product decays. Let us suppose that at the time $t_{\alpha 1}$ and at the position $x_{\alpha 1}$ a signal with an energy $E_{\alpha 1}$ was detected. Further we can assume that at the time $t_{\alpha 2}$ and at the position $x_{\alpha 2}$ the next signal with energy $E_{\alpha 2}$ is detected. In case that all signals are coming from the implantation and decay of the reaction product and subsequent decay of its daughter nucleus the position differences $|x_{ER} - x_{\alpha 1}|$ and $|x_{\alpha 1} - x_{\alpha 2}|$ must be lower than position sensitivity of used detector. The time differences $|t_{ER} - t_{\alpha 1}|$ and $|t_{\alpha 1} - t_{\alpha 2}|$ should correspond to the lifetimes of the implanted evaporation residue and its daughter products.

[5] In all experiments described in this work was this part disabled, due to the long expected lifetime.

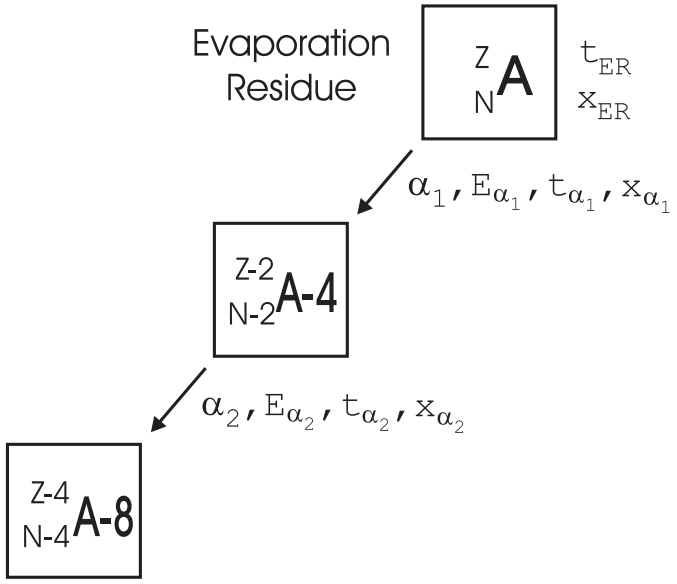


Figure 3.5: Principle of position and time correlation method for identification of the reaction products.

The efficiency of the background suppression using the TOF system for distinction of reaction products and alpha decay is shown in figure 3.6. The spectra shown on this figure are taken from the reaction of $^{54}$Cr + $^{208}$Pb at a beam energy corresponding to the production of $^{261}$Sg (1n channel) from 4.695 AMeV to 4.810 AMeV. The black line shows the complete $\alpha$-spectrum collected over 120 hours of irradiation for the energy range from 6000 keV to 11000 keV. Only less than 1 % of all events come from alpha decay and the complete decay energy structure is hidden in this background. The energy spectrum of the decays in anti-coincidence with TOF system is shown by a red line. In this spectrum the background is significantly reduced and it is possible to identify all main alpha lines. The green line shows signals coming in the pause between the beam pulses. The background is reduced 5 - 10 times compared to the use of "antiTOF" events but at the cost of 20 % loss of counts. Using only pause events is not suitable in the case when the decay lifetime is shorter than several milliseconds because most of the $\alpha$-decays will occur during the pulse. Practically complete reduction of the background is possible using the correlation method. With a blue line the alpha spectrum of the events correlated to the recoils is shown. The structure in the energy range of 9350 - 9600 keV corresponds to the decay of $^{261}$Sg. In this part the blue and green spectra are almost identical what is the indication of high efficiency for the search of Re - $\alpha$ correlations with used conditions for the recoil and alpha decay. The peak at the energy 8.77 MeV corresponds to Re - $\alpha$ correlations of $^{257}$Rf which is the daughter product of $^{261}$Sg and is partially covered by the correlation search in the used correlation time window (1.3 second). The rest of the correlation spectrum has two different sources. The first source of unwanted background are random

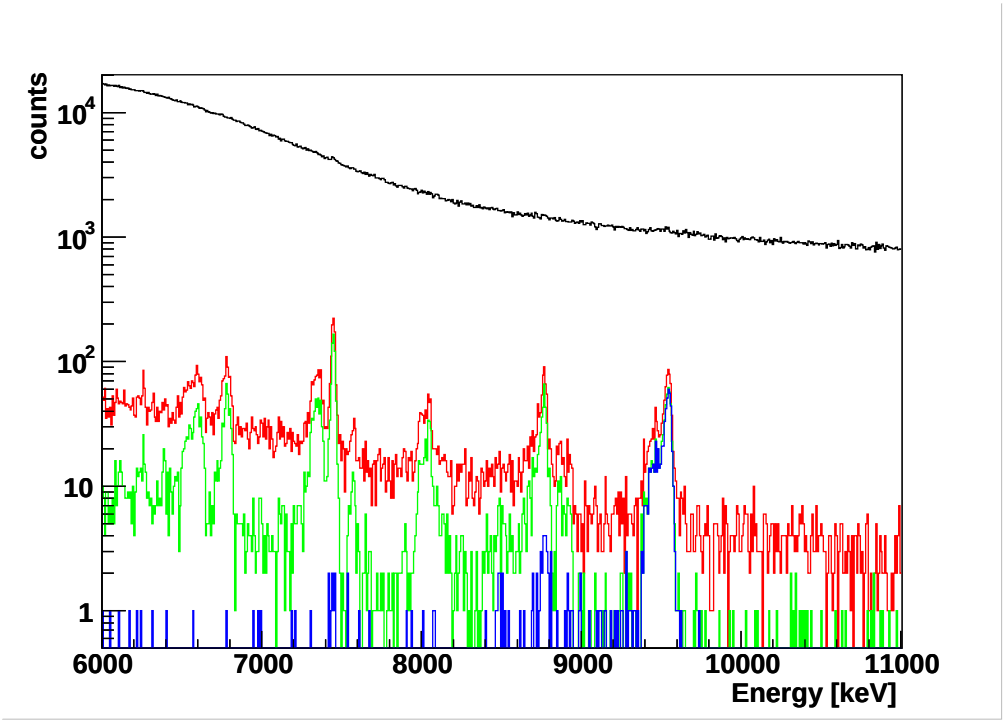


Figure 3.6: The low energy spectra (6000 - 11000 keV) collected in the reaction of $^{54}$Cr + $^{208}$Pb as an example of background suppression by different methods (anti-coincidence with TOF system, beam pulsing and using correlation method). Black line - total energy spectrum, Red line - spectrum anti-coincident to TOF system, green line - spectrum in pause between a beam pulses, blue line - spectrum of correlated alphas.

correlations. The other source of background are the Re - $\alpha$ correlations of transfer reaction products which are covered partially by given conditions for the energy and TOF value of the complete fusion reaction products. For example the typical "background" line in the experiment with use of the lead and bismuth targets is $^{211}$Po line at the energy of $E_\alpha$ = 7450 keV.

With an increasing number of the chain members the random correlation probability decreases and nearly unambiguous identification is achieved when known decay products are present in the decay chain. The reliability of described method is decreased when some chain members are missing because of emission of $\alpha$ particle out of the detector. As was described before this can be partially solved by using the backward detectors but sometimes it is not possible to assign the position in stop detector for such an events because of missing position information or its large uncertainty due to a low energy deposited in the stop detector. Even worse situation can arise when the decay chains are too short. Such a situation can happen for example when produced isotope or its daughter product has a large fission branch.

# Chapter 4

# Physical background

## 4.1 Alpha decay

Alpha decay is an useful tool for the study of the heavy and superheavy elements properties. Discrete decay energy gives us the possibility to identify the isotopes in this region. From the fine structure of alpha decay one can estimate the excited levels of daughter nucleus. Measuring of alpha decay energy, in case where the mass excesses of daughter nuclei are known, gives us the possibility to estimate the mass excesses of the mother nuclei. Because most of the results in this work are obtained from the study of alpha decay in following section some of its basic characteristic will be presented.

The process of alpha decay can be schematically written as:

$$ {}^{A}_{Z}X_N \rightarrow {}^{A-4}_{Z-2}Y_{N-2} + {}^{4}_{2}He_2 + Q_\alpha \tag{4.1} $$

The $Q_\alpha$ is exothermic for spontaneous alpha decay and the emission of the $\alpha$ particle lowers the Coulomb energy of the nucleus. In essence, all nuclei with a mass greater than A $\approx$ 150 are thermodynamically unstable[1] against alpha emission [Hod97]. The energies of alpha decay can range from 1.83 MeV ($^{144}$No) to 11.6 MeV ($^{212m}$Po) [FiS96]. Typical $\alpha$ decay energies are in the range from 4 MeV to 9 MeV.

The $Q_\alpha$ value can be calculated as a difference between the initial and final binding energies or binding energy of the system.

$$ Q_\alpha = B(Z-2, A-4) + B(\alpha) - B(Z, A) \tag{4.2} $$

The released energy is divided between the $\alpha$ particle ($E_\alpha$) and daughter nucleus ($E_R$). From the momentum conservation law (relativistic) can be written:

$$ E_R = E_\alpha \frac{m_\alpha}{M(Z-2, A-4)} + \frac{E_\alpha^2}{2M(Z-2, A-4)c^2} \tag{4.3} $$

[1] There is also a small island of $\alpha$-emitters around A $\approx$ 100 just above the tin

Because the recoil mass is in the order of AxGeV and typical $\alpha$ energy is up to 10 MeV the second term in equation 4.3 is of the order of 0.1 keV and is usually neglected. For the recoil energy we obtained simplified form:

$$E_R = E_\alpha \frac{m(\alpha)}{M(Z-2, A-4)} \tag{4.4}$$

In the first approximation $Q_\alpha$ can be calculated from the measured kinetic energy of released $\alpha$ particle:

$$Q_\alpha = E_\alpha + E_R = E_\alpha \frac{M(Z, A)}{M(Z-2, A-4)} \tag{4.5}$$

The detected energy is measured after the alpha particle passed through the electron cloud around the nucleus. Therefore the initial energy is larger. The so called "screening correction" can be estimated by the equation:

$$\Delta Q_\alpha \approx 65.3 Z^{7/5} - 80 Z^{2/5} eV \tag{4.6}$$

Beside the energy measurements the very important information source obtained from a data analysis is the half-life of the studied $\alpha$ decay. When more decay modes are possible the decay constant $\lambda$ is given as a sum of partial decay constants:

$$\lambda = \lambda_\alpha + \lambda_{EC} + \lambda_{sf} \tag{4.7}$$

where

$$\lambda_\alpha = b_\alpha \lambda\,,\ \lambda_{EC} = b_{EC} \lambda\,,\ \lambda_{sf} = b_{sf} \lambda \tag{4.8}$$

and the coefficient $b_\alpha$, $b_{EC}$ and $b_{sf}$ are the branching rations for the various decay modes.

For even - even nuclei the ground state spins are zero and for these nuclei the $l = 0$ alpha particle emission is the most probable alpha transition and the decays to the excited states are (strongly) suppressed. For the odd-odd or even-odd nuclei the $l = 0$ alpha decay usually leads to some of the excited states. For example for the $^{249}$Cf the most intensive (82.2 %) alpha decay goes into $7^{th}$ excited state of $^{245}$Cm with an energy of $E_{exc}$ = 388.18 keV above the groundstate because of the same Nilsson configuration as the groundstate of $^{249}$Cf. In the case when several daughter levels are populated the alpha decay constant $\lambda$ is the sum of all possible transitions:

$$\lambda_\alpha = \sum_i \lambda_{\alpha i} \tag{4.9}$$

where

$$\lambda_{\alpha i} = b_{\alpha i} \lambda\,, \tag{4.10}$$

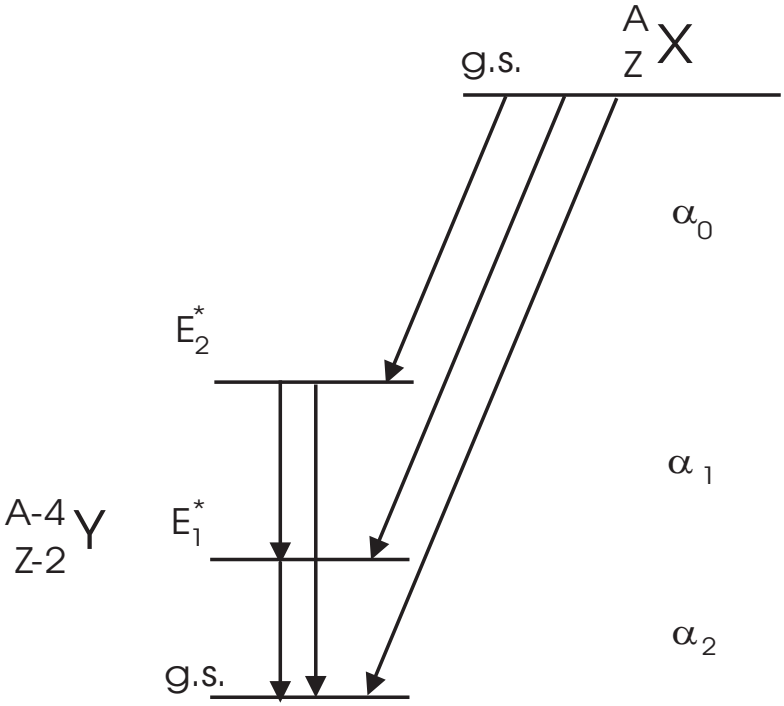


Figure 4.1: A schematic alpha decay scheme to different excited states in the daughter nucleus .

and $b_{\alpha i}$ are the relative intensities for these transitions.

The relation between the $\alpha$ energy $E_\alpha$ and the decay constant $\lambda$ is given by the Geiger-Nuttall law:

$$log\ \lambda = A\ logE_\alpha - B \tag{4.11}$$

where $A$ and $B$ are constants. To explain this law together with large variation in half-lives, Gamow and Condon and Gurney developed the theory of the quantum mechanical tunnelling of the $\alpha$-particle through the Coulomb barrier [Hod97] which results in the relation:

$$log\ \lambda = A - B\ \frac{Z}{\sqrt{E_\alpha}} \tag{4.12}$$

Several semiempirical approaches are used for the theoretical half-life value evaluation. In this work the formula developed by *Poenaru et al.* [Poe80] will be used:

$$log\ T = (B_1 + B_2 y + B_3 z + B_4 y^2 + B_6 z^2)\frac{K_s}{ln10} - 20.446 \tag{4.13}$$

where

$$K_s = 2.52956 Z_d \sqrt{\frac{A_d}{A Q_\alpha}} (\arccos\sqrt{x} - \sqrt{x(1-x)}) \tag{4.14}$$

and

$$x = 0.4253 Q_\alpha \frac{(1.5874 + A_d^{1/3})}{Z_d}. \tag{4.15}$$

The values $Z_d$ and $A_d$ are proton and mass numbers for the daughter nucleus ($A_d = A - 4$ and $Z_d = Z - 2$). The $y$ and $z$ express the relative distance of $N$ and $Z$ between the closest magic numbers plus one for the neutrons and protons $N_i$, $Z_i$ ($N_I < N \leq N_{i+1}$ and $Z_I < Z \leq Z_{i+1}$):

$$y = \frac{(N - N_i)}{(N_{i+1} - N_i)} \tag{4.16}$$

$$z = \frac{(Z - Z_i)}{(Z_{i+1} - Z_i)} \tag{4.17}$$

where

$$N_i = ...., 51, 83, 127, 185, .... \tag{4.18}$$

$$Z_i = ...., 51, 83, 115, 121, .... \tag{4.19}$$

The $Q_\alpha$ value can be calculated from the equation 4.5. Instead of parameterization coefficients $B_i$ used by *Poenaru et al.* a modified values recommended by *Rurarz* [Rur83] where used.

$$\begin{aligned} B_1 &= \ \ 0.988662 \\ B_2 &= \ \ 0.016314 \\ B_3 &= \ \ 0.020433 \\ B_4 &= \ \ 0.027896 \\ B_5 &= -0.003033 \\ B_6 &= -0.003033 \end{aligned} \tag{4.20}$$

The additional important characteristic of the $\alpha$ transition is the hindrance factor, defined as:

$$HF = \frac{T_\alpha(exp)}{T_\alpha(ee)} \tag{4.21}$$

where $T_\alpha(exp)$ is the measured partial half-live and $T_\alpha(ee)$ is calculated half-live for a given $\alpha$-transition from the simple one-body theory applied to even-even nuclides.

In general the hindrance factors for odd-mass nuclei may be divided into five classes:

a. The hindrance factor between 1 and 4 is for "favored" transition. In such decays the emitted $\alpha$ particle is assembled from two low lying pairs of nucleons in the parent nucleus, leaving the odd nucleon in its initial orbital.

b. The hindrance factor of 4-10 indicates a mixing or favorable overlap between the initial and final nuclear states involved in the transition.

c. The hindrance factor of 10-100 indicates that spin projections of initial and final states are parallel, but the wave function overlap is not favorable.

d. Factors of 100-1000 indicate transitions with a change in parity but with projections of initial and final states being parallel.

e. Factors $>$ 1000 indicate that the transition involves a parity change and initial and final spin projections are antiparallel. This requires substantial reorganization of the nucleon in the parent when the alpha particle is emitted.

An other possibility to define the hindrance factor is the ratio of reduced widths for g.s. - g.s. transition $\delta^2_{gs}$ and g.s. - excited state transition $\delta^2_{exc}$.

$$HF = \frac{\delta^2_{gs}}{\delta^2_{exc}} \tag{4.22}$$

As a $\delta^2_{gs}$ for even-odd nuclei the reduced width for neighbouring isotope can be taken. The reduced alpha decay width $\delta^2$ is given by equation:

$$\delta^2 = \frac{\lambda_\alpha h}{P} \tag{4.23}$$

where $h$ is Planck's constant, $P$ is barrier penetrability and $\lambda_\alpha$ is a partial alpha decay probability calculated from a half-live $T_{1/2}$:

$$\lambda_\alpha = \frac{b_\alpha \; ln \; 2}{T_{1/2}} \tag{4.24}$$

## 4.2 Gamma Ray Decay

Gamma decay occurs when a nucleus in excited state goes to the ground-state by emission of the photon. Schematically it can be written as:

$${}^A_Z X^*_N \rightarrow {}^A_Z X_N + \gamma \tag{4.25}$$

There is no change in $Z$ or $A$ in this type of decay, only the energy is released. The energy of the gamma rays can vary from 10 keV to a few MeV. Sometimes, when is necessary to release a $\gamma$ ray with high multipolarity, the nucleus can survive

in excited state rather long time. This kind of excited state is called isomeric state. This can decays, following the usual law of radioactive decay, either to the ground state by an isomeric or internal transition (see the section 4.3), that is emitting a $\gamma$ ray or a converted electron, or by $\alpha$- or $\beta$ decay.

Because each state is defined by a spin and parity the gamma transition can be classified by the angular momentum and parity change. The transitions carrying angular momentum $l$ is named as $2^l$ transition. For $l$=1 the name dipole transition is used, $l$=2 is called quadrupole transition, $l$=3 is octupole transition, etc. Each multipole transition may have a character of the electric transition with the parity $(-1)^l$ and magnetic transition with the parity $(-1)^{l+1}$. The name electric is connected with the charge distribution and magnetic with the current density. For the parities of initial and final state following selection rules are applied:

a. $\underline{\pi_i = \pi_f}$ for even radiation, i.e. even electric and odd magnetic multipoles

b. $\underline{\pi_i = -\pi_f}$ for odd radiation, i.e. odd electric and even magnetic multipoles

If the spins of initial state and final state are $J_i$ and $J_f$ the angular momentum $l$ can range from $|J_i - J_f|$ and $|J_i + J_f|$. The minimum angular momentum that can be carried by a gamma ray is one unit. The transition between two states of spin zero are forbidden (except of internal conversion - see below).

The different classes of gamma emission have different probabilities to occur. This probability can be estimated using the following Weisskopf equations [Lov00]:

$$\lambda_{electric} = 10^{21} \frac{4.4(l+1)}{l[(2l+1)!!]^2} \left(\frac{3}{l+3}\right)^2 \left(\frac{E_\gamma}{197}\right)^{2l+1} R^{2l} \; sec^{-1} \tag{4.26}$$

$$\lambda_{magnetic} = 10^{21} \frac{1.9(l+1)}{l[(2l+1)!!]^2} \left(\frac{3}{l+3}\right)^2 \left(\frac{E_\gamma}{197}\right)^{2l+1} R^{2l-2} \; sec^{-1} \tag{4.27}$$

$l$ is the angular momentum carried away by the photon, $E_\gamma$ is the transition energy in MeV and $R$ is the nuclear radius in fm and is calculated as $R = 1.25\ A^{1/3}$. These equations are usually reliable to within a factor of ten and represent maximum values for the transition probabilities.

Using these formulas one can show that probability for electric transitions are $\sim$ 100 times larger in comparison with magnetic transitions of the same multipolarity and energy. This difference depends only on nuclear radius.

$$t_{magnetic}/t_{electric} \approx 2.32R^2 = 2.9\ A^{2/3} \tag{4.28}$$

One can also see that for the transition of the same type and multipolarity the probability rapidly drops down with the decrease of energy. For the E1 transition change of energy $E_\gamma$ from 1 MeV to 0.1 MeV leads to decrease of transition probability $\lambda$ by three orders. Even larger effect is the change of transition multipolarity. The difference of transition probability $\lambda$ for E1 and E2 transitions with $E_\gamma$=1 MeV energy is around 5 orders of magnitude.

Generally speaking, large spin difference and low energy hinder transition probability. This is also an explanation for the existence of "islands of isomerism".

## 4.3 Internal conversion

Another possibility for a nucleus to deexcite is an *internal conversion*. This process is competitive to gamma ray emission and occurs when an excited nucleus interacts electromagnetically with an orbital electron. The excitation energy is transferred to the electron which is than ejected. The energy of this electron $E_e$ is a difference between the energy of de-excitation $\Delta E$ and binding energy of the electron in atomic shell $B_e$.

$$E_e = \Delta E - B_e \tag{4.29}$$

The vacancy left in the atomic shell after the emission of a conversion electron is filled by one from a higher shell, and the difference in energy between the two shells is released in the form of a X-ray or by radiation less transition e.g. Auger electron emission.

The competition of gamma ray emission and internal conversion process can be described by the *internal conversion coefficient* $\alpha$ which is defined as ratio of number of internal conversion decays and gamma ray decays. It can be written as a ratio of decay probabilities $\lambda$:

$$\alpha = \frac{\lambda_{IC}}{\lambda_\gamma} \tag{4.30}$$

In general, the internal conversion coefficient is higher for magnetic transitions and increases with decreasing energy, increasing Z and increasing angular momentum change in the decay. The values for internal conversion coefficient for the elements up to the Rutherfordium can be found for example in *Rösel et al.* [Rös78]. Calculation for heavier elements up to the element 120 can be found in *Dragoun et al.* [Dra00].

# Chapter 5

# Experiments

## 5.1 Reaction $^{40}$Ar + $^{209}$Bi

Two experiments aimed for detailed spectroscopy measurements of $^{246}$Md and $^{247}$Md were realized in last years at SHIP.

The first one was performed in September 2001. In this experiment compound target - $BiF_3$ - was used, to avoid a problem with a low melting point of pure bismuth target. The target thickness was 430 $\mu$g/cm$^2$ and was evaporated on the carbon backing with a thickness of 40 $\mu$g/cm$^2$. The chosen energy were $E_{beam}$ = 4.93 AMeV ($E_{exc}$ = 35.7 MeV) and $E_{beam}$ = 5.08 AMeV ($E_{exc}$ = 40.0 MeV), however the detailed off-line analysis shows the problem with beam energy measurements. Because the experiment was running with shifted beam energy, compared to the planed value, the mixture of isotopes $^{246}$Md and $^{247}$Md was produced. Because it was impossible to make any detail spectroscopy analysis, due to the similar half-life of these isotopes and impossibility to distinguish them, an other experiment was necessary. Some details of this experiment and the preliminary results of the data analysis can be found in [Ant03].

The second experiments was running from 7th of April 2003 until 11th of April 2003 using complete fusion reaction of $^{40}$Ar + $^{209}$Bi at two beam energies, $E_{lab}$ = 4.67 AMeV and $E_{lab}$ = 4.95 AMeV. These energies were chosen according to the predicted maximum production cross-section for 2n and 3n channel (see later). The experiment was performed at the velocity filter SHIP at GSI, Darmstadt using an intense $^{40}$Ar beam, with a beam intensity up to 8x10$^{12}$ ions/s ($\approx$ 1.33 p$\mu$A), delivered by the UNILAC accelerator. The detection and analysis technique described in previous chapters was employed. The used target wheel consisted from 450 $\mu$g/cm$^2$ of $^{209}$Bi evaporated on 40 $\mu$g/cm$^2$ carbon backing and covered by 10 $\mu$g/cm$^2$ carbon layer to avoid a sputtering of the target material and increase an emissivity of the target.

Results of calculations using code HIVAP together with the used beam energies for this reaction are shown in figure 5.1. The chosen beam energies were corrected to energy losses in 2/3 of the target using computer code SRIM [ZiB03]. Two energies were chosen to avoid an ambiguities in estimating decay properties that

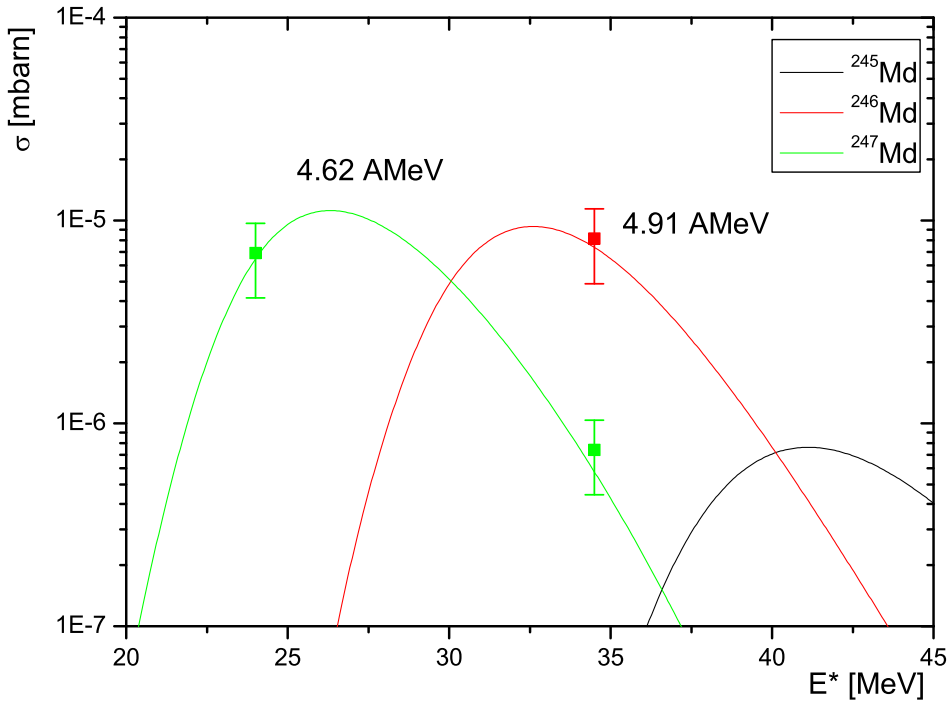


Figure 5.1: The production cross-section for Mendelevium isotopes corresponding to 2n, 3n and 4n channels in the reaction of $^{40}$Ar + $^{209}$Bi. The measured cross-sections for the applied beam energies are marked as well (see text for more details). The beam energies were corrected for energy losses in 2/3 of the target. The statistical and systematic uncertainty were taken into an account.

could arise from similar production cross-section for both isotopes. For the beam energy of $E_{beam}$ = 4.62 AMeV ($E_{exc}$ = 24.7 MeV) the only expected product of complete fusion reaction was $^{247}$Md. The expected reaction cross-section for this beam energy is 6 nb. For the beam energy $E_{beam}$ = 4.95 AMeV ($E_{exc}$ = 34.3 MeV) the mixture of isotopes $^{246}$Md and $^{247}$Md was expected with the ratio 12:1 in favor of $^{246}$Md. The calculated reaction cross-sections at the excitation energy of $E_{exc}$ = 34.3 MeV are 7 nb for $^{246}$Md and 560 pb for $^{247}$Md. It should be mentioned here that the target thickness may lead to broadening of the cross-section functions and the measured production ratios may differ slightly from calculated values. Because of large number of semi-empirical and empirical parameters used as an input of the HIVAP code the difference of the measured cross-sections up to the half of the order are usually expected.

## 5.2 Reaction $^{48}$Ca + $^{209}$Bi

The experiment aimed at the production of $^{255}$Lr, $^{254}$Lr and their daughter products was performed from 24th of February 2003 until 11th of March 2003. This experiment was performed parasitic to an experiment of the chem. group aimed to investigate the chemical properties of the element 112. Our irradiations were performed in breaks of this experiment and the "beam on target time" was only around 5 % of the total beam time. The complete fusion reaction of $^{48}$Ca + $^{209}$Bi at two beam energies - $E_{beam}$ = 4.69 AMeV and $E_{beam}$ = 4.81 AMeV was used. These energies were chosen in respect to old measurements of the excitation function for this reaction [Gag89] (see figure 5.2). The beam intensity during the measurement was up to ≈ 410 pnA.

The backward detectors were not used for the data analysis due to their malfunction and the system of TOF measurements was changed as well. Due to a technical problem the signal from the silicon detector was used as a "stop" signal instead of the signal from TOF detectors. All other detection and analysis techniques were used as usual on experiments performed at SHIP and as was described already in chapter 3.

The used target consists from 450 $\mu$g/cm$^2$ of $^{209}$Bi evaporated on 40 $\mu$g/cm$^2$ carbon backing and covered by 10 $\mu$g/cm$^2$ carbon layer. These targets were mounted on the target wheel with a diameter of 310 mm as was described already in the section 3.2.

Based on the previous excitation function measurements of Lawrencium [Gag89] the calculation using HIVAP code [ReS81],[ReS92] were performed (see figure 5.2) for production estimation of studied isotopes and contribution of unwanted reaction channels. As was already mentioned, the HIVAP code includes many empirical and semi-empirical parameters and the difference between experimental values and calculation may differ usually up to the half of the order. For the cross-section experimental values themselves the systematic uncertainties up to 60% have to be also taken into account. The reasons are usually the uncertainties of the separator efficiency, beam current measurements etc. The statistical uncertainties of the reaction cross-section values itself can be neglected for the measurements discussed in this work, due to the high statistics.

The experimental points of the excitation energies in figure 5.2 were corrected for energy losses [ZiB03] and are given for 2/3 of the target. For spectroscopy studies of $^{255}$Lr and $^{254}$Lr the excitation energies of $E_{exc}$=25.4 MeV and $E_{exc}$=30.6 MeV were used. The expected ratio of reaction products for $E_{exc}$ = 25.4 MeV is $N_{3n}/N_{2n} \approx 1/60$. For the excitation energy of $E_{exc}$ = 30.6 MeV the ratio of $N_{3n}/N_{2n} \approx 1/10$ was expected. Based on the results presented below the evaluated cross-sections are $\sigma \approx$ 159 nb for the $E_{exc}$=25.4 MeV ($E_{lab}$=4.69 AMeV) and $\sigma \approx$ 22.6 nb for the $E_{exc}$=30.6 MeV ($E_{lab}$=4.81 AMeV). These values are in agreement with previous measurements and with the HIVAP calculations (see figure 5.2).

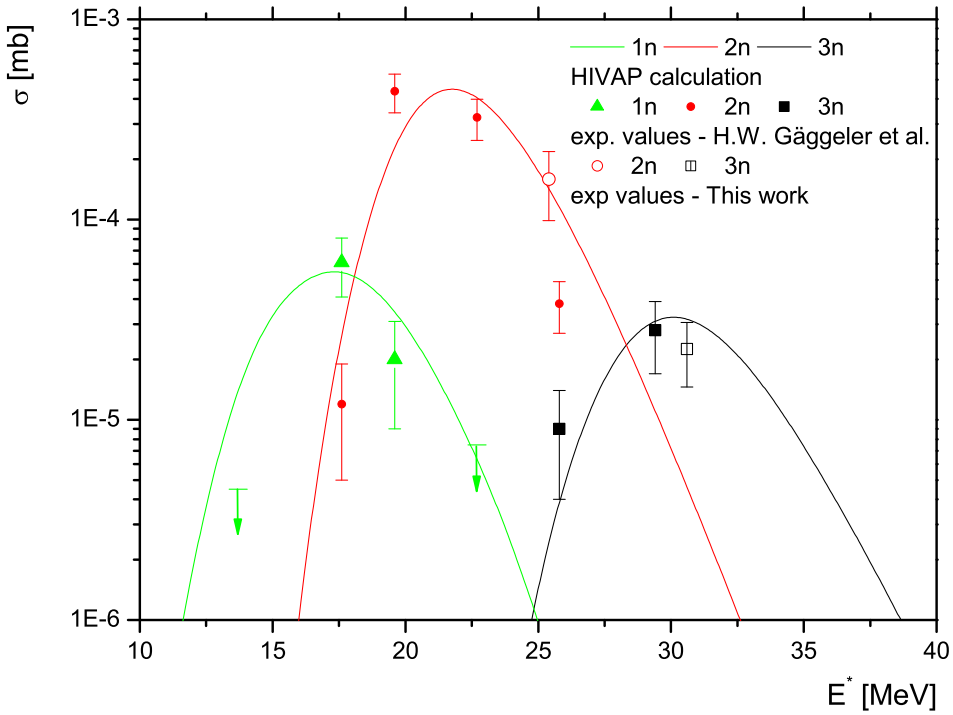


Figure 5.2: The cross-section function for the Lawrencium isotopes produced by a complete fusion reaction of $^{48}$Ca + $^{209}$Bi corresponding to the 1n, 2n and 3n channels. The solid line represents the results of HIVAP calculation. The reaction cross-section points measured by *H.W. Gäggeler et al.* [Gag89] are shown with solid symbols. Two points measured at the beam energies discussed in this work are shown with open symbols. The errors include both - statistical and systematic - uncertainties, however for the measurements discussed in this work a statistical uncertainties itself may be neglected due to a high number of counts. Excitation energies are corrected to energy loss in the target and are equivalent to the beam energy in 2/3 of the target.

## 5.3 Calibrations

The techniques of calibrations used for this analysis were described in detail in section 3.4. The following remarks to calibrations of experiments described above point out the most important features:

a. *The gamma calibrations* of the clover detector, as was mentioned already, were done using a $^{152}$Eu and a $^{133}$Ba sources. This calibration was repeated and checked several times during the experiments to test the detector

stability.

b. *The alpha calibration* of the stop detector, in the reaction of $^{40}$Ar + $^{209}$Bi aimed to production of $^{247}$Md and $^{246}$Md, was done using two calibration reactions - before and after the measurement. Two calibration measurements were necessary due to the calibration shift during the measurement.

   1. For the measurements at the beam energy of $E_{beam}$ = 4.67 AMeV the reactions $^{40}$Ar + $^{169}$Tm and $^{40}$Ar + $^{176}$Yb were chosen. The used alpha lines are shown in table 5.1 Resulting resolution for the $^{211}$Po peak with the energy of $E_{^{211}Po}$ = 7450 keV - which, as the transfer product, is typical for the measurements using Bi targets - was $\Delta E_{FWHM}$ = 18.8 keV. The energy difference for this peak compared to reference value [FiS96] was $\approx$ 1 keV.
   2. For the measurements at the beam energy 4.95 AMeV the separator settings were optimized for transfer products and these nuclei were used for calibrations. The used alpha lines are shown in table 5.2. Resulting resolution for the $^{211}$Po peak of $E_{^{211}Po}$ = 7450 keV in this case was $\Delta E_{FWHM}$ = 25.8 keV and the energy difference for this peak compared to the reference value [FiS96] was $\approx$ 5 keV.

   All $\alpha$ decay energies used for both calibrations are given below (see tables 5.1 and 5.2).

| **Isotope** | **$E_\alpha$ [keV]** | **Isotope** | **$E_\alpha$ [keV]** |
|---|---|---|---|
| $^{208}$Rn | 6143 ± 21 | $^{205}$Fr | 6915 ± 4 |
| $^{212}$Rn | 6264 ± 3 | $^{207}$Rn | 6131 ± 4 |
| $^{201}$At | 6344 ± 2 | $^{211}$Ra | 6910 ± 5 |
| $^{204}$Rn | 6418 ± 25 | $^{210}$Ra | 7019 ± 5 |
| $^{206}$Fr | 6790 ± 4 | | |

Table 5.1: Alpha lines used for calibration of the first measurement - the reaction of $^{40}$Ar + $^{209}$Bi - at the beam energy of $E_{beam}$ = 4.67 AMeV. The isotopes were produced by reactions $^{40}$Ar + $^{169}$Tm and $^{40}$Ar + $^{176}$Yb. All energies are taken from the *Table of isotopes* [FiS96]

c. *The alpha calibrations*, in the reaction of $^{48}$Ca + $^{209}$Bi aimed to production of $^{254}$Lr and $^{255}$Lr, were done using a reaction of $^{48}$Ca + $^{170}$Er at the beam energy of $E_{beam}$ = 4.47 AMeV. The $\alpha$ lines used for the energy calibration are shown in table 5.3. The stability of the detector calibration was later

| **Isotope** | **$E_\alpha$ [keV]** | **Isotope** | **$E_\alpha$ [keV]** |
|---|---|---|---|
| $^{212}$Rn | 6264 ± 3 | $^{212}$At | 7679 ± 6 |
| $^{213}$Fr | 6775 ± 17 | $^{212m}$At | 7900 ± 6 |
| $^{211}$Po | 7450 ± 5 | $^{213}$Rn | 8088 ± 8 |

Table 5.2: Alpha lines used for calibration of the second measurement - the reaction of $^{40}$Ar + $^{209}$Bi - at the beam energy of $E_{beam}$ = 4.95 AMeV. The isotopes are transfer reaction products created in the $^{40}$Ar + $^{209}$Bi reaction. These nuclei were collected during the short time when SHIP settings were optimized for their separation. All energies are taken from the *Table of isotopes* [FiS96]

| **Isotope** | **$E_\alpha$ [keV]** | **Isotope** | **$E_\alpha$ [keV]** |
|---|---|---|---|
| $^{209}$At | 5647 ± 2 | $^{207}$Rn | 6131 ± 4 |
| $^{209}$Rn | 6039 ± 3 | $^{212}$Ra | 6899.2 ± 1.7 |
| $^{208}$Rn | 6143.8 ± 2.1 | $^{214}$Ra | 7137 ± 3 |
| $^{212}$Fr | 6261.9 ± 2.1 | $^{213}$Rn | 8088 ± 8 |
| $^{213}$Ra | 6731 ± 3 | $^{214}$Fr | 8427 ± 4 |
| $^{213}$Fr | 6775.0 ± 1.7 | | |

Table 5.3: Alpha lines used for $\alpha$ calibrations of detector setup for the measurements $^{48}$Ca +$^{209}$Bi. The isotopes were produced by the reaction $^{48}$Ca + $^{170}$Er at the beam energy of $E_{beam}$ = 4.47 AMeV. All energies were taken from the *Table of isotopes* [FiS96]

checked using an external $\alpha$ source containing a mixture of three $\alpha$ emitters - $^{241}$Am, $^{239}$Pu and $^{244}$Cm.

d. Because of technical problems *the backward detectors* were not used in these experiments and therefore their calibration was not performed.

e. For *the high energy region*, calibration based on measurements of $^{252}$Cf fission fragments was used. This calibration was performed in a preceding experiment. The energies of the fission fragments were corrected for the PHD [Wil71].

# Chapter 6

# Results and Discussion

## 6.1 Reaction $^{40}$Ar + $^{209}$Bi

Although $^{246}$Md and $^{247}$Md isotopes have been known for a longer time, no detailed spectroscopic investigation was performed so far and only some rough information about these nuclei were known.

The first successful synthesis of $^{247}$Md was reported in the year 1981 [Mun81b]. Only five events with energy of $E_\alpha = 8428 \pm 25$ keV and half-life of $T_{1/2} = 2.9^{+1.7}_{-1.2}$ s were measured at that time. Two of them were correlated with a correlation time 6 s and 17 s to events with the energy of $E_\alpha = 7889 \pm 25$ keV which were attributed to the decay of $^{243}$Es. Further investigation was performed in the year 1993 [Hof94]. The known alpha activity for $^{247}$Md was confirmed. At a beam energy of $E_{beam} = 4.78$ AMeV two fission events with half-life $T_{SF} = 0.23^{+0.19}_{-0.12}$ s were detected and were tentatively assigned to spontaneous fission of isomeric $1/2^-$ state of $^{247}$Md.

In the same experiment, at beam energies of $E_{beam} = 4.93$ AMeV and $E_{beam} = 5.12$ AMeV, two energy groups of alpha activity were measured - an energy of $E_\alpha = 8740 \pm 20$ keV and an energy range of $E_\alpha = 8500$ - 8560 keV [Nin96]. The measured half-life was $T_{1/2\alpha} \approx 1 \pm 0.4$ s. This activity was attributed to a new isotope $^{246}$Md. Besides these alpha decays also ten fission events with a half-life of 1 second were observed. These fissions were ascribed to $^{246}$Fm. The fission branch obtained for this isotope $b_{sf} = 0.15 \pm 0.05$ was significantly higher than known value $b_{sf} = 0.045 \pm 0.013$. This difference was explained by an EC-delayed fission (ECDF) of $^{246}$Md. A probability of $p_{ECDF} \approx 0.065$ was estimated.

### 6.1.1 Decay chain of $^{247}$Md

During the time of 35 hours of irradiation a total beam dose of 7.76 x $10^{17}$ ions was collected at a beam energy of $E_{beam} = 4.67$ AMeV. Altogether 24 fission events were registered in pause. The alpha spectrum in the energy region, from 7000 keV to 9000 keV, is shown in figure 6.1 a) where the most intensive $\alpha$ lines are marked. In figure 6.1 b) the $\alpha$ events correlated to the ER in defined energy and TOF

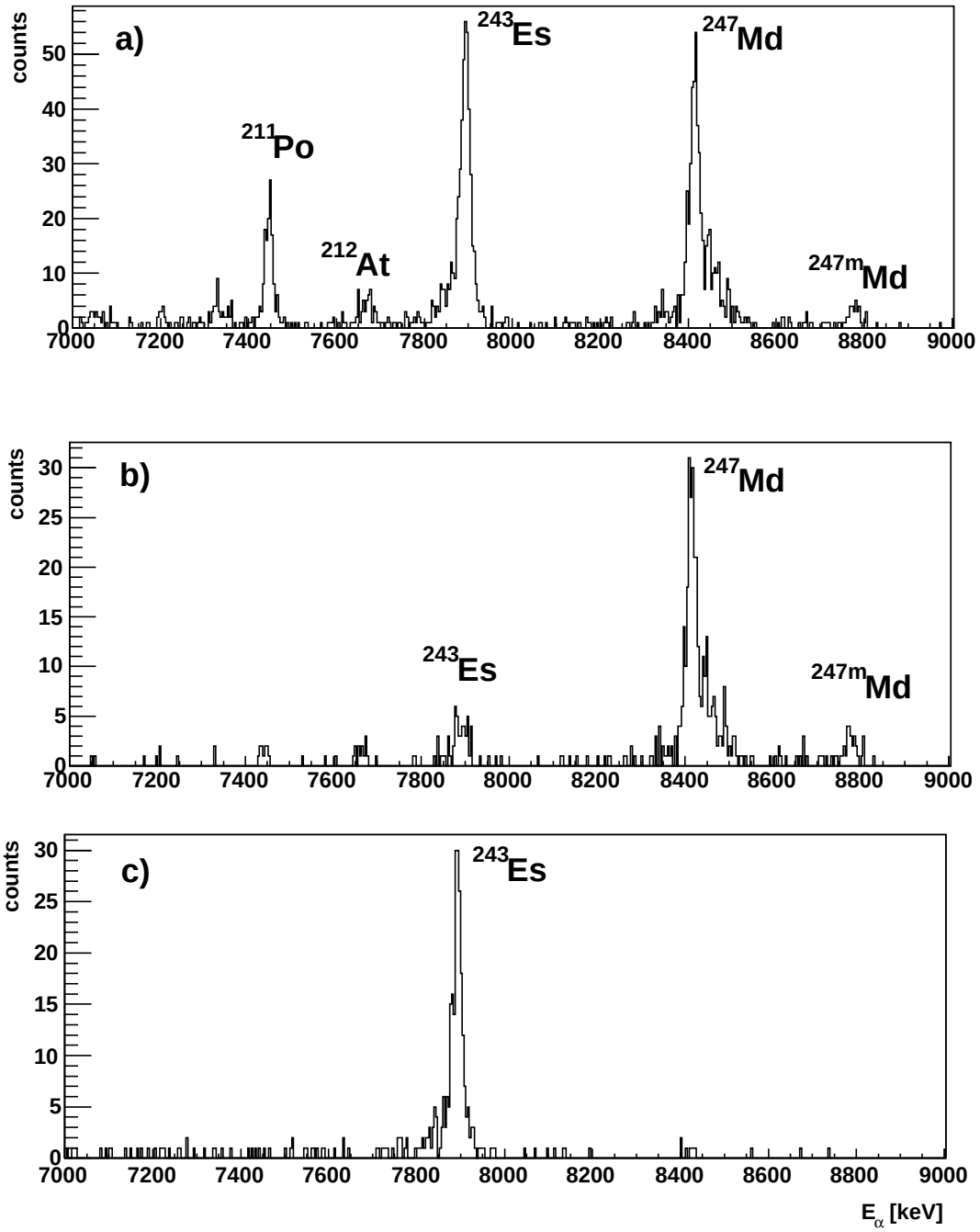


Figure 6.1: a) Alpha spectrum in the reaction of $^{40}$Ar + $^{209}$Bi collected in pause. The marked, most intense peaks belong to reaction products $^{243}$Es, $^{247}$Md and $^{247m}$Md and to transfer products $^{211}$Po and $^{212}$At b) Spectrum of $\alpha$ decays correlated to implanted nuclei. The $\alpha$-events were expected in anti-coincidence with TOF system. c) Spectrum of $\alpha$-events is correlated to the $\alpha$-events of $^{247}$Md.

windows are shown. The correlation time was chosen to $\Delta t = 2.2$ s and the position window to $\Delta x = \pm 0.25$ mm. The most intense peaks arise from $^{247}$Md and from its daughter isotope $^{243}$Es. The rest of the spectra is created by unwanted and random correlation with the background (e.g. the correlations with transfer products).

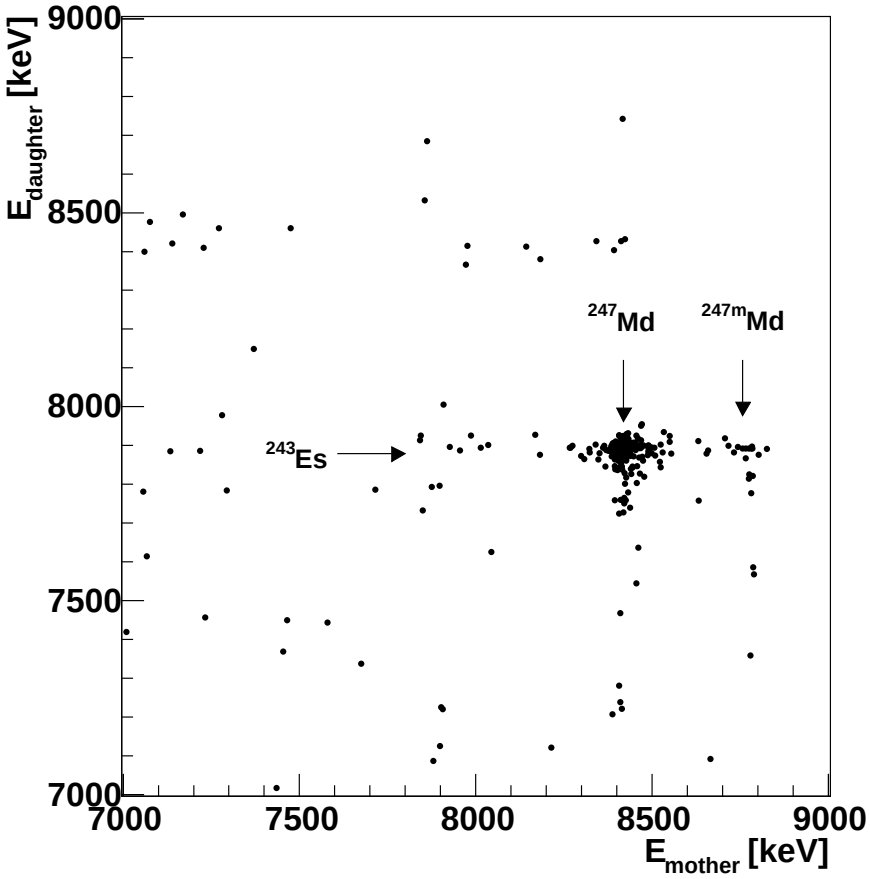


Figure 6.2: The spectrum with observed $\alpha$ - $\alpha$ correlations was obtained using a position window $\Delta x = \pm 0.25$ mm, correlation time of $\Delta t = 120$ seconds and requirement that at least one alpha particle from the correlated pair must be in pause. Two $\alpha$ - $\alpha$ groups with mother energies around 8416 keV and 8780 keV are visible. A weak group of $\alpha$ - $\alpha$ correlations with a mother energy of 8416 keV and daughter energy of 7860 keV indicates a possibility of decay to the excited level of $^{243}$Es.

Based on the measured time distribution of ER-SF correlations the half-life for spontaneous fission activity was calculated to be $T_{1/2} = 0.278 \pm 0.100$ s and previously tentatively reported isomeric fission activity [Hof94] could be confirmed.

The previously measured decay properties of $^{247}$Md were confirmed in this experiment with a value of $E_\alpha = 8416 \pm 10$ keV. The half-life of $^{247}$Md measured

using recoil-alpha correlation technique was determined to 1.3 ± 0.1 s. The calculated half-life using the Poenaru formula (4.13) in case of 8416 keV $\alpha$ decay is $T_\alpha \approx 1.14$ s. The hindrance factor of this transition is close to one what indicates equal spin and parity states for the ground-state of the mother nucleus ($^{247}$Md) and the final state of this decay in daughter nucleus ($^{243}$Es).

Beside the 8416 keV $\alpha$-line a previously unknown alpha activity at the energy of $E_\alpha = 8783 \pm 40$ keV with the half-life of $T_{1/2} = 0.257 \pm 0.033$ s was detected. According to the similar half-life this activity was attributed to the decay from the same state as the detected spontaneous fission. The alpha decay branching ratio for isomeric state of $^{247}$Md was evaluated to be $b_\alpha = 76.8 \pm 4.5$ %.

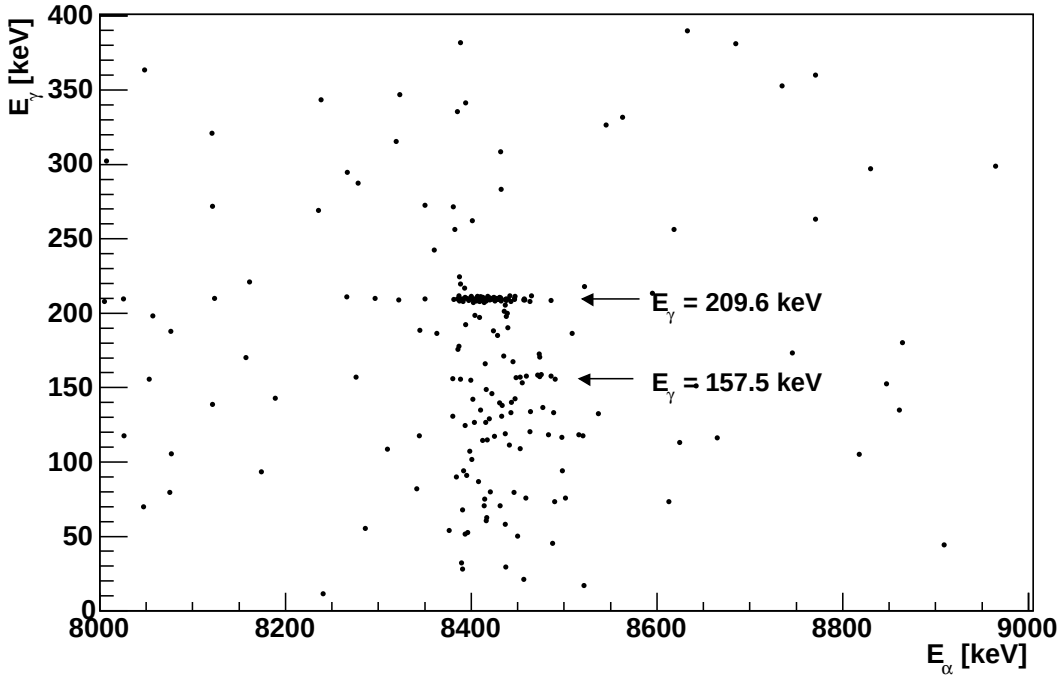


Figure 6.3: The $\alpha$ - $\gamma$ coincidence spectrum collected for the events in anti-coincidence with TOF system. Two coincidence groups assigned to the $\alpha$ decay of $^{247}$Md and subsequent $\gamma$ de-excitation in $^{243}$Es are shown.

There is an indication of g.s. - g.s. transition represented by a small group around the energy of $E_\alpha = 8670 \pm 20$ keV but this assignment is not unambiguous and needs to be checked in the future because of small statistic. The same is the situation for the small "bump" at the energy of $E_\alpha = 8330$ keV. This can be a decay to a different Nilsson level but because of missing gamma coincidences and low statistics one can assign this line only tentatively as an $\alpha$ decay of $^{247}$Md.

In the scatter plot of $\alpha$ - $\gamma$ coincidences (see figure 6.3) two $\alpha$ - $\gamma$ groups are visible and, similarly, in figure 6.4 two $\gamma$ lines with energies $E_\gamma = 209.6 \pm 0.5$ keV

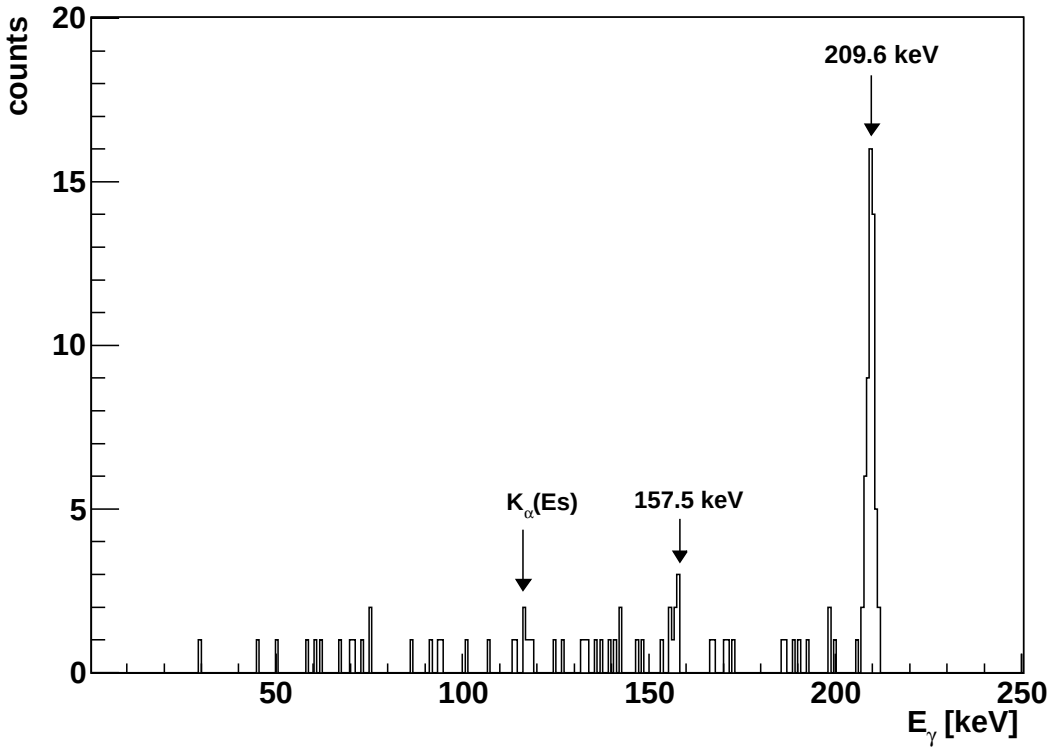


Figure 6.4: The $\gamma$ spectrum measured in coincidence with the $\alpha$ particles of energy from 8380 keV to 8900 keV. The two lines of energy $E_\gamma$ = 209.6 keV and $E_\gamma$ = 157.5 keV a clearly visible.

and $E_\gamma = 157.5 \pm 0.5$ keV can be identified in coincidence with $\alpha$-particles in energy range from 8380 to 8800 keV. These lines can be assigned to the de-excitation from the level at the energy of 209.6 keV populated by $\alpha$ decay of $^{247}$Md. The energy structure of the pause $\alpha$ spectrum in figure 6.1 a) in the energy range of 8440 - 8500 keV suggest an energy summing with the K- conversion electrons. The $\alpha$ - $\gamma$ coincidences with $\gamma$ line of $E_\gamma$ = 157.5 keV seems to be influenced by energy summing with conversion electrons and shows broader distribution of coincident $\alpha$ decays (see figure 6.3) compare to the distribution of the $\alpha$ decays in coincidence with $E_\gamma$ = 209.6 keV $\gamma$ transitions. Therefore $\gamma$ line of $E_\gamma$ = 209.6 keV is ascribed to the decay into the ground state of $^{243}$Es and the $\gamma$ line of $E_\gamma$ = 157.5 keV is assigned to a transition into an excited level with the energy of $E_{exc}$ = (209.6 - 157.5) keV = 52.1 keV. It should be mentioned here that for an one event $\alpha$ - $\gamma$ - $\gamma$ coincidence was detected, with an $E_\alpha$ = 8364 keV, $E_{\gamma 1}$ = 156.3 keV and $E_{\gamma 2}$ = 53.8 keV. This supports the previous conclusion, however also the possibility of the random coincidence can not be excluded.

The measured upper limit of K conversion coefficient, $\alpha_K$, for $\gamma$ line of energy

| | $\alpha_K$ | $\alpha_{L\ tot}$ |
|---|---|---|
| E1 | 0.0787 | 0.020 |
| E2 | 0.131 | 0.861 |
| E3 | 0.239 | 12.10 |
| E4 | 0.425 | 107.0 |
| M1 | 4.43 | 1.032 |
| M2 | 12.6 | 6.853 |
| M3 | 20.9 | 52.01 |
| M3 | 31.3 | 422.7 |

Table 6.1: Calculated internal conversion coefficients of Einsteinium [Rös78] for the different type of transitions with energy of $E_\gamma = 210$ keV. For the $\alpha_L$ coefficient a total value is given.

$E_\gamma = 209.6$ keV obtained from the ratio of X-ray and gamma intensities is $\alpha_K < 0.13$. The upper limits of K- and L- conversion coefficient, $\alpha_{L\ tot}$, measured using $\alpha$ particles energy summing are $\alpha_K < 0.3$, $\alpha_L < 0.1$. Based on comparison with calculated values (see table 6.1) [Rös78] the transition 209.6 keV was assigned as E1, but possibility of E2 transition cannot be completely excluded either.

For the evaluation of the reaction cross-section the relevant alpha and fission activity in pause was used. The influence of transfer reaction products - mainly the $\alpha$ decay of the isotope $^{214}$Fr - was not significant. Only for 6 alpha decays the correlation with the half-life typical for the $^{214}$Fr were found. Beside this 555 events were assigned to the $\alpha$ decay of $^{247}$Md in the energy region from 8300 keV to 8650 keV in pause and additionally 63 events around the energy of $E_\alpha = 8700$ keV. Assuming the separator efficiency of 30 % the cross-section was evaluated to the value of $6.9 \pm 2.7$ nbarn[1].

The recommended ground state for $^{247}$Md is $1/2^-[521]$ (see table 6.2) [Cwi94] however from the systematics one can expect $7/2^-[514]$ state [Hes01],[FiS96]. One needs to take into an account also low hindrance factor for $\alpha$ decay of 8416 keV, what indicates the same Nilsson level for ground state of $^{247}$Md and corresponding daughter level in $^{243}$Es. Since $1/2^-[521]$ state in $^{243}$Es is not populated by this $\alpha$ decay (see discussion below) assignment of $1/2^-[521]$ Nilsson level as a ground-state of $^{247}$Md is not anticipated either. Therefore the value of $7/2^-[514]$ will be used for a ground state of $^{247}$Md (see figure 6.5).

The ground state for the $^{243}$Es is proposed, based on calculation, as $7/2^+[633]$

[1]The both - statistical and systematic uncertainties - were included. The statistical uncertainty is expected usually up to the 5 % for this reaction. Systematic uncertainties may change all cross-section values up to the 60 %.

Nilsson level and $3/2^-[521]$ is predicted with the excitation energy of $E^{th}_{exc} = 270$ keV (see table 6.2) [Cwi94]. But based on the EC decay measurements of $^{251}$Fm the ground-state in the isotope $^{251}$Es is assigned to $3/2^-[521]$ Nilsson level while $7/2^+[633]$ is located at $E_{exc} = 8.3$ keV [Ahm00]. Theory predicts more-less constant place for $3/2^-[521]$ in the energy range of $E^{th}_{exc} = 270$ - 300 keV for odd-mass Es isotopes (from $^{243}$Es to $^{257}$Es). Therefore for isotopes discussed in this work, e.g. $^{243}$Es, one can expect similar behavior of experimental values i.e. a rather constant energy difference of the $7/2^+[633]$ state and $3/2^-[521]$ levels around $\Delta E \approx 0$ keV. This means that the $3/2^-[521]$ level may also be the ground-state in at least some lighter odd mass Es - isotopes while $7/2^+[633]$ may appear at low excitation energy. In case of small energy difference - less then 10 keV - between these levels one will not see any distortion in alpha spectrum and then it is not possible to decide which one from these two states is ground state of $^{243}$Es.

The 209.6 keV transition can be attributed as a transition between $7/2^-[514]$ - populated by 8416 keV $\alpha$ decay of $^{247}$Md - and $7/2^+[633]$ Nilsson levels. Although a possibility of E2 transition cannot be completely excluded, one should think about the possibility of the transition between the $7/2^-[514]$ and $3/2^-[521]$ level. Based on predicted values of conversion coefficients (see table 6.2) and measured conversion coefficient upper limits for 209.6 keV $\gamma$ line, the possibility of E3, E4 and all magnetic transitions are ruled out. The possibility that $1/2^-[521]$ state, expected by theory at 450 keV, as level populated by 8416 keV $\alpha$ decay is therefore excluded because it requires de-excitation by E3 transition to $7/2^+[633]$ or M1 transition to $3/2^-[521]$.

Considering the theoretical calculation [Cwi94] (see table 6.2) one can expect assignment of the level at $E_{exc} = 52.1$ keV to $5/2^+[642]$ Nilsson level. Instead of this the assignment to $9/2^+[624]$ is proposed in this work. This is based on knowledge that in deformed nuclei a "rotational band" is built up on each Nilsson -level (bandhead), leading to a sequence e.g. $7/2^+$, $9/2^+$, $11/2^+$ etc. or $1/2^-$, $3/2^-$, $5/2^-$ etc. The transition $9/2^+[624] \rightarrow 7/2^+[633]$ is M1 and thus is highly converted [Rös78]. An energy summing with conversion electrons is a reason for small shift of the $\alpha$ - $\gamma$ group for $E_\gamma = 157.5$ keV in figure 6.3 to the higher energy for this transition compare to the group with $E_\gamma = 209.6$ keV. Due to a low

| **Isotope** | $\mathbf{E^*_{th}}$ **[MeV]** | | | | |
|---|---|---|---|---|---|
| $^{247}$Md | 0 ($1/2^-$) | 0.28 ($7/2^-$) | 0.4 ($7/2^+$) | 0.71 ($9/2^+$) | 0.82 ($3/2^-$) |
| $^{243}$Es | 0 ($7/2^+$) | 0.27 ($3/2^-$) | 0.45 ($1/2^-$) | 0.67 ($7/2^-$) | 0.93 ($5/2^+$) |

Table 6.2: Results of theoretical calculations of the energies, spins and parities of $^{247}$Md and $^{243}$Es excited level.

statistic for a gamma line of energy $E_\gamma = 157.5$ keV is not possible to recognize the character of this transition, however E1 character resulting from a proposed decay scheme, proposed below, is not in contradiction with a measurement.

The hindrance factor of 8783 ± 40 keV $\alpha$ decay from isomeric state was $\approx 3$. This indicates the possibility of the $\alpha$ transition $1/2^-[521] \rightarrow 1/2^-[521]$. There is no indication of any $\gamma$ line in coincidence with $\alpha$ transition from isomeric state of $^{247m}$Md and position of proposed levels $1/2^-[521]$ in $^{243}$Es and $1/2^-[521]$ level in $^{247}$Md are hard to locate.

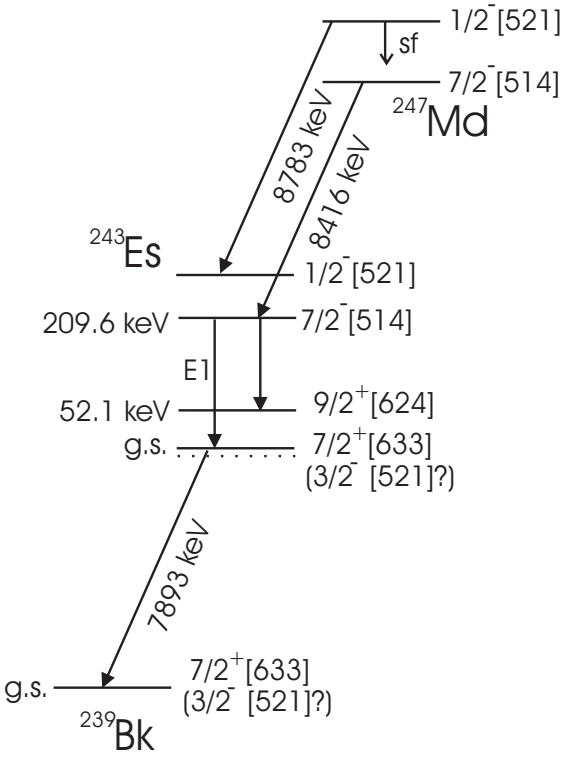


Figure 6.5: Decay scheme of $^{247}$Md and $^{243}$Es drawn on the basis of the measured $\alpha$ decay energies, $\gamma$ transition energies and their coincidences. The $\gamma$ transitions marked by the solid arrow were detected in coincidence with the relevant $\alpha$ decays as it follows from the proposed decay scheme. The ground-state level assignment for $^{243}$Es is only tentative (see text for more details).

Using the method of delayed $\alpha$ - $\alpha$ coincidences with $^{247}$Md the $\alpha$ spectrum of its daughter isotope $^{243}$Es was obtained as it is shown in figure 6.1 c). The energy window for mother $\alpha$ decays was set from 8380 keV up to the 8800 keV and covers the decay of $^{247}$Md from a ground-state and from an isomeric state as well. Correlation time window was chosen to $\Delta$t = 120 s and the position window of $\Delta$x = ± 0.25 mm was used. The strong $\alpha$ decay line with energy of $E_\alpha = 7893 \pm 10$ keV was detected and attributed to the decay of $^{243}$Es. This value corresponds to an already known decay with an energy of $E_\alpha = 7899 \pm 3$ keV. Also

| **Isotope** | $E_\alpha$ [keV] | $T_{1/2}$ [s] | $b_\alpha$ | $E_\gamma$ [keV] | $b_{SF}$ | Ref. |
|---|---|---|---|---|---|---|
| $^{247}$Md | 8416±10 | 1.3±0.1 | | 209.6±0.5<br>157.5±0.5 | | This work |
| | 8660±20[A] | | | | | This work |
| | 8424±20 | 1.12±0.22 | | | | [Hof94] |
| $^{247m}$Md | 8783±40 | 0.257±0.033 | ≈ 0.77 | | ≈ 0.23 | This work |
| | | $0.23^{+0.19}_{-0.12}$ | | | ≈1[B] | [Hof94] |
| $^{243}$Es | 7893±10 | 22.9±2.2 | ≈ 0.6 | | | This work |
| | 7860±20[A] | | | | | This work |
| | 7895±20 | $40^{+40}_{-20}$ | | | | [Hof94] |
| | 7939±10 | 21±5 | | | | [Hat89] |
| | 7899±3 | | | | | [Hat89] |

Table 6.3: Summary of the measured decay spectroscopic data for $^{247,247m}$Md and its daughter product $^{243}$Es. [A)] - the assignment is only tentative and because of small statistics the additional measurement is needed [B)] only three SF events were detected.

on the two dimensional plot 6.2 two intensive correlation groups of mother energies attributed to $^{247}$Md and its isomeric state with daughter energy $E_\alpha$ = 7893 keV are clearly visible. There is an indication for small group of events around the energy of $E_\alpha$ = 7860 ± 20 keV correlated to the mother energy 8420 keV (see figures 6.1 c) and 6.2). This structure can indicate the $\alpha$-decay into an excited level with energy around 40 keV but the quality of the data does not allow to draw a definite conclusions and more sensitive measurements are necessary. The weak line with the energy of $E_\alpha$ = 7939 keV reported by *Hatsukawa et al.* [Hat89] was not confirmed.

By comparing the number of $^{247}$Md and $^{243}$Es decays the $\alpha$-branch of $^{243}$Es can be estimated to be $b_\alpha$ = 59.7 ± 2.5 %. The measured half-life of $^{243}$Es was $T_{1/2}$ = 22.9 ± 2.23 s what is in agreement with the values measured before [FiS96]. The hindrance factor is HF ≈ 2 and thus the transition between the same type of levels is expected as it is shown in figure 6.5.

The already discussed situation about the $^{243}$Es ground state level will be not clear even after considering of $\alpha$ decay information obtained for $^{243}$Es. The HF of the $E_\alpha$ = 7893 keV decay is close to one what indicates the same mother and daughter level. But the ground-state levels for Berkelium isotopes are partly $7/2^+[633]$ and partly $3/2^-[521]$, what are the candidates for a ground state level of $^{243}$Es too.

There was no clear evidence of $^{239}$Bk $\alpha$ decay correlated to $^{243}$Es. Only an

upper limit around 0.5 % can be evaluated. However this fact could be explained considering rather high predicted ratio of EC decay and long $\alpha$ half-life for $^{239}$Bk. Calculated half-life for EC decay is around 300 seconds [Hes04]. For $\alpha$ half-life according to the trend of measured experimental data for $Q_\alpha$ value ($Q_\alpha$ = 7.2 MeV [Zho03]) and using the Poenaru formula 4.13 [Poe80] the value around 24 000 seconds can be expected. This results in $\alpha$ branch of $^{239}$Bk in the order of $b_\alpha \approx 1$ %.

### 6.1.2 Decay chain of $^{246}$Md

The isotope $^{246}$Md was produced using the same reaction as $^{247}$Md - $^{40}$Ar+$^{209}$Bi - at the beam energy of 4.95 AMeV. The production of both isotopes was expected but the new knowledge of $^{247}$Md decay characteristics (see sec. 6.1.1 and table 6.3) gives us the good possibility to evaluate a contribution of the $^{247}$Md produced at this beam energy. During 48.5 hours of irradiation a total beam dose of 1.165 x $10^{18}$ projectiles was collected. The total amount of 1439 $\alpha$ decay events in the energy range from 8000 keV to 9000 keV and 62 events with the energy from 50 MeV to 200 MeV were registered in the pause. Most of these decay events might be attributed to the decay of $^{246}$Md or $^{246}$Fm (mainly produced by EC decay of $^{246}$Md) however also a different origin and contribution of other isotopes to these groups of decays needs to be checked.

a. *$\alpha$ decay of $^{247}$Md* is the most important parasitic contribution for this reaction energy. At the previous beam energy $E_{beam}$ = 4.67 AMeV - during the pause - 555 events in energy range from 8300 keV to 8650 keV were attributed to the decay of $^{247}$Md. In coincidence with these $\alpha$ decays 54 $\gamma$ transitions within the energy range of $E_\gamma$ = 207 - 211 keV were found. At the beam energy 4.95 AMeV and in the energy region 8300 - 8650 keV, what is the region where the $^{247}$Md decays can be expected only 9 $\alpha$ decays were in coincidence with the 207 - 211 keV $\gamma$ quants. Based on this fact the number of $^{247}$Md events was estimated to $N_{^{247}Md} \approx 92$.

b. *Spontaneous fission and $\alpha$-decay of $^{247m}$Md.* Using similar procedure as in case of ground-state decay of $^{246}$Md the estimated number of $^{247m}$Md can be evaluated. The expected amount of $\alpha$-decays is only $N_{^{247m}Md} \approx 7$ and the number of $^{247m}$Md SF is $\approx 4$.

c. *Decay of $^{214}$Fr.* This isotope is created by transfer reaction and has a 100 % alpha branch. It decays predominantly in energy range from 8420 keV to 8547 keV with a typical - very short - half-lives of $T_{1/2}$ = 5 ms in case of ground - state decay and $T_{1/2}$ = 3.35 ms in case of decay from an isomeric state. This short half-life gives us a possibility to identify them easily. Using recoil - $\alpha$ correlation search with a time window 30 ms altogether 39 events were identified as a decay of $^{214}$Fr.

d. *Decay of $^{246}Fm$* - produced by p2n de-excitation of the compound nucleus. Some of the $^{246}$Fm nuclei may be produced directly via p2n channels and should not be used for an evaluation of the properties of studied nuclei (like an estimation of cross-section and branching ration of $^{246}$Md). Using HIVAP calculation, the ratio between the p2n channel and 3n channel at excitation energy $E^* = 34$ MeV is expected to be around 4 %. Because expected EC branch of $^{246}$Md is $b_{EC} = 20$ - 30 % only around 15 % of all $^{246}$Fm events may have origin in p2n de-excitation of the compound nucleus $^{249}$Md and this estimate will not be taken into the account in further calculations.

Using the previous conclusions one can estimate the number of synthesized $^{246}$Md events as a difference of he sum of "parasitic" decays mentioned above and the sum of all $\alpha$-events in the range from 8180 keV to 8800 keV and SF events in the energy range from 50 MeV to 200 MeV. After considering a detector efficiency of 54 % for alpha decay, 100 % detector efficiency for spontaneous fission events and 30 % separation efficiency of SHIP we get a value of 8.1 $\pm$ 3.2 nbarn for the production cross-section of $^{246}$Md. For the $^{247}$Md the measured cross-section is 740 $\pm$ 290 pbarn. It is seen from figure 5.1 that both cross-section fit quite well to a calculated curves.

The lifetime distribution of spontaneous fission events detected in the measurement at the energy of $E_{beam} = 4.95$ AMeV is shown in figure 6.6. These values were obtained using recoil - SF correlation search. Although the number of counts is quite small it is possible to identify two well separated groups. One group centered around $\approx$ 320 ms should represents SF of $^{247}$Md. The second group has a time distribution from 1 second up to 12 seconds. The maximum number of counts is around $\approx$ 7 seconds what corresponds to the half-life of $T_{1/2} \approx 4.8$ seconds. The fission events in this group are attributed to SF of the isotopes $^{246m}$Md and $^{246}$Fm, which cannot be distinguished unambiguously.

The $\alpha$ spectrum displayed in figure 6.7 shows $\alpha$ decays collected in pause between the accelerator pulses. A strong influence of the energy summing with electrons from internal conversion on $\alpha$ decay $^{246}$Md is visible at the first sight. As it will be shown later, its energy spectrum lies more less continuously in the energy region from 8180 keV up to the 8800 keV and is hard to recognize the energy structure of $^{246}$Md $\alpha$ decay.

The most intensive group of $^{246}$Md $\alpha$ decays lies in the interval from the 8300 keV to 8640 keV but it is overlapped by $\alpha$ decays of $^{247}$Md. Both isotopes can not be unambiguously distinguished using correlation method because of similar decay characteristics (lifetime and decay energy) of these isotopes and their daughter products. Therefore for the precise decay properties evaluation of $^{246}$Md and its daughter products the energy region from 8380 keV to 8480 keV must be excluded to avoid the influence of $^{247}$Md and $^{243}$Es.

Using maximum likelihood method the half-life of the $^{246}$Md, as a result of recoil - alpha correlation search, was evaluated to the value of $T_{1/2}$ 1.3 $\pm$ 0.4 s. One can divide this energy range into the subintervals around the energies of

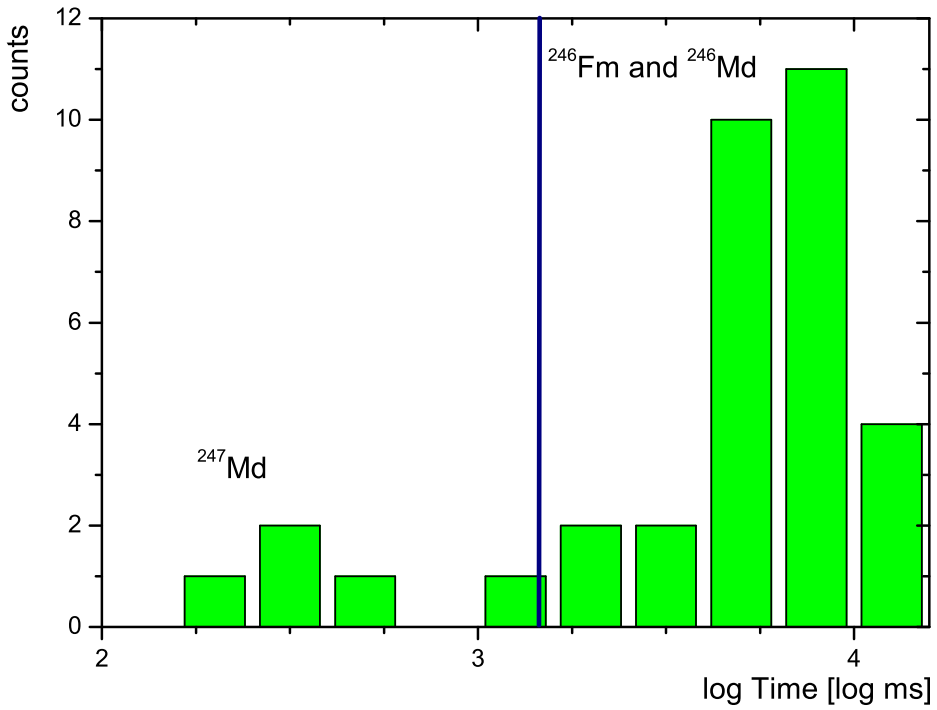


Figure 6.6: Logarithmic distribution of spontaneous fission lifetimes achieved by recoil - SF correlation search. The group of fissions with a short life-time represents SF of $^{247}$Md. The long lived fission events belong to SF of $^{246m}$Md and $^{246}$Fm (see text for more details).

$E_\alpha$ = 8350 keV, $E_\alpha$ = 8450 keV and $E_\alpha$ = 8560 keV with the relative intensities for these $\alpha$ energy sub-regions in the order of 20 % [2]. Assuming this relative intensity and the estimated $\alpha$ branching of $^{246}$Md from analyzed data (around 74 %) one can roughly evaluate the hindrance factors. These values vary from HF $\approx$ 7 for the decays around 8350 keV and 8450 keV up to the value HF $\approx$ 25 for the region around 8560 keV. It should be noticed that large uncertainty of the relative intensities (up to the factor of two) and decay energies (up to the several tens of keV) are expected due to the strong influence of energy summing with

[2] Thinking about all these facts one should have in mind that this structure is not a clear $\alpha$ structure but a combination of the "phantom" structure created by energy summing with conversion electrons and by "clean" $\alpha$ decays. Therefore the conclusions about the decay of the $^{246}$Md should be taken as a tentative results and should be tested in other experiments. One of the improvements which can solve this puzzle is including of the additional detector system optimized for energy measurement of escaped conversion electrons.

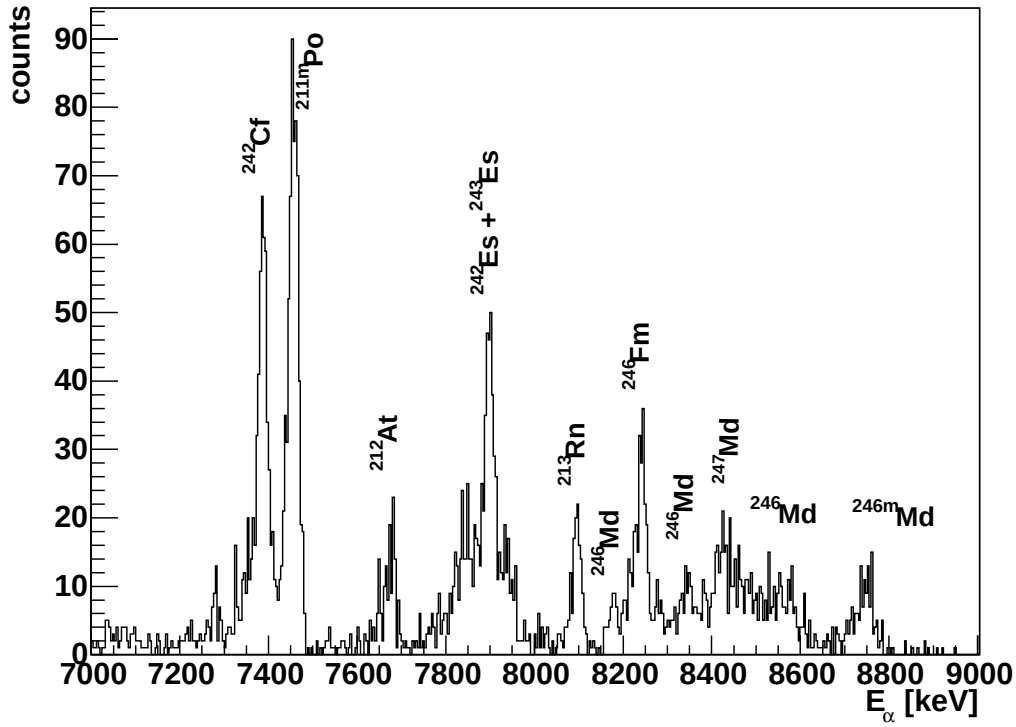


Figure 6.7: The $\alpha$ spectrum collected in the reaction $^{40}$Ar + $^{209}$Bi at the beam energy of $E_{beam}$ = 4.95 AMeV. The most intensive lines are coming from the products of complete fusion reaction or transfer reactions.

conversion electrons. Therefore the calculated hindrance factors may vary up to the factor of two.

Near to the strong 8244 keV line of $^{246}$Fm (see more details later) a small line with the energy 8178 ± 10 keV is visible. In the figure 6.8 c) one can see that the daughter decays correlated to this line have the same energy distribution as the daughter decays correlated to the $\alpha$-decays from the main energy region of 8300 - 8640 keV. Therefore this line was unambiguously assigned to the decay of $^{246}$Md. The half-life of $T_{1/2}$ = 4.4 ± 0.8 s was evaluated for this line using the maximum likelihood method. The hindrance factor for this transition is HF ≈ 10, suggesting a favored transition. The different value of the $\alpha$ decay half-life for this $\alpha$ energy gives us the indication about the existence of the isomeric state in the $^{246}$Md.

Because of the rather long half live one can think about the influence of the random correlations. This can be tested easily: One can search for recoil - $\alpha$ correlations of a long-living isotope for which no real correlations are expected. In this case a $^{211}$At line with an energy of $E_\alpha$ = 5867 keV and a known half-life of 7.2 hours was used for this test. Both time distributions (for $\alpha$ decay of energy $E_\alpha$ = 8178 keV and $E_\alpha$ = 5867 keV) are shown in figure 6.9 - normalized to 100 of

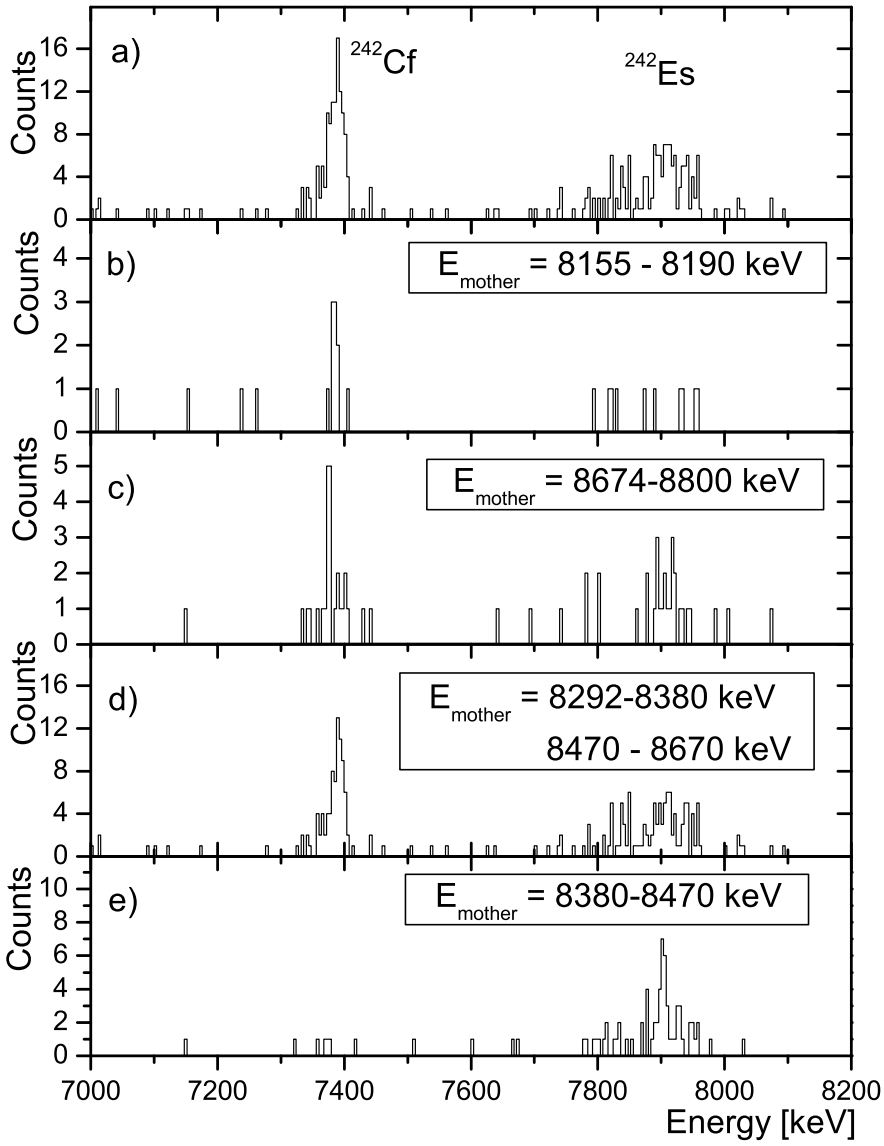


Figure 6.8: The spectra of the $\alpha$ decays correlated to the different energy regions of mother $\alpha$ decays. At the top (part a) ) is the sum spectrum from the part b), c) and d). These parts shows a various $\alpha$ decay energy region of $^{246}$Md, however regions with a strong contribution of $^{247}$Md (8380 - 8470 keV) and $^{246}$Fm (8190 - 8292 keV) are excluded. In the part d) the $\alpha$ decays correlated to the mother decays of energy 8380 - 8470 keV with a typical energy structure for the daughter products of $^{247}$Md.

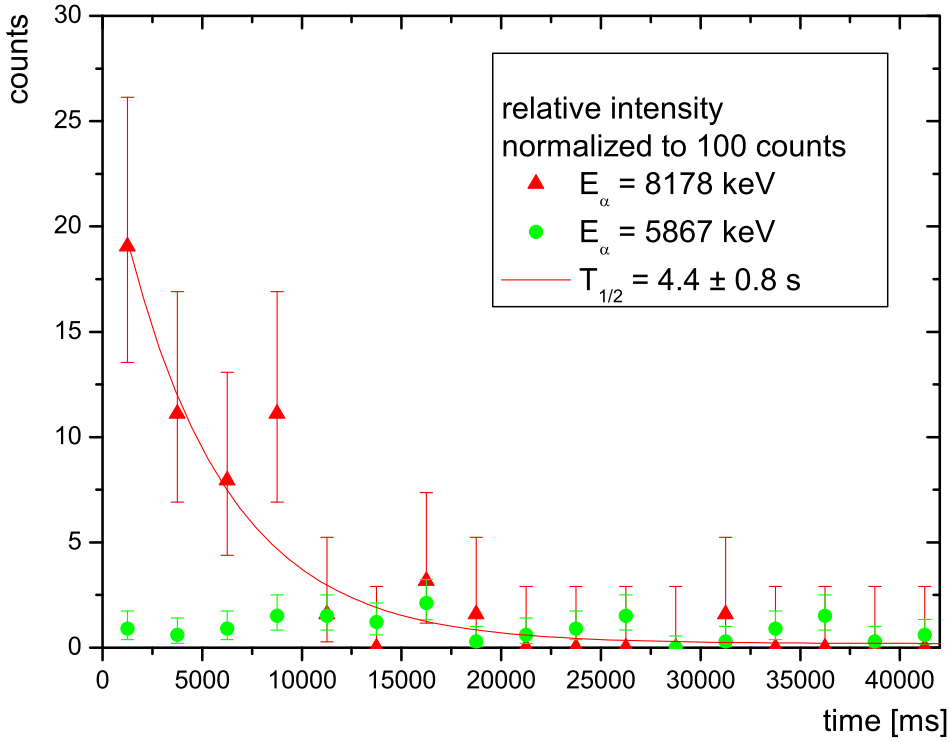


Figure 6.9: The decay curve for the $\alpha$ decay of energy 8178 keV attributed to $^{246}$Md as results of recoil - $\alpha$ correlation search (marked by red triangles). For information about the expected number of random recoil - $\alpha$ correlation the correlation with the $^{211}$At $\alpha$ decay of energy 5867 keV line was searched (marked by green circles). Both distributions and their statistical uncertainties are normalized to 100 counts due to different intensities of 5867 keV and 8178 keV line. The isotope $^{211}$At is transfer reaction product and because of its long half-life (7.22 hours) all of the found correlation should be random.

counts. This unambiguously shows that there is only a small influence of random correlations for the line of $E_\alpha = 8178$ keV. However it must be noted that because of small number of counts and large errors the value of the half-life may differ and needs to be approved by additional measurement.

It is evident that the $E_\alpha = 8178$ keV $\alpha$ decay half-life of $T_{1/2}(\alpha) \approx 4.4$ s is similar to $T_{1/2}(SF) \approx 4.8$ s half-life of SF events what leads to conclusion about decay from the same $^{246}$Md isomeric level. Moreover this can be the explanation of the higher number of SF events detected. The existence of isomeric state with SF branch seems to be more likely than the unexpected high EC-delayed fission of $^{246}$Fm suggested by *V. Ninov et al.* [Nin96]. It is not possible effectively measure the EC

decay using SHIP detectors, and therefore the SF events of $^{246m}$Md and $^{246}$Fm can not be distinguished. Consequently only only an upper limits $b_{SF} \approx 30$ % for the SF branch of this isomeric state may be evaluated.

Similarly as in the case of $^{247}$Md also for $^{246}$Md a well separated $\alpha$ decay peak around the energy of $E_\alpha = 8744 \pm 40$ keV is present in the spectrum. Although there are no $\gamma$ transitions or X-rays in coincidence with this $\alpha$ line, the FWHM of this peak is around 40 keV and it seems to be influenced by energy summing with conversion electrons. Therefore one can expect that this line does not represent $\alpha$ decay to the ground-state but, decay to the low lying excited state - close to the ground-state - with an energy around few tens of keV. The half-life for this peak is slightly shorter as half-life measured for the the main $\alpha$ group of energy 8.3 - 8.6 MeV mentioned before - $T_{1/2} = 750 \pm 180$ ms. But the existence of an additional isomeric state with such an intensity seems to be unlikely, especially with respect to the large uncertainty of the half-life for the $\alpha$ decays in the region of 8.4 - 8.6 MeV.

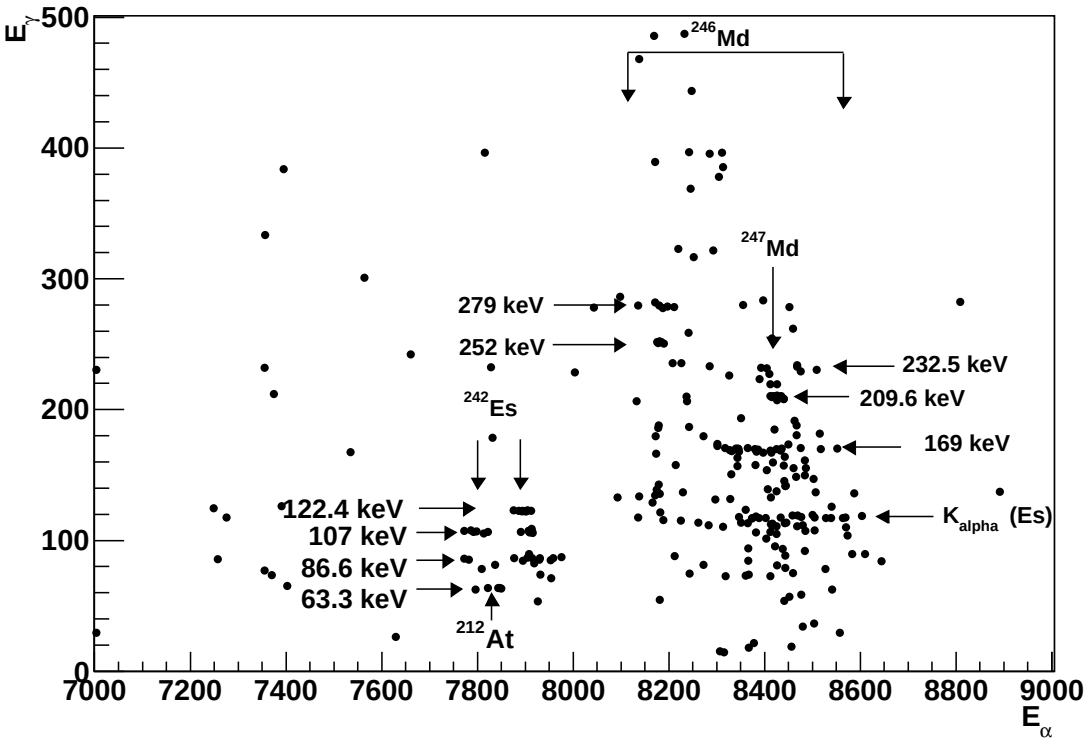


Figure 6.10: The $\gamma$ spectrum of transitions in coincidence with $\alpha$ decays of energy from 7000 keV to 9000 keV collected in pause. In the $\alpha$ energy range typical for $^{246}$Md a rather complicated structure of the $\alpha$ - $\gamma$ coincidence groups strongly influenced by internal conversion is visible. Clear $\alpha$ - $\gamma$ coincidence groups are detected also for the $\alpha$ decay of $^{242}$Es.

The $\alpha$ line of $E_\alpha$ = 8178 keV clearly represents decay into an excited state (see figure 6.10) and thus a contribution of the decay from this isomeric state to the energy region 8.3 - 8.6 MeV can not be ruled out completely. This will have an influence on the measured half-lives for these $\alpha$ decays, what can explain a difference between the measured half-life for the 8744 keV $\alpha$ line and a 8.3 - 8.6 MeV $\alpha$ group.

In figure 6.10 the $\alpha$ - $\gamma$ coincidences registered in pause are shown. There are several coincidence groups which belong to the decay of $^{246}$Md, $^{247}$Md and $^{242}$Es and de-excitation of their daughter products. As it is indicated already in the $\alpha$ spectrum also the $\alpha$ - $\gamma$ coincidence spectrum of $^{246}$Md is strongly influenced by energy summing of $\alpha$ particles with the electrons from the internal conversion process. The groups attributed to $\alpha$ decay of $^{246}$Md are spread over the area of 500 keV.

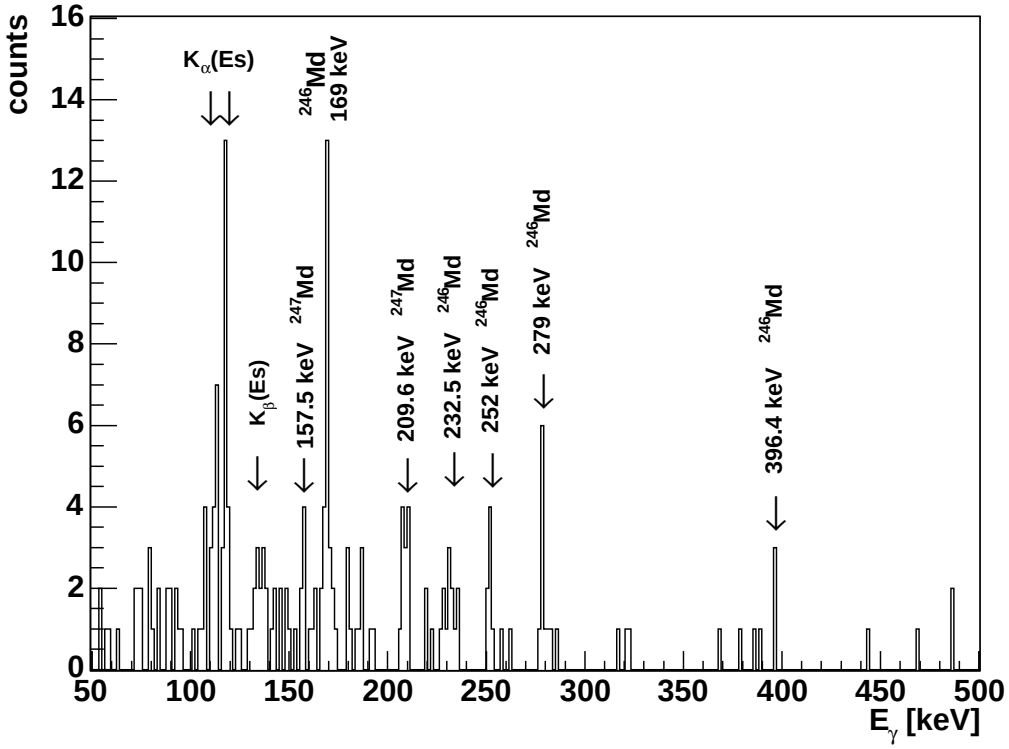


Figure 6.11: The spectrum of $\gamma$ transitions in coincidence with the $\alpha$ decays of energy from 8000 keV to 8650 keV in pause.

These gamma transitions gated by $\alpha$ decays with an energy from 8000 keV up to 8650 keV are shown in figure 6.11. Several lines are clearly coming up and can be assigned as follows:[3]

a. *The region 110 keV - 120 keV* contains the X-rays coming from the internal conversion (IC) process - $K_\alpha$ lines.

b. In *the region of 131 keV - 139 keV* the $K_\beta$ X-rays created in IC process are detected.

c. *The 157.5 keV and 209.6 keV $\gamma$ lines* were already identified as the de-excitation of the $^{243}$Es accompanying the $^{247}$Md $\alpha$ decay in the measurement at the beam energy 4.67 AMeV (see section 6.1.1).

d. *The 169.0 keV, 232.5 keV and 396.4 keV $\gamma$ lines* appear in coincidence with $\alpha$ decay of $^{246}$Md and therefore were assigned to the de-excitation of $^{242}$Es. Origin of mentioned decays was tested using $\alpha$ - $\alpha$ correlation search. The 396.4 keV line which appears in coincidence with $\alpha$ decay of the energy from 8260 keV to 8320 keV should be assigned only tentatively due to low statistics.

e. *The 252.0 keV and 279.0 keV $\gamma$ lines* appears in coincidence with $^{246m}$Md and therefore are also assigned to the de-excitation of $^{242}$Es.

As can be seen from figure 6.10 the coincidence group with $E_\alpha$ = 8180 keV and $E_\gamma$ = 252 keV is not influenced by energy summing with electrons from internal conversion, compare to the broad distribution measured for the $\alpha$ decays in coincidence with $\gamma$ line of $E_\gamma$ = 169 keV. Similar trend is measured also for the $\gamma$ transitions with the energy of $E_\gamma$ = 279 keV when most of them comes in the coincidence with the $E_\alpha$ = 8180 keV $\alpha$ decays. However some of them may be found in coincidence with higher energetic $\alpha$ decays too.

It should be noted that the sum of the energies 232.5 keV and 169 keV lines is very close to the energy of 396.4 keV transition. This may indicate that the 232.5 keV and 169 keV transitions come parallel to the third one however the difference of 7 keV is too large to draw definite conclusions - especially with respect to a low number of counts in the 396.4 keV line. It needs an additional assumption about existence of two close levels around 90 keV with an energy difference of some keV. This may also help to explain rather broad ($\Delta$ (FWHM) = 6 keV) distribution of 232.5 keV line in compare to typical width of other $\gamma$ lines ($\Delta$ (FWHM) $\approx$ 1.9 keV) measured in this experiment.

The group of $\alpha$ - $\gamma$ coincidences with $\gamma$ transition of $E_\gamma$ = 232.5 keV and $\alpha$ decay of $E_\alpha \approx$ 8400 - 8500 keV. Taking into the account the detector resolution and, mainly, the influence of energy summing with conversion electrons one can

[3] All assignments to presented isotopes in this work were also tested using of the recoil - $\alpha$ - $\gamma$ and the $\alpha$ - $\alpha$ - $\gamma$ correlation method.

tentatively assign the $\gamma$ transition with energy of $E_\gamma = 232.5$ keV as a transition between the levels populated by the $\alpha$ decay with energy around $\approx 8450$ keV and $\approx 8720$ keV

It should be noted that the energy of 90 keV for the first excited state is deduced from the structure of the 8700 - 8790 keV area which seems to be influenced by energy summing with conversion electrons.

The energy spectra of $\alpha$ decays correlated with the $\alpha$ decay of $^{246}$Md are shown in figure 6.8. The typical signature of the energy spectrum for all $\alpha$ events correlated to the various energy regions attributed to $^{246}$Md may be divided in two separate parts:

a. *The energy region from 7300 keV to 7450 keV* is attributed to the decay of $^{242}$Cf. This isotope is produced by EC decay of $^{242}$Es. The measured energies of $^{242}$Cf ($E_{\alpha 1} = 7389 \pm 10$ keV and $E_{\alpha 1} = 7360 \pm 30$ keV) are in agreement with the known values [FiS96].

b. *The energy region from 7700 keV to 8050 keV* is the region of $^{242}$Es $\alpha$ decay. Compared to $^{243}$Es the $\alpha$ decays of $^{242}$Es have a very broad distribution due to a strong influence of energy summing with conversion electrons.

The structure typical for the $^{243}$Es is clearly visible in the energy spectrum of the $\alpha$ decays correlated to the mother decays from energy range of 8380 - 8470 keV (see figure 6.8 d) compared to the figure 6.1 c)). Therefore, one can expect only small number of $^{246}$Md daughter products because only few $\alpha$ decays were registered with an energy typical for $^{242}$Cf $\alpha$ decay - one of the expected decay products. Therefore the energy region from 8380 keV to 8470 keV can be excluded from the analysis to avoid an influence on the calculated values of branching ratio and lifetimes.

The half-life of $^{242}$Es was evaluated using maximum likelihood method to a value of $T_{1/2} = 17.8 \pm 1.6$ s what is in agreement with a value measured before $T_{1/2} = 16^{+6}_{-4}$ s [Nin96]. The branching ratio may be estimated from the measured number of events in the energy regions of $^{242}$Es and $^{242}$Cf decay which are correlated to the $^{246}$Md decay (see figure 6.8). The correlations were searched using correlation time of 1000 second and therefore up to the 94 % of all $^{242}$Cf should be observed. After including this correction the $\alpha$ branch of $^{242}$Es was calculated to $b_\alpha = 45.6 \pm 2.6$ %.

In case of $^{242}$Es the half-life of 11 seconds is expected for the 7900 keV $\alpha$ decay. Assuming the measured values for the branching ratio and half-life the HF $\approx 4$ is typical for the $\alpha$ decay of $^{242}$Es what indicates an unhindered transition between the energy levels with the same spin a parity.

The published data on observed ECDF branch of $^{242}$Es with a branching ratio of $b_{ECDF} = 1.4 \pm 0.8$ % [Hin85] were confirmed in this experiments. Totally 440 $\alpha$ decays correlated to $^{246}$Md decay and attributed to the $\alpha$ decay of $^{242}$Es and $^{242}$Cf were found. Beside these $\alpha$ decays also three $\alpha$ - SF correlations were observed

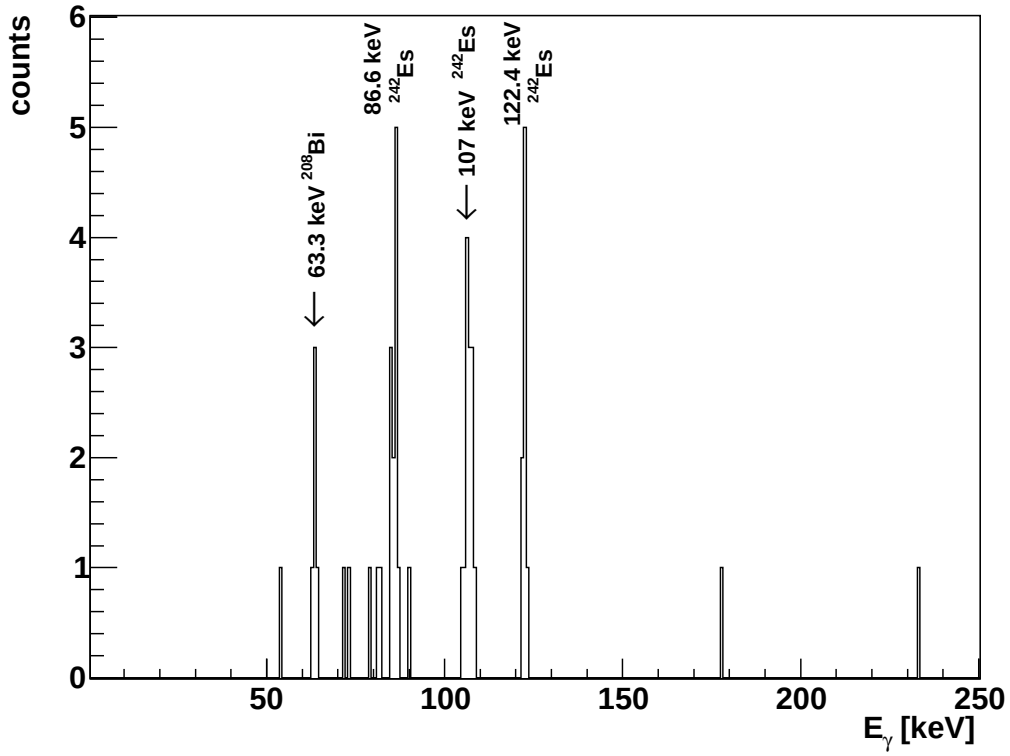


Figure 6.12: The spectrum of $\gamma$ transitions in coincidence with the $\alpha$ decays of energy from 7750 keV to 8000 keV in pause.

in data analysis[4] within the correlation time window of $\Delta$t = 120 s and position window of $\Delta$x = 1.2 mm. The $\alpha$ decay and SF events in this three correlations were detected in pause and the possibility of such a random correlation is not expected.[5] The evaluated error probability that three found $\alpha$ - SF correlations are random was calculated - according to the formalism of *K.-H. Schmidt et el.* [Sch84] - to the value of $P_{err} = 2x10^{-10}$. Based of these three $\alpha$ - SF correlation the value for a ECDF branch of $^{242}$Es is $b_{ECDF} = 0.67\ ^{+0.61}_{-0.39}$ %.

As it can be seen from figures 6.10 and 6.8 there is an indication of fine structure in the $\alpha$ decay group for isotope $^{242}$Es. The spectrum can be roughly divided into regions around the energies 7785 keV, 7830 keV, 7900 keV, 7940 keV and 8020 keV.

[4]Found SF events were not attributed directly to a SF of $^{242}$Es. The SF is hindered process for all odd-even and (even more) odd-odd isotopes due to a presence of unpaired nucleon(s) and therefore also the SF of $^{242}$Es are not expected.

[5]The possibility for observation of similar random correlation was tested also by searching for a $\alpha$ - SF correlation (both were required to be in pause) using a correlation time of 1000 seconds and alpha energy 7300 - 7500 keV which covers a region of $^{211}$Po $\alpha$ decay. Such an $\alpha$ - SF correlation should not exist. As expected - no candidate was found for a random $\alpha$ - SF correlation with required conditions.

Since some of them might be created by summing with conversion electrons one should take into account a possibility that these areas (especially weak lines) do not correspond to the real $\alpha$ lines. The line $E_\alpha \approx 8025$ keV may correspond to the g.s - g.s. transition but it should be assigned only tentatively because of its weak statistic.

In figure 6.12 the $\gamma$ transitions coming in coincidence with the $\alpha$ decays of energy from 7750 keV to the 8000 keV are shown. Similarly as in figure 6.10 there are clear $\alpha$ - $\gamma$ coincidence groups visible. The groups with the $\gamma$ energy of $E_\gamma = 63.3$ keV and $\alpha$ decay of $E_\alpha \approx 7830$ keV was attributed to the de-excitation of $^{208}$Bi after an $\alpha$ decay of $^{212}$At. Three other groups with the $\gamma$ energies of $E_\gamma = 87$ keV, $E_\gamma \approx 107$ keV and $E_\gamma = 122.7$ keV have an origin in the de-excitation of isotope $^{238}$Bk, which is produced by $\alpha$ decay of $^{242}$Es. Using these data one can estimate the excited levels of $^{238}$Bk but there were no clear decay data observed for this isotope and from measured data in this experiment one can expect the EC branch $b_{EC} > 99$ %.

Although the 107 keV line fits quite well to the $K_{\alpha 2}$ X-ray energy of Berkelium (107.1 keV), such an assignment is questionable, since one expects an intensity ratio $i(K_{\alpha 2})/i(K_{\alpha 1}) = 0.64$. The $K_{\alpha 2}$ line, however, is completely missing in analyzed data (see figure 6.12). Therefore the 107 keV $\gamma$ transition should come from direct de-excitation and in proposed decay scheme (see figure 6.13) also the level at this energy is placed. The other conclusion from non observation of any 112 keV X-rays is that all transition mentioned above should be E1 transition. However this seems to be in contradiction with the character of $\alpha$ spectrum which indicates strong influence of summing with internal conversion electrons and therefore the X-rays from the internal conversion should be present. This may be explained by de-excitation via internal conversion on L-shell. Unfortunately this can not be solved from presented data since the energy of expected X-rays is below the threshold of used $\gamma$ detectors.

Assuming the assignment of $E_\alpha \approx 8025$ keV line as a g.s - g.s. decay of $^{242}$Es the additional levels populated by the $\alpha$ decay from energy region 7700 - 7800 keV should have the excitation energy of $E_{exc} \approx 235$ keV and $E_{exc} \approx 285$ keV. These energies correspond to the differences between the $8020 \pm 20$ keV decay and lowest energetic $\alpha$ decay assigned to $^{242}$Es with energies of $E_\alpha = 7740 \pm 20$ keV and $E_\alpha = 7785 \pm 20$ keV. The idea about an existence of $E_{exc} = 235$ keV level in $^{238}$Bk may be supported also by one single gamma transition with energy $E_\gamma = 233.5$ keV detected in coincidence with $\alpha$ decay of energy $E_\alpha \approx 7800$ keV in pause. It must be pointed out that because of the low statistics the assignments for $E_{exc} = 235$ keV and $E_{exc} = 285$ keV levels should be taken only tentatively. The proposed decay and level scheme is shown in figure 6.13. All obtained information about the $\alpha$ decay and spontaneous fission are summarized in table 6.4.

Table 6.4: Summary of the measured spectroscopic data for the $^{246}$Md and its daughter products. $^{A)}$ The assignment is only tentative and the additional measurements are needed because of small statistics $^{B}$) Besides the $\alpha$ branch and EC branch also the ECDF branch of 0.67 $^{+0.61}_{-0.39}$ % was tentatively identified in this work. $^{C)}$ Because the $\alpha$ lines can not be resolved unambiguously only the energy range is given.

| **Isotope** | $E_\alpha$ [keV] | $I_\alpha$ | $T_{1/2}$ [s] | $b_\alpha$ | $E_\gamma$ [keV] | $b_{SF}$ | Reference |
|---|---|---|---|---|---|---|---|
| $^{246}$Md | 8250-8690$^{C}$ | $\approx$ 0.75 | 1.3 $\pm$ 0.4 | $\approx$ 0.74 | 169.0<br>232.5$^{A}$<br>252.0<br>279.0<br>396.4$^{A}$ | | This work |
| | 8744 $\pm$ 10<br>8500-8560<br>8740 $\pm$ 20 | $\approx$ 0.25 | 0.75 $\pm$ 0.18<br>1.0$\pm$0.4 | | | | This work<br>[Nin96] |
| $^{246m}$Md | 8178 $\pm$ 10 | | 4.4$\pm$0.8 | | | $\approx$ 0.3 | This work |
| $^{242}$Es | 7780-7960$^{C}$ | $\approx$ 0.95 | 17.8 $\pm$ 1.6 | 0.456$\pm$ 0.026$^{B}$ | 86.6<br>107.0<br>122.4 | | This work |
| | 8025 $\pm$ 20$^{A}$<br>7920 $\pm$ 20 | $\approx$ 0.05 | $22^{+1.6}_{-9.9}$<br>$16^{+6}_{-4}$ | | | | This work<br>[Nin96] |

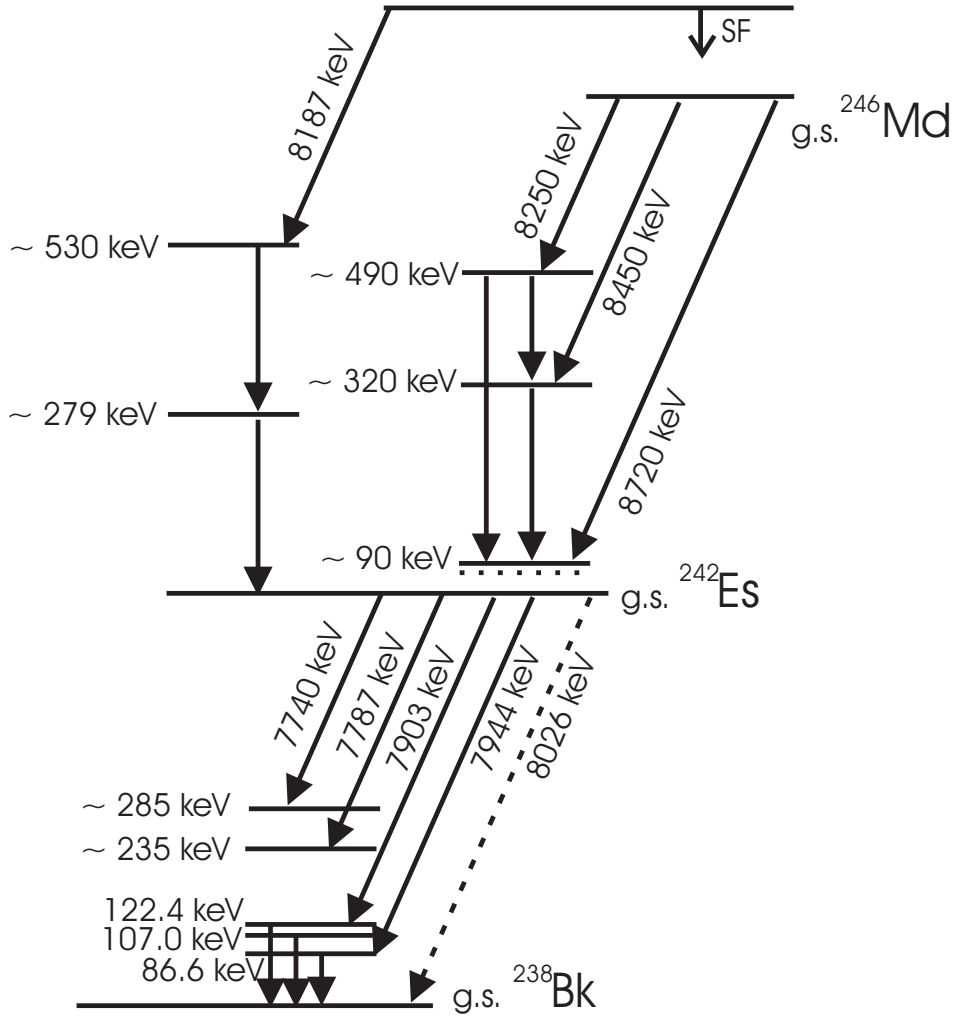


Figure 6.13: The proposed decay and level scheme of $^{246}$Md and its daughter products $^{242}$Es and $^{238}$Bk. It must be pointed out that the part concerning $\alpha$ decay of $^{246}$Md and the excited levels of $^{242}$Es should be taken as a tentative assignment. Spin and parity values are not attributed to proposed energy levels since no systematics is known until now. The transitions marked by the solid arrow were detected in coincidence with the relevant $\alpha$ decays as it follows from the proposed decay scheme.

## 6.2 Reaction $^{48}$Ca + $^{209}$Bi

As was already mentioned (see section 1) some basic spectroscopic information about the isotopes $^{254}$Lr, $^{255}$Lr and their daughter products were studied in the past. For more detail see the work of *F.P. Heßberger et al.* [Hes85], *K. Eskola et al.* [EsK71] or *V.A. Druin* [Dru70]. Some excited levels were also deduced based on previously measured $\alpha$ energy structure (see below).

The isotope $^{255}$Lr decays predominantly by $\alpha$ decay with an energy of $E_{\alpha 1}$ = 8410 ± 20 keV ($I_{\alpha 1} \approx 40 \pm 10$ %) and $E_{\alpha 2}$ = 8360 ± 13 keV ($I_{\alpha 2} \approx 60 \pm 10$ %). Only upper limits for the EC decay branch ($b_{EC} < 30$ %) and spontaneous fission branch ($b_{SF} < 0.1$ %) are given [FiS96]. The decay half-life of this isotope is $T_{1/2}$ = 22 ± 4 s [FiS96]. The daughter product of $^{255}$Lr $\alpha$ decay is an isotope $^{251}$Md. The EC branch of this isotope is more than 90 % with 4 minutes half-life. This gives a requirement for a high production rate of $^{255}$Lr in th order to study the spectroscopic properties of this isotope. Until now only one decay energy was known - $E_\alpha$ = 7550 ± 20 keV. An information (however uncertain) about the ground-state spin and parity of $^{247}$Es gives the possibility for prediction of the spin and parity states of $^{251}$Md and $^{255}$Lr excited levels. In case of successful assignments of these levels one can compare them with existing theoretical predictions (e.g. [Cwi94]).

Isotope $^{254}$Lr, produced by 3n de-excitation channel, has an $\alpha$ decay branch $b_\alpha \approx 80\%$. Until now two $\alpha$ lines were known for this isotope - $E_{\alpha 1}$ = 8460 ± 20 keV ($I_{\alpha 1} \approx 64$ %) and $E_{\alpha 2}$ = 8408 ± 20 keV ($I_{\alpha 2} \approx 36$ %) [Hes85]. Its daughter product $^{250}$Md decays predominantly by EC ($b_{EC} \approx 93$ %) and two $\alpha$ decay energies are known - $E_{\alpha 1}$ = 7830 ± 20 keV ( with a relative intensity $I_{\alpha 1} \approx 25$ %) and $E_{\alpha 2}$ = 7750 ± 20 keV ($I_{\alpha 2} \approx 75$ %) [FiS96]. Some levels of $^{250}$Md and $^{246}$Es were estimated from known information about $\alpha$ decay [FiS96].

Using the $\gamma$ detectors and $\alpha$ - $\gamma$ coincidence measurements with higher statistics one can get new and more precise spectroscopic data and can construct accurate decay schemes for these isotopes.

In our experiment aimed at production of $^{254}$Lr and $^{255}$Lr performed at SHIP the new data about these isotopes and their daughter products (mainly $^{251}$Md, $^{250}$Md, $^{247}$Es and $^{246}$Es) were obtained. The results of data analysis obtained at SHIP and their physical interpretation, as well as comparison of these results with some known theoretical and experimental results will be presented in following sections. These data were confirmed recently at RITU in Jyväskylä (Finland) [Hes04].

### 6.2.1 Decay chain of $^{255}$Lr

The total beam dose of 3.5 x $10^{16}$ ions was collected at the beam energy of $E_{beam}$ = 4.69 AMeV during 19 hours of irradiation. The spectrum of the $\alpha$ decays detected in anti-coincidence with TOF system is shown in figure 6.14. There is no significant influence of the un-wanted $\alpha$ decays (e.g. the $\alpha$ decay of the transfer

reaction products). All peaks in the energy range from 7000 keV up to 9000 keV were attributed to the $\alpha$ decay of $^{255}$Lr and its daughter decay products $^{255}$No, $^{251}$Md and $^{247}$Es.

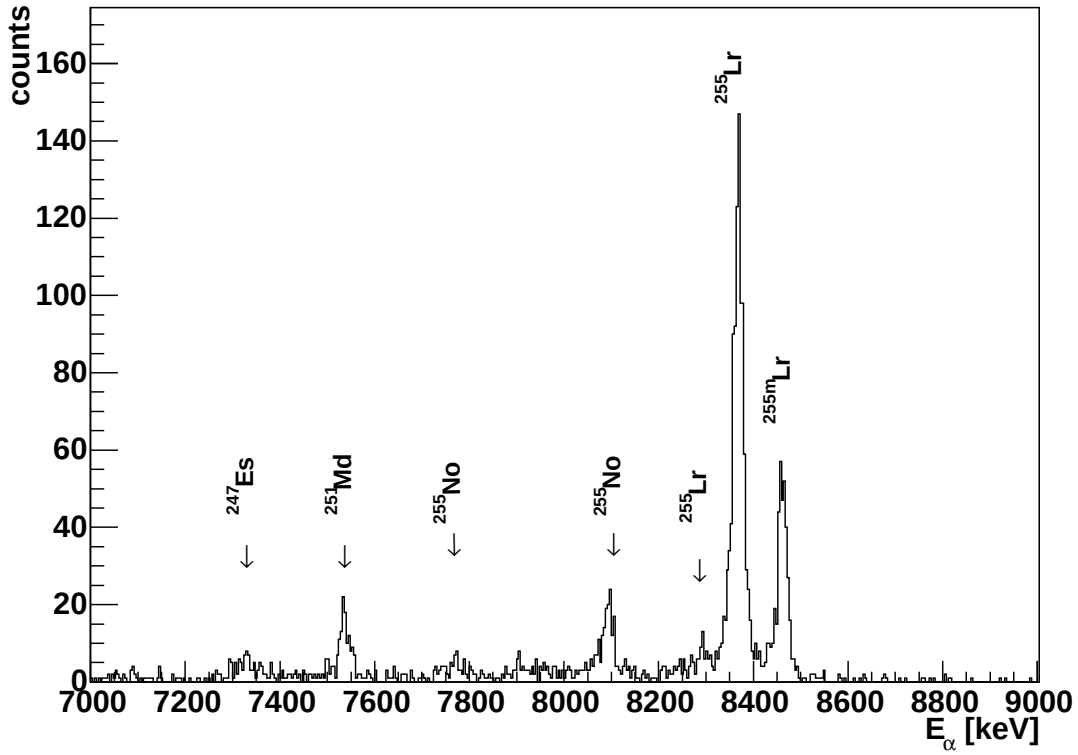


Figure 6.14: The spectrum of $\alpha$ decays detected in anti-coincidence with TOF system in reaction $^{40}$Ar + $^{209}$Bi. All intense peaks arise from the reaction product - $^{255}$Lr and its daughter decay products - $^{251}$Md, $^{247}$Es (produced by $\alpha$ decay) and $^{255}$No (produced by EC decay of $^{255}$Lr)

Both, already known, $\alpha$ decay energies of $^{255}$Lr were unambiguously identified by means of recoil - $\alpha$ and $\alpha$ - $\alpha$ correlation search also in this experiment with the measured - more precise - energies of $E_\alpha = 8462 \pm 10$ keV and $E_\alpha = 8369 \pm 10$ keV. But in contradiction with reported decay data [FiS96] two different half-lives of $T_{1/2} = 19.9 \pm 5.3$ s and $T_{1/2} = 2.56 \pm 0.25$ s were measured for these $\alpha$ lines. Both relevant decay curves are shown in figure 6.15. The possible explanation for the transition with the half-life of $T_{1/2} = 2.56$ s is an existence of long-living isomeric state of $^{255}$Lr decaying by the $\alpha$ decay of $E_\alpha = 8462$ keV energy.

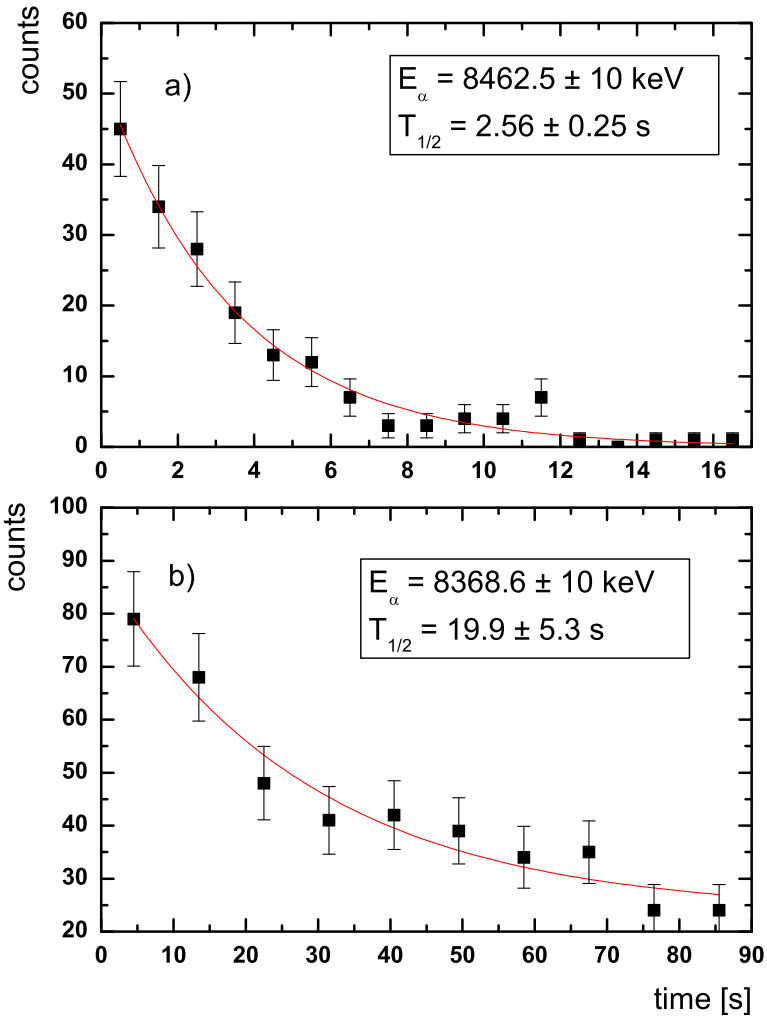


Figure 6.15: Decay curves for the two most intensive $\alpha$ lines of $^{255}$Lr. They clearly show the existence of an isomeric state for this isotope. The part a) shows a decay curve of the $E_\alpha = 8462$ keV $\alpha$ decay with a half-life of $T_{1/2} = 2.56 \pm 0.25$ s. The part b) shows a decay curve of $E_\alpha = 8369$ keV decay with the half-life of $T_{1/2} = 19.9 \pm 5.3$ s. Both $\alpha$ decay half-lives were obtained by means of recoil - $\alpha$ correlation search.

The calculated hindrance factors for both $\alpha$ transitions are close to one and therefore they are considered to be un-hindered transitions between the states without the spin and parity change [6].

[6] The existence of the isomeric state for this isotope was later confirmed in similar experiment performed at RITU in Jyväskylä

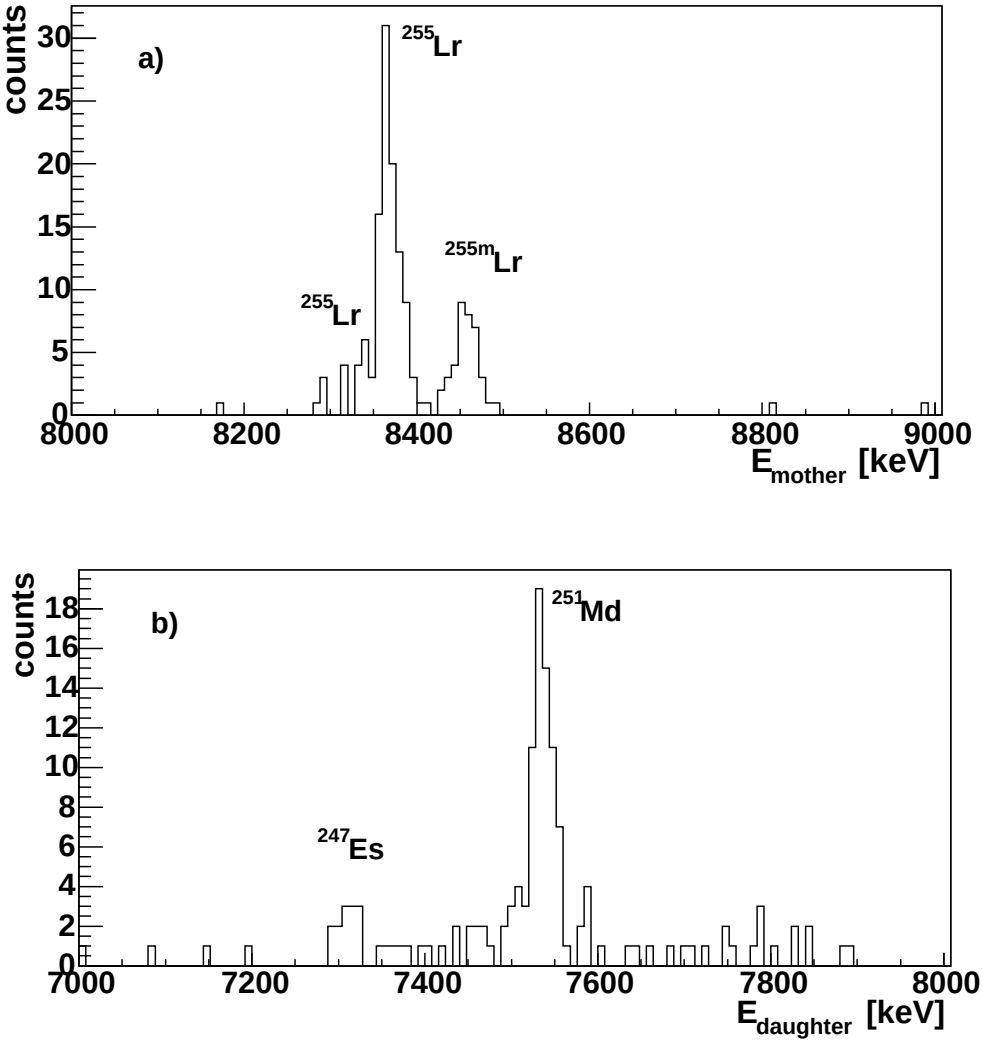


Figure 6.16: Mother and daughter $\alpha$ energy spectra as a results of $\alpha$-$\alpha$ correlation search between the $\alpha$ energy range of 8000 - 9000 keV and the energy range of 7000 - 8000 keV within a correlation time window of 1200 s and a position window of 0.25 mm. Part a) shows a mother $\alpha$ decays attributed to $^{255}$Lr and its isomeric state (see text for more details). The part b) includes its decay products $^{251}$Md and $^{247}$Es. It is not clear from analyzed data if the energy structure from 7600 keV to 7900 keV belongs to the real or random correlation.

In figure 6.16 a) the spectrum of $\alpha$ decays correlated to the $^{251}$Md - expected daughter product of $^{255}$Lr - is shown. Beside the $E_\alpha = 8462$ keV and $E_\alpha = 8369$ keV $\alpha$ lines, a group of events around the energy of $E_\alpha = 8310$ keV is visible. Using mentioned $\alpha$ - $\alpha$ correlation method these decays were also attributed to the decay

of $^{255}$Lr. From the recoil - $\alpha$ correlation analysis their half-life was calculated according to the formalism of *Schmidt et al.* [Sch84] to the value of $T_{1/2} = 24.2^{+5.1}_{-3.6}$ s. Due to its half-life this $\alpha$ decay is attributed to the decay from the same level as the $\alpha$ decay of energy $E_\alpha$ = 8369 keV but populating a different level in the daughter nucleus with an energy difference around 60 keV. No $\gamma$ transitions have been observed in coincidence with $\alpha$ decay of $E_\alpha$ = 8369 keV, however there is an influence of the broadening of the $\alpha$ line due to a energy summing with conversion electrons.

$^{251}$Md decays by $\alpha$ transition of energy $E_\alpha$ = 7535 keV (see figure 6.16 b) ). Due to a low statistics the measured half-life - $T_{1/2} = 6.7 \pm 1.5$ min has a large uncertainty, but within the statistical error is still in agreement with previously published value ($T_{1/2} = 4 \pm 0.5$ min) [EsP73]. Based on the HF $\approx$ 4 transition between levels with the same spin and parity is expected.

The daughter $\alpha$ activity correlated to $^{251}$Md with the energy close to the expected $\alpha$ decay energy for $^{247}$Es was identified properly in agreement with known decay data. But due to the high EC decay branch of $^{247}$Es and $^{251}$Md and low statistics it is not possible to improve data measured in past or obtained some new spectroscopic results.

Because of the existence of isomeric state only the limits for the EC decay branch of $^{255}$Lr can be given. The upper limit for 8462 keV $\alpha$ line is $b_{EC} < 60 \pm 2$ % and for the 8368 keV $\alpha$ decay is $b_{EC} < 38 \pm 2$ %. For $^{251}$Md only limit for decay branch was evaluated until know. Comparing of $^{255}$Lr and $^{251}$Md peak intensities for measurement discussed in this work results to $^{251}$Md EC branch of $b_{EC} = 90.2 \pm 0.9$ %. There was no sign of any spontaneous fission in analyzed data and only the upper limits for the fission branch of discussed isotopes were calculated - for $^{255}$Lr $b_{SF^{255}Lr} < 0.03$ % for $^{251}$Md $b_{SF^{251}Md} < 0.04$ % and for $^{255}$No $b_{SF^{255}No} < 0.08$ %.

The figure 6.17 shows a scatter plot of measured $\alpha$ - $\gamma$ coincidences. Although few single $\alpha$ - $\gamma$ coincidences were detected for the $^{255}$Lr there is no indication of any group - neither for the $K_\alpha$ X-rays from internal conversion nor from a $\gamma$ transition from direct de-excitation. For the $\alpha$ decay of $E_\alpha$ = 8369 keV, with a width of $\Delta$E (FWHM) = 24 keV, this may be explained by decaying into the ground-state of $^{251}$Md. Also the width of the line $E_\alpha$ = 8462 keV is small ($\Delta$E (FWHM) = 21 keV) without any evidence of energy summing with conversion electrons.

The strong $\gamma$ line of $E_\gamma$ = 294 keV was identified in coincidence with discussed $^{251}$Md $\alpha$ decay (see figures 6.17 and 6.18). There is almost no indication of any X-rays with the energy typical for internal conversion of Einsteinium. The limit for internal conversion coefficients on K-shell and L-shell of this $\gamma$ transition is $\alpha_K < 0.11$ and $\alpha_L < 0.13$, respectively. According to calculated values of internal conversion coefficients of Einsteinium [Rös78] this $\gamma$ line is assigned as a E1 transition, however the possibility of E2 transition must be taken into an account, too.

With regard to the proton single-particle states in the region of Lawrencium isotopes, calculations based on a Woods-Saxon potential predicts a $7/2^-[514]$ Nils-

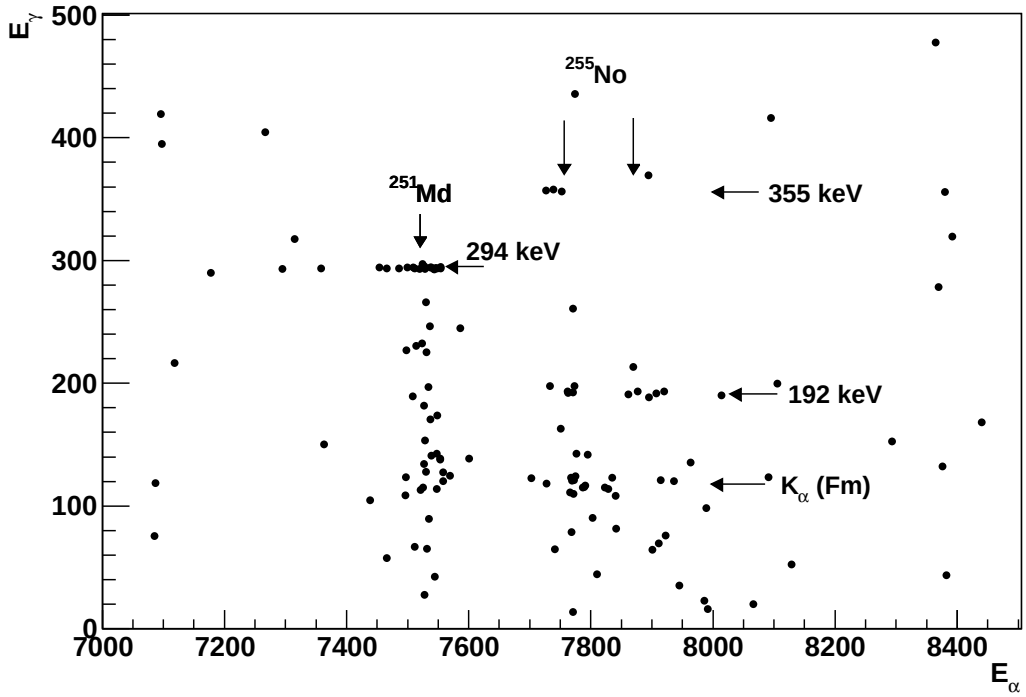


Figure 6.17: The $\alpha$ - $\gamma$ coincidence spectrum showing the $\alpha$ decays and $\gamma$ transitions within 4 $\mu$s time window. One can see a strong group for the $\alpha$ decay of $^{251}$Md in coincidence with a 294 keV transition. For the decay of $^{255}$No it is possible to identify the coincidence group with - already known - gamma transition of energy 192 keV and with X-rays coming from internal conversion of $^{251}$Fm. There is an indication of the coincidence with a gamma events of energy 355 keV which was also confirmed also by recent SHIP experiments.

son level [Cwi94]. Since it is in agreement also with the systematic also in this work the ground-state for $^{255}$Lr was assigned to $7/2^-[514]$ level and the isomeric state to the $1/2^-[521]$ Nilsson level.

Based on the expected similarity for mendelevium isotopes studied in this work, also in case of $^{251}$Md the ground-state spin of $7/2^-[514]$ can be expected, since for the $^{255}$Md and $^{257}$Md the spin of $7/2^-[514]$ was attributed, too [FiS96]. As was mentioned already, for the ground-state of $^{255}$Md spin of $7/2^-[514]$ has been proposed also in recent measurement of $^{255}$Md EC decay [Ahm00]. This supports an idea of un-hindered g.s. - g.s. $\alpha$ transition with energy of $E_\alpha \approx 8369 \pm 10$ keV between $^{255}$Lr and $^{251}$Md with the ground-state assignments to $7/2^-[514]$ Nilsson level.

The excited level, populated by the 8462 keV decay, was attributed to the $1/2^-[521]$ Nilsson level. The expected M3 transition, $1/2^-[521] \rightarrow 7/2^-[514]$, should be highly converted. But the typical transition time in case of M3 transi-

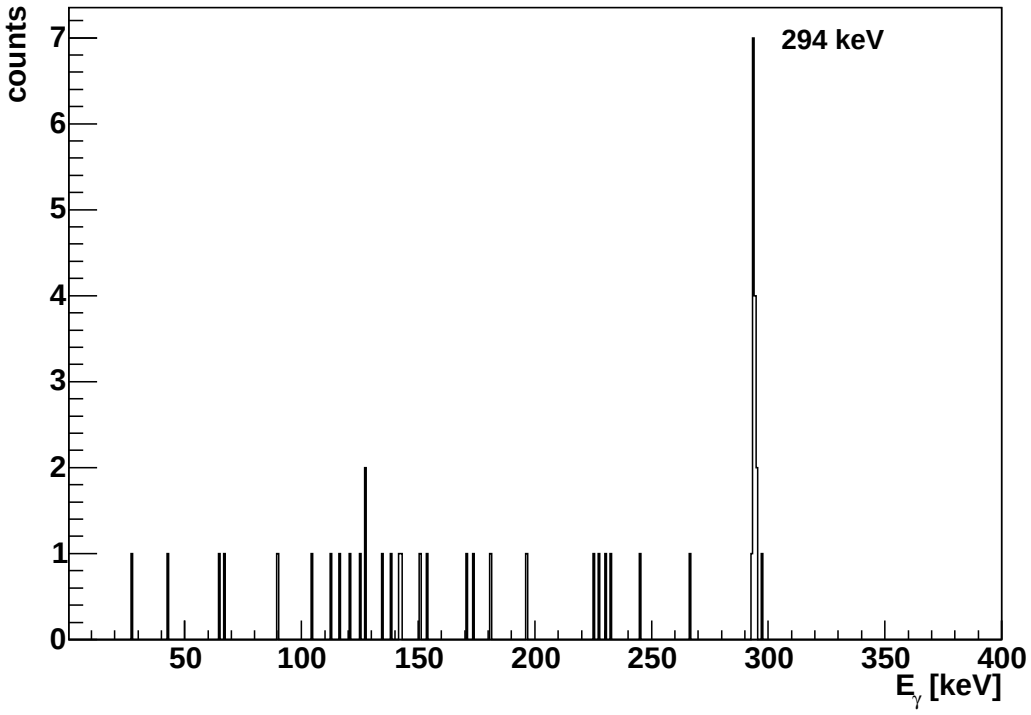


Figure 6.18: The spectrum of $\gamma$ transitions detected in coincidence with an $\alpha$ decay of $^{251}$Md from 7200 keV to 7600 keV.

tion with the energy of few hundred keV, corrected for internal conversion, is in the order of 0.1 - 1 seconds and therefore this transition can not be detected in coincidence with $\alpha$ decay within used 4 $\mu$s coincidence interval. This is also the explanation of narrow energy distribution for 8462 keV $\alpha$ line. Since, there were no $\alpha$ - $\gamma$ coincidences observed with the 8462 keV transition it is not possible to determine the excitation energy of $1/2^-[521]$ level neither in $^{255}$Lr nor $^{251}$Md.

For the $^{255}$Lr $\alpha$ decay of energy 8310 keV the populated, daughter, level can be tentatively assigned to the first member of rotational band - $9/2^-[505]$ Nilsson level. The energy of 60 keV for this level is assumed from the difference of $\alpha$ decay energies and therefore its exact position is uncertain. The proposed decay scheme of $^{255}$Lr is drawn in figure 6.19.

The small HF of $^{251}$Md $\alpha$ decay suggest the same level for the excited state of $^{247}$Es was assigned as for the groundstate of $^{251}$Md - $7/2^-[514]$ Nilsson level. The energy of this level is at least 294 keV.

The possibility of two levels with the spin and parity of $3/2^-[521]$ and $7/2^+[633]$ as candidates for the ground-state of $^{243}$Es was discussed already in section 6.1.1. The similar situation is expected also for $^{247}$Es. The E1 character of 294 keV $\gamma$ line suggest the transition $7/2^-[514] \rightarrow 7/2^+[633]$, however the possibility of

| **Isotope** | $E_\alpha$ [keV] | $T_{1/2}$ [s] | $b_\alpha$ | $E_\gamma$ [keV] | $b_{SF}$ | Reference |
|---|---|---|---|---|---|---|
| $^{255}$Lr | 8369±10 | 19.9±5.3 | >0.62±0.02 | | <0.0003 | This work |
| | 8310±20 | $24.2^{+5.1}_{-3.6}$ | | | | This work |
| $^{255m}$Lr | 8462±10 | 2.56±0.25 | >0.4±0.02 | | | This work |
| $^{251}$Md | 7535±10 | 420±90 | 0.0.098±0.009 | 294 | <0.0004 | This work |
| | 7550±20 | 240±30 | | | | [FiS96] |
| $^{247}$Es | 7310±20 | | | | | This work |
| | 7323±1 | 273±16 | | | | [FiS96] |

Table 6.5: Summary of the measured spectroscopic data for the $^{255}$Lr and its daughter products.

| **Isotope** | **$E^{th}$ [MeV]** | | | | |
|---|---|---|---|---|---|
| $^{255}$Lr | 0 $(7/2^-)$ | 0.14 $(9/2^+)$ | 0.15 $(1/2^-)$ | 0.73 $(5/2^-)$ | 0.87 $(7/2^+)$ |
| $^{251}$Md | 0 $(1/2^-)$ | 0.30 $(7/2^-)$ | 0.43 $(7/2^+)$ | 0.63 $(9/2^+)$ | 0.82 $(3/2^-)$ |
| $^{247}$Es | 0 $(7/2^+)$ | 0.27 $(3/2^-)$ | 0.41 $(1/2^-)$ | 0.74 $(7/2^-)$ | 0.88 $(5/2^+)$ |

Table 6.6: Theoretical calculation for the energies, spins and parities of $^{255}$Lr, $^{251}$Md and $^{247}$Es excited level. [Cwi94]

$7/2^-[514] \rightarrow 3/2^-[521]$ transition - based on the possibility E2 character - can not be ruled out. Therefore the ordering of these levels and the ground-state of $^{247}$Es is still uncertain.

The proposed decay scheme of $^{255}$Lr and its decay chain members is shown in figure 6.19.

The ordering of the levels proposed for $^{247}$Es is in agreement with the calculated values[7] (see table 6.6), however there is some disagreement between theoretical and experimental energies of these levels. The measured differences between the levels are significantly smaller than a calculated, but this fact is known also for the other

[7] One should not forget on an assignment of uncertainty for $^{247}$Es ground-state (see discussion above) due to a possibility of very low energy difference between $3/2^-$ and $7/2^+$ level.

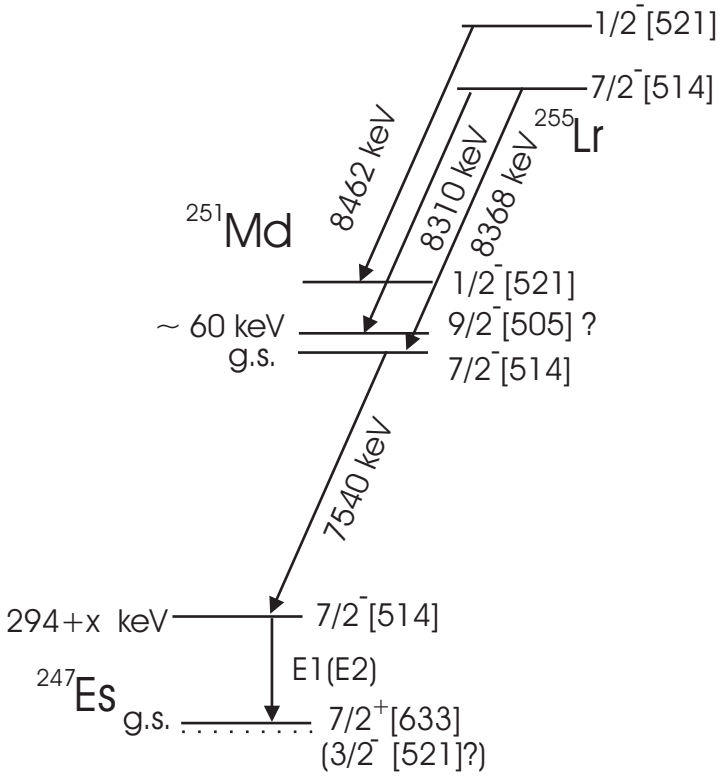


Figure 6.19: The proposed decay and level scheme of $^{255}$Lr and its daughter product $^{247}$Es. The transition marked by the solid arrow was detected in coincidence with the $\alpha$ decays of 7540 keV.

isotopes (see also the discussion in section 6.1.1).

The $^{255}$No - a daughter product of $^{255}$Lr EC decay - shows a complicated $\alpha$ energy structure. Since the excited $5/2^+[622]$ level of energy 192 keV has a tabulated life-time value of 15 $\mu$s no $\alpha$ - $\gamma$ coincidences with the $\gamma$ energy of 192 keV are expected. But the recent measurements shows that decays of energy from 7750 keV to 8020 keV and $\gamma$ energy of 192 keV were detected within 4 $\mu$s interval (see figure 6.17). The $\alpha$ energy distribution of the $\alpha$ decay in coincidence with the 192 keV $\gamma$ transition is also in disagreement with published data [FiS96]. The possible explanation is that the transition 192 keV does not lead to the ground-state, as it was proposed before [FiS96], but its final state is one of the excited levels - at least 100 keV above the ground-state. Additionally three $\alpha$ - $\gamma$ coincidences of $E_\alpha$ = 7740 keV and $E_\gamma$ = 355 keV were detected (see figure 6.17)[8].

[8] The 355 keV $\gamma$ transition was confirmed recently in experiment at SHIP. The measured, more precise value, is $E_\gamma$ = 357.4 keV. The energy of $5/2^+[622]$ was also corrected to the energy of $E_{exc} \approx 197$ keV.

### 6.2.2 Decay chain of $^{254}$Lr

As was already mentioned another isotope - $^{254}$Lr - was produced using the same reaction - $^{48}$Ca + $^{209}$Bi - at the beam energy of $E_{beam}$ = 4.81 AMeV. The total beam dose of 1.165 x $10^{18}$ projectiles was collected over 135 hours of irradiation using parasitic beam. Figure 6.20 shows cumulative $\alpha$ decay spectrum taken of $\alpha$ energy range from 6000 to 9000 keV.

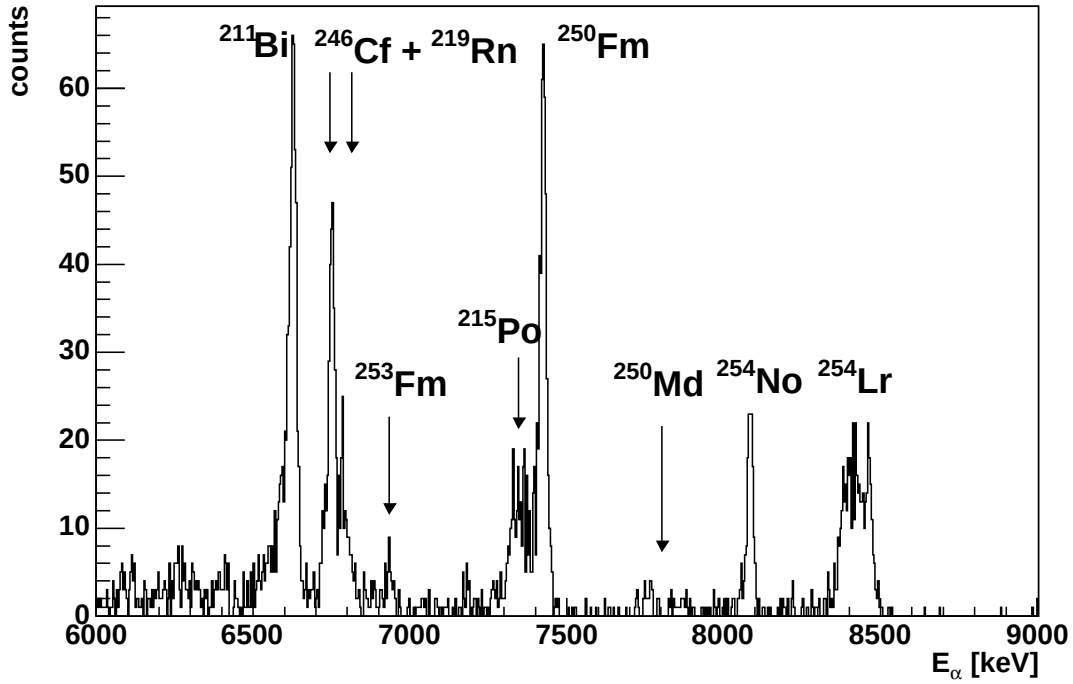


Figure 6.20: Spectrum of the $\alpha$ decays detected for the reaction $^{48}$Ca + $^{209}$Bi at the beam energy $E_{beam}$ = 4.81 AMeV. All decays were detected in the pause between the beam pulses. The alpha decays of $^{211}$Bi, $^{215}$Po and $^{219}$Rn appear due to a badly shielded $\alpha$ source of $^{227}$Ac which emits a gaseous radon isotope - $^{219}$Rn. All other lines come from an implanted reaction products - $^{254}$Lr - and its daughter decay products. The isotope $^{253}$Fm originates from EC-decay of $^{253}$No produced in a preceding irradiation.

During this time 445 events, assigned to $^{254}$Lr, were detected in the range of 8300 - 8550 keV in pause. Beside this 158 pause events of $^{254}$No, produced by EC decay of $^{254}$Lr, were detected in energy range of 8020 - 8125 keV. Considering 90 % $\alpha$ branch of $^{254}$No, 30 % expected SHIP transmission, 54 % geometry efficiency of stop detector and 76.5 % duty factor, the resulting production cross-section is around 22 $\pm$ 6 nb. During the measurement two spontaneous fission events were

detected[9].

The measured EC decay branch of $^{254}$Lr of $b_{EC} = 28.3 \pm 1.9$ % is in an agreement with the already known value [Hes85]. The lifetime for $^{254}$Lr was evaluated to be $T_{1/2} = 18.4 \pm 1.8$ s. This value was confirmed also using indirect production of $^{254}$Lr, produced in later SHIP experiments, when this isotope was studied as a daughter product of $^{258}$Db.

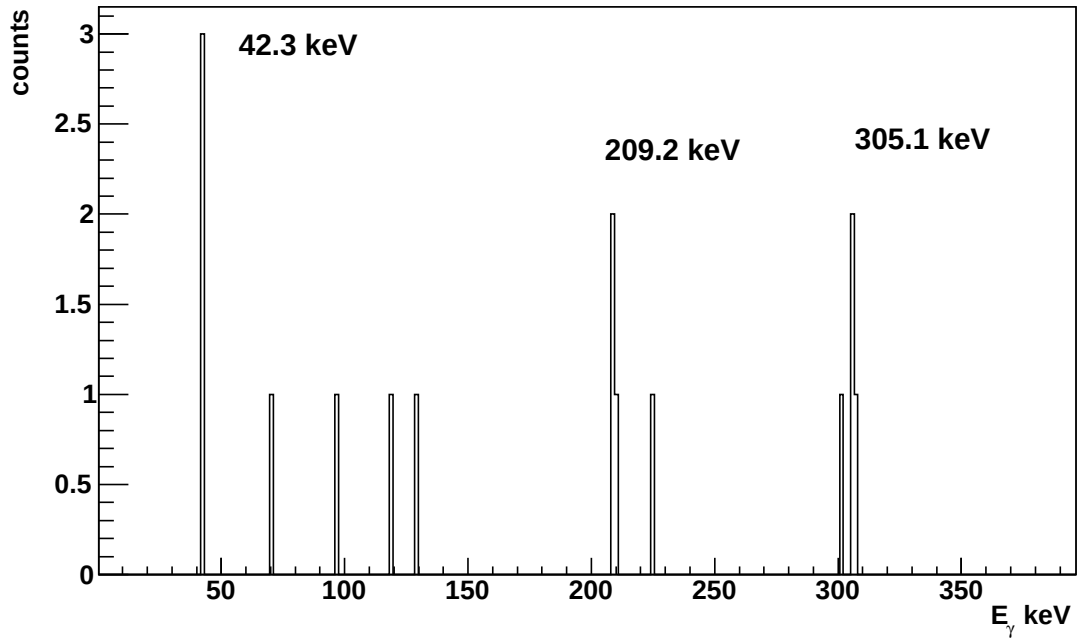


Figure 6.21: Spectrum of $\gamma$ transitions detected in coincidence with $^{254}$Lr $\alpha$ decays of energy region from 8310 keV to 8530 keV. The clear indication of three $\gamma$ transitions are visible in coincidence with these $\alpha$ decays. Al three $\gamma$ lines were confirmed later in the experiment aimed on production of $^{258}$Db.

Important is that three $\gamma$ transitions were detected in coincidence with $^{254}$Lr $\alpha$ decay (see figure 6.21) however with weak statistics. A bit confusing seems to be a strong influence of energy summing with conversion electrons but non-observation of $\alpha$ - X-rays coincidences. This is probably due to transitions between excited levels predominantly having energy differences below the K-binding energy - $E_K \approx 146$ keV. The de-excitation between the levels with smaller energy difference than is the electron binding energy on K-shell may be converted only via internal conversion on L-shell. However the energy summing with conversion electrons is detected the X-rays are below the threshold of used detection system and therefore are not identified.

[9]It was required that event assigned to the spontaneous fission must by accompanied by $\gamma$ ray emission to avoid a problem of increased high energy background during this measurement.

In spite of this low statistics three $\gamma$ lines of energies $E_\gamma = 42.3$ keV (in coincidence with $\alpha$ decay from energy interval of 8400 - 8412 keV), $E_\gamma = 209.2$ keV (in coincidence with 8390 - 8490 keV $\alpha$ decay) and $E_\gamma = 305.1$ keV (in coincidence with $\alpha$ decay from 8355 keV to 8390 keV) were detected. These $\gamma$ transitions were attributed as $\gamma$ de-excitation of $^{250}$Md due to their coincidence with $\alpha$ decay energies typical for the $^{254}$Lr (see values in brackets). These gamma lines were confirmed in, already mentioned, later experiments performed on SHIP aimed on production of $^{258}$Db.

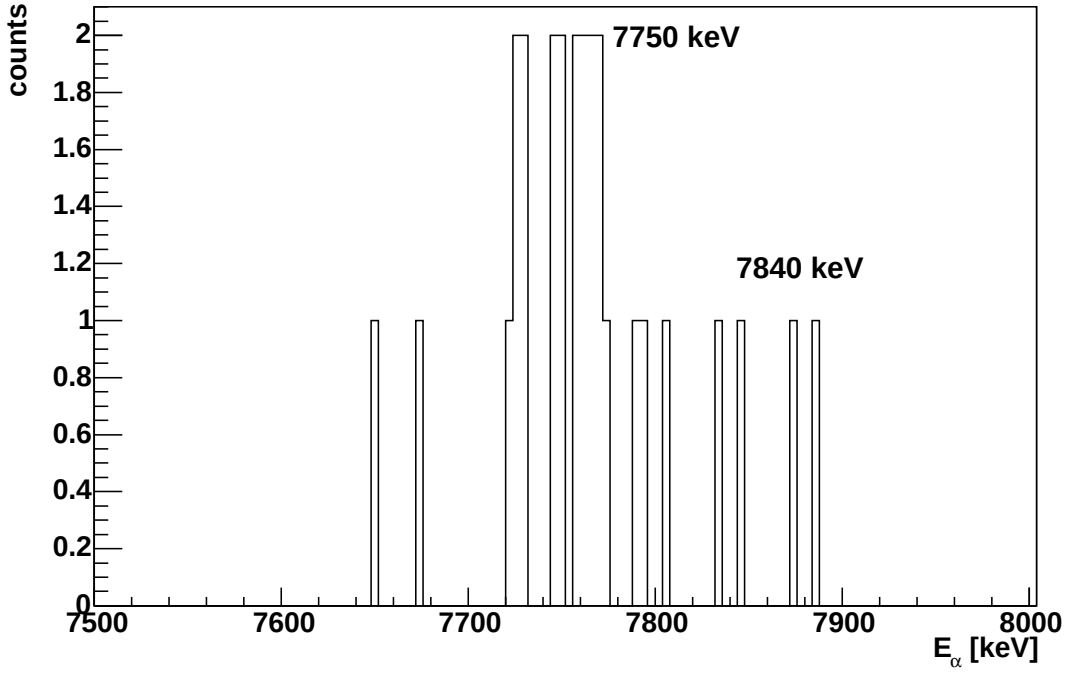


Figure 6.22: Spectrum of $\alpha$ decays correlated to the decay of $^{254}$Lr and attributed to the $\alpha$ decay of $^{250}$Md. One can see the strong influence of energy summing with electrons from internal conversion.

In the $\alpha$ decay energy spectrum of $^{254}$Lr the evidence of structure is visible but considering weak statistics, missing coincidences with X-rays and problems with energy summing it is not possible, using these data, to propose a decay scheme for the decay of $^{254}$Lr.

Strong energy summing with conversion electrons is also typical for the $\alpha$ decay of $^{250}$Md. In figure 6.22 spectrum of $\alpha$ decays correlated to the decays of $^{254}$Lr within a position window of $\Delta x = 0.3$ mm and time interval up to $\Delta t = 300$ s is shown. The energy spectrum can be roughly divided into two regions - group of $\alpha$ decays around the energy of $E_\alpha \approx 7750$ keV and group of events around the $\alpha$ energy of $E_\alpha \approx 7840$ keV.

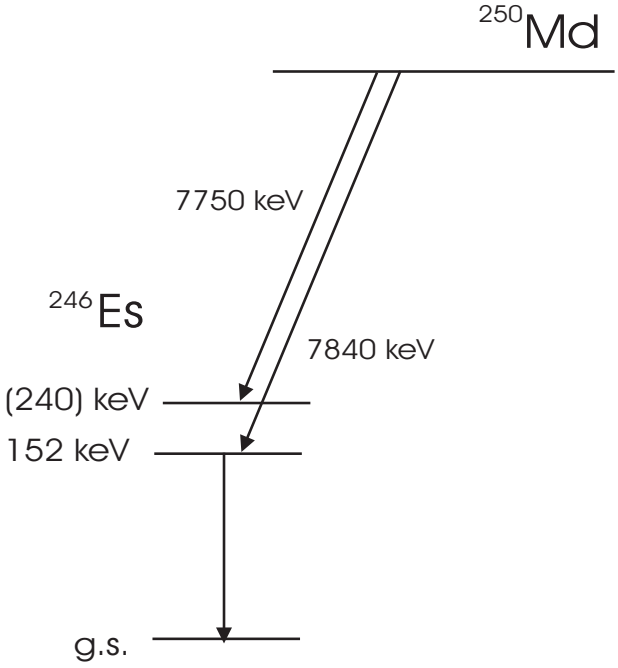


Figure 6.23: The proposed decay scheme of $^{250}$Md.

| **Isotope** | $E_\alpha$ [keV] | $T_{1/2}$ [s] | $b_\alpha$ | $E_\gamma$ [keV] | $b_{SF}$ | Reference |
|---|---|---|---|---|---|---|
| $^{254}$Lr | 8460±20 | 13 ± 2 | 0.78±0.06 | | <0.0016 | [Hes85] |
| | 8408±20<br>8300 - 8550 | 18.4 ± 1.8 | 0.72±0.02 | 42.3<br>209.2<br>305.1 | | This work |
| $^{250}$Md | 7830±20<br>7750±20 | 52 ± 6 | 0.07±0.03 | | | [Hes85] |
| | 7840±40<br>7750±20 | $50^{+10}_{-7}$ | 0.070±0.008 | 152 | | This work |

Table 6.7: Summary of the measured spectroscopic data for the $^{254}$Lr and its daughter product $^{250}$Md.

Based on the number of found $^{254}$Lr - $^{250}$Md correlations and total number of $^{254}$Lr $\alpha$ decays the EC branching ratio for $^{250}$Md was evaluated to the value of $b_{al} \approx 93.0 \pm 0.8$ %. The $\alpha$ decay half life of $^{250}$Md was, according to the formalism of *Schmidt et al.* [Sch84], evaluated to the value of $T_{1/2} = 50^{+10}_{-7}$ s. The hindrance factor for this transition is HF $\approx 5$ what suggest an unhindered transition between the levels with the same spin and parity.

As a part of two Re-$\alpha_1$-$\alpha_2$ correlation chains, in coincidence with $^{250}$Md decay, the $\gamma$ transition with energy of $E_\gamma = 151.8$ keV and $E_\gamma = 152.8$ keV was observed. Therefore the energy of 152 keV might be attributed tentatively as an energy of first excited level in $^{246}$Es. According to measured $\alpha$ energy distribution the additional excited level may be placed around the energy of $E_{exc} = 240 \pm 40$ keV. The proposed decay scheme for $^{250}$Md is shown in figure 6.23.

Although some $\alpha$ - $\alpha$ correlations of $^{250}$Md and $^{246}$Es were observed, due to low statistic it was not possible to obtained any new information about the $\alpha$ decay of $^{246}$Es.

# Chapter 7

# Conclusion and Outlook

This work was motivated by recent experiments on the synthesis of heavy and superheavy elements performed in the region of elements with proton number around 100, and heavier. For most of the isotopes in this region only basic data, obtained by means of $\alpha$ spectroscopy, are available. Usually there is no $\gamma$ spectroscopy information available for the isotopes in this region. Experiments discussed in this work were performed with intention to obtained a spectroscopic data of better quality for some isotopes of odd elements around Z=100. The results presented in this work deliver valuable information on the nuclear structure and help to enlarge the basis of experimental data as support for the various theoretical models.

The results, presented here, were obtained using a method of $\alpha$ and $\alpha$ - $\gamma$ coincidence spectroscopy combined with $\alpha$ - $\alpha$ and recoil - $\alpha$ correlation search. These results show that used spectroscopy method, combined with using of the separator of heavy ion reaction products, is powerful tool for study of decay properties of products with very low cross-section - around 1 nb - and short lifetime - with lower limit of few $\mu$s. Using the $\alpha$ - $\gamma$ spectroscopy method, energy differences between the low-lying excited levels can be obtained with high precision - in the order of few keV.

The obtained data were studied as a part of long-term project of spectroscopy studies of superheavy elements. This project is primarily aimed to the study of elements with odd proton number around $Z > 100$.

Decay chains of four isotopes were described in this work:

a. *The decay chain of $^{247}$Md.* The already known data about $\alpha$ decay of $^{247}$Md were confirmed with an improved precision. The $\alpha$ decay with a energy of $E_\alpha = 8416 \pm 10$ keV was assigned to originate from a ground-state $7/2^-[514]$ Nilsson level of $^{247}$Md. Additional $\alpha$ decay with the energy of $E_\alpha = 8660 \pm 20$ keV (tentatively assigned to a g.s. - g.s. transition) was detected for this isotope.

   The $\alpha$ decay of the isomeric state with a lifetime of $T_{1/2} = 0.257 \pm 0.033$ s and energy of $E_\alpha = 8783 \pm 40$ keV was observed for the first time. This level was assigned to $1/2^-[521]$ Nilsson level. Until now only tentative indication

based on a few fission events were known [Hof94].

The gamma transitions with energies of $E_\gamma$= 209.6 ± 0.5 keV and $E_\gamma$= 157.5 ± 0.5 keV were observed in coincidence with $\alpha$ decay of $^{247}$Md. These transitions were attributed to the direct de-excitation from low lying excited levels of $^{247}$Md daughter product - $^{243}$Es. The spin and parity for low-lying Nilsson levels of $^{243}$Es was assigned to $7/2^-[514]$ at $E_{exc}$ = 209.6 keV and $9/2^+[624]$ at $E_{exc}$ = 52.1 keV. Additionally a level of energy $1/2^-[521]$ is populated by an $\alpha$ decay of $^{247m}$Md. The Nilsson levels of $7/2^+[633]$ and $3/2^-[521]$ can be assigned as a ground-state level and/or first excited levels of $^{243}$Es - tentatively located close to the ground state (see discussion in section 6.1.1).

In case of $^{243}$Es $\alpha$ decay only one of the known line was confirmed by $\alpha$ decay with energy of $E_\alpha$ = 7893 ± 10 keV. The previously reported $\alpha$ decay with energy of 7939 keV was not observed. An additional line - tentatively assigned to decay of $^{243}$Es - at the energy of $E_\alpha$ = 7860 ± 20 keV was detected.

All known data are summarized in the table 6.3. Based on new data - evaluated in this thesis work - the level assignment and decay scheme was drawn (see figure 6.5).

b. *The decay chain of $^{246}$Md.* The complicated $\alpha$ decay energy structure reported before [Nin96] was confirmed. Recent measurements analyzed and described in this thesis work show the existence of three separated $\alpha$ decay groups. The area of $\alpha$ decay energy from 8250 keV to 8690 keV with half-life of $T_{1/2}$ = 1.3 ± 0.4 s and the line of the $E_\alpha$ = 8744 ± 10 keV with a half-life of $T_{1/2}$ = 0.75 ± 0.18 s are attributed to ground-state decay of $^{246}$Md.

An additional $\alpha$ decay of energy $E_\alpha$ = 8178 ± 10 keV and a half-life of $T_{1/2}$ = 4.4 ± 0.8 s was observed for the first time. This $\alpha$ activity was assigned to a decay of isomeric state $^{246m}$Md. The spontaneous fission branch ($b_{SF}$ < 30 %) of this isomeric state can be also the explanation for the higher number of fission events detected for this isotope - compare to value expected from known fission branch of $^{246}$Fm[1].

Similarly as for $^{246}$Md, also for $\alpha$ decay of $^{242}$Es a strong influence of energy summing with conversion electrons was observed. The $\alpha$ decay assigned to $^{242}$Es are spread over a region from 7780 keV to 7960 keV. The EC branch of $^{242}$Es was evaluated to value of $b_{EC}$ = 54.4 ± 2.6 %.

Several $\gamma$ transitions were observed in coincidence with $\alpha$ decay of $^{246}$Md (see figure 6.11) and $\alpha$ decay of $^{242}$Es (see figure 6.12). All spectroscopic data for $^{246}$Md and its daughter products are summarized in table 6.4. A tentative decay scheme was drawn for $^{246}$Md and $^{242}$Es (see figure 6.13). Due to a

[1]The unexpected high number of fission events was previously ascribed to ECDF branch - $b_{ECDF} \approx 6\%$ - of $^{246}$Md [Nin96].

complicated decay structure of the $^{246}$Md and $^{242}$Es it was not possible to assigned spin and parity to suggested levels.

c. *The decay chain of $^{255}$Lr.* The $^{255}$Lr and $^{251}$Md were a blank spot in the nuclear chart. Although both isotopes were known around 30 years [EsP73] there were no detailed $\alpha$ spectroscopy experiment performed until now[2]. The $\alpha$ spectroscopy data were measured with better precision. The spin and parity of $^{255}$Lr ground-state was assigned to $7/2^-[514]$ Nilsson level. An additional $\alpha$ line of energy $E_\alpha = 8310 \pm 10$ keV was identified as an $\alpha$ decay of $^{255}$Lr and attributed as the decay to $^{251}$Md excited level of $E^* \approx 60$ keV. The $\alpha$ decay of $E_\alpha = 8462 \pm 10$ keV was assigned to the decay from an isomeric state ($1/2^-[521]$) in $^{255}$Lr with a decay half-life of $T_{1/2} = 2.56 \pm 0.25$ s.

   For $^{251}$Md the quality of the data was improved too. An 294 keV $\gamma$ line, of E1 or E2 character, transition was identified in coincidence with $\alpha$ decay of energy $E_\alpha = 7535 \pm 10$ keV for the first time. The level populated by this $\alpha$ decay was tentatively assigned to a $7/2^-[514]$ Nilsson level.

d. *The decay chain of $^{254}$Lr.* The $\gamma$ lines with the energies of $E_\gamma = 42.3$ keV, $E_\gamma = 209.2$ keV and $E_\gamma = 305.1$ keV were observed to be in coincidence with $^{254}$Lr $\alpha$ decays. Due to the low statistics collected in this experiment and complicated decay structure it is not possible to propose any decay scheme based on these data. Some tentative decay scheme can be drawn in case of $^{250}$Md $\alpha$ decay (see figure 6.23). For this isotope a new transition of energy $E_\gamma = 152$ keV was observed as a part of Re-$\alpha$-$\alpha$-$\gamma$ chain.

The comparing of the recent experimental data and theoretical calculations shows a disagreement and necessity to improve a prediction power of theory. For example figure 7.1 shows the comparison of experimental results and theoretical calculation for a low lying Nilsson levels of neutron deficient Einsteinium isotopes. The theoretical values are taken from *S. Cwiok et al.* [Cwi94]. Experimental values for $^{251}$Es are taken from *I. Ahmad et al.* [Ahm00]. The data for $^{243}$Es and $^{247}$Es are results of the data analysis discussed in this thesis work. The results for $^{245}$Es and $^{249}$Es were obtained in different SHIP experiments [Hes04].

As was mentioned already for $^{251}$Es the $7/2^+[633]$ level was located close - only 8.3 keV - above the ground-state and assigned to $3/2^-[521]$ [Ahm00]. A similar behavior cannot be excluded for the more neutron deficient isotopes, but this cannot be proven with the detector set-up presently used at SHIP. The $\alpha$ spectroscopy method can not be used due to an insufficient detector resolution of stop detector and the insensitivity of $\gamma$ detectors at SHIP setup to the $\gamma$ emission with energy of few keV. In addition these low energetic transitions are highly converted and may have lifetimes $\gg 1$ $\mu$s. The $7/2^-$ [514] level increases with increased neutron

[2] As was already mentioned, beside the SHIP experiment aimed to the study of $^{255}$Lr, an additional two experiments were performed in Jyväskylä (Finland) and GANIL (France) [Hes04]. The results of these experiments were in agreement with the conclusion of this thesis work.

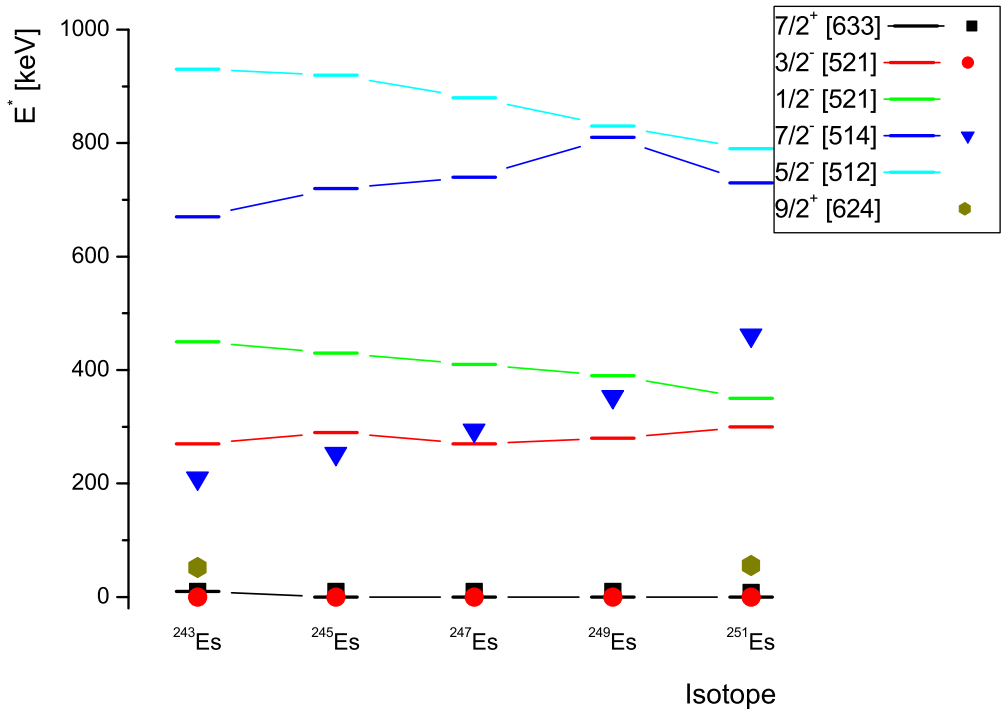


Figure 7.1: Comparison of experimental results - shown by marks - and theoretical calculations - shown by lines - for low lying Nilsson levels Z=99 isotopes. Calculation are taken from *S. Cwiok et al.* [Cwi94]. Experimental values for $^{251}$Es are taken from the *I. Ahmad et al.* [Ahm00]. The experimental results for $^{243}$Es and $^{247}$Es are the results obtained in the SHIP experiment and evaluated in this thesis work. The results for $^{245}$Es and $^{249}$Es were measured in other, recent, SHIP experiments.

number. The excitation energy of this level increases from 200 keV to 400 keV, but the theory [Cwi94] predicts this level at 650 - 800 keV.

For the neutron deficient isotopes of Mendelevium with odd mass ranging from $^{247}$Md to $^{255}$Md the ground-state was assigned to the $7/2^-[514]$ Nilsson level. Close to the ground-state an existence of $1/2^-[521]$ level was observed at SHIP experiments, but from collected data it was not possible to evaluate the excitation energy of this level. Similarly, based on measured $\alpha$ characteristic, also the ground-states of $^{253}$Lr (synthesized in one of the recent SHIP experiment), $^{255}$Lr (studied in this work) were preliminary attributed to $7/2^-[514]$ Nilsson level.

As was already mentioned, this work is a part of long-term and continuous project and further spectroscopy investigation of the superheavy region is planed at SHIP in the future. The aim is to continue with study of more neutron deficient

nuclei and also the isotopes of heavier elements with higher proton number.

For odd-even elements the measurements using existing setup of SHIP detectors give a good possibility to evaluate the decay scheme and spin - parity characteristic of low lying Nilsson levels. For odd-odd isotopes the situation is more difficult due to a strong effect of energy summing with electrons coming from internal conversion process. To improve the situation, it is necessary to measure the energy spectrum of escaped electrons in coincidence with $\alpha$ decay. These measurements are already realized on some other experimental setup, e.g. at RITU in Jyväskylä (Finland), where the detector device GREAT (Gamma Recoil Electron Alpha Tagging) is used.

To observe the $\alpha$ decays and $\gamma$ transitions of low intensity it is necessary to increase a collected statistics for the isotopes of our interest. It is necessary to increase the total efficiency of the current experimental setup, improve reliability of analysis technique, increase beam intensity delivered by accelerator, improve a target properties etc. These changes require lot of effort and beam time.

For example, one of the obstacles is a low melting point of the lead and bismuth targets what is a limiting factor for an increasing of the beam intensity. Recently, this problem was partially solved by applying of the chemical compounds of lead and bismuth with sulfur or fluoride with higher melting point [Lom02],[Kin00]. Experiments with other projectile-target combinations seem promising. Recently the production of superheavy elements with platinum target was tested successfully [Cag02]. The other possibility, for the increase of beam intensity accepted by target, is the target cooling. The active cooling with Helium atmosphere was tested in last years with promising results [Ant04].

Necessary technical development will allow not only the production of new isotopes and study of the elements synthesized in last years but also the research of nuclear structure in case of superheavy elements. This is stringent test and base of theoretical calculation which needs to be improved, as was clearly shown in this thesis work.

# Appendix A

# Reaction $^{40}$Ar + $^{208}$Pb

As a part of the work presented in previous chapters also one brief test of $^{246}$Fm decay properties was done. This measurement was necessary for clarifying of the fission branch value for this isotope because of the unexpectedly high number of spontaneous fission events detected during the production of $^{246}$Md. At the time, when the experiment was performed, the reason for this high number of fission events information was preliminary explained by existence of electron capture delayed fission branch of $^{246}$Fm. Due to the uncertainties of older measurements the more precise data were needed. The experiment was performed in April 2001 at SHIP and its main aim was a test of the excitation function for Fermium production using reactions $^{40}$Ar + $^{208}$Pb and $^{50}$Ti + $^{198}$Pt, and test of the various types of lead targets. Some details about this comparison can be found in the *P. Cagarda, Thesis work* [Cag02]. During this experiment not only the targets with pure lead were used but also the targets based on the chemical compound with Thulium (Pb3Tm) and Sulfur (PbS) were applied.

The data for the reaction $^{40}$Ar + $^{208}$Pb were taken at the beam energies of 4.46 AMeV, 4.5 AMeV, 4.6AMeV, 4.7 AMeV, 4.78 AMeV, 4.9 AMeV and 5.05 AMeV. These energies were corrected for an energy losses in the middle of the target[1]. Used lead targets with a thickness of 430 - 440 $\mu$g/cm$^2$ were evaporated on the carbon foil with thickness of 35 $\mu$g/cm$^2$ and covered with additional carbon foil of 10 $\mu$g/cm$^2$ thickness to avoid target material sputtering and to increase of the target emissivity. The measured data and calculated excitation functions are shown in figure A.1. This figure shows rather good agreement of measured experimental results with the excitation function calculated using HIVAP code [ReS81],[ReS92].

The advantage, in the data analysis, for $^{246}$Fm fission branch evaluation in the data analysis is the fact that neither $^{245}$Fm nor $^{247}$Fm have a notable fission branch. Therefore all detected fission events can be attributed to the decay of $^{246}$Fm. Any unwanted contribution of $^{244}$Fm, which have 100 % fission branch, can be easily distinguished, based on the very short half-life of this isotope - around 3 ms. To

[1]The excitation energy equivalents are 19.1 MeV, 20.5 MeV, 23.9 MeV, 27.3 MeV, 29.9 MeV, 33.9 MeV and 38.5 MeV

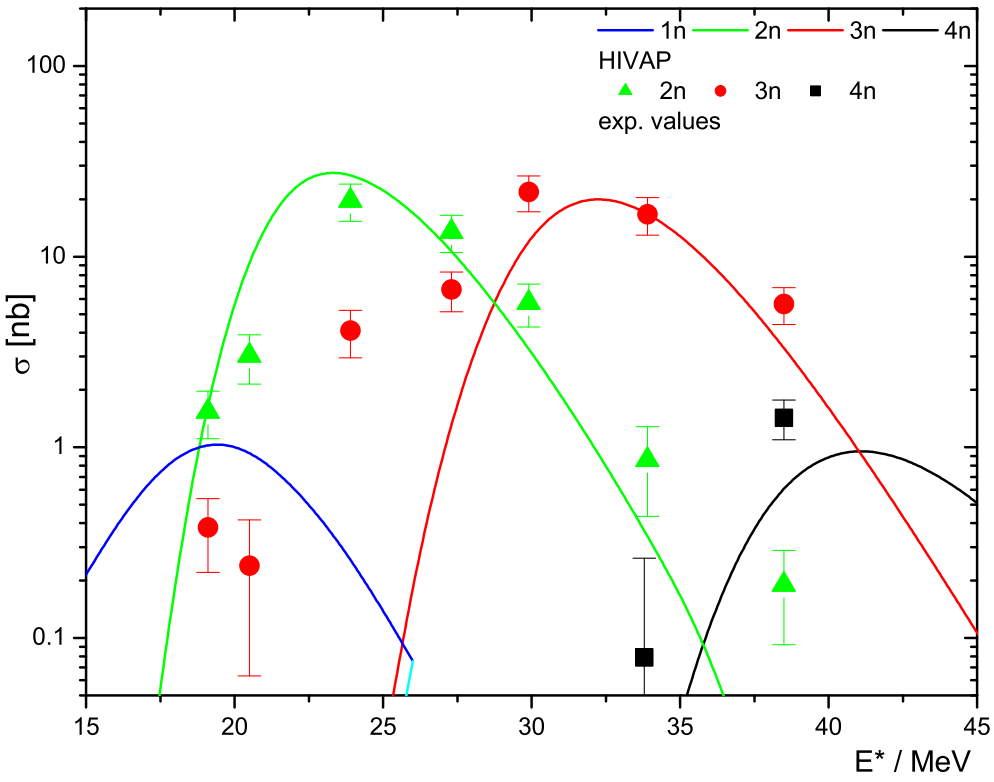


Figure A.1: The production cross-sections for fermium isotopes corresponding to 1n, 2n, 3n and 4n channels produced in the reaction $^{40}$Ar + $^{208}$Pb as a result of HIVAP calculation. The measured cross-sections for applied beam energies are marked as well (see text for more details) [Cag02]. The beam energies were corrected for energy losses in 1/2 of the target thickness. The statistical and systematic uncertainty were taken into an account.

the $\alpha$ decay of $^{246}$Fm were attributed the decays with the energy from 8190 keV to 8280 keV.

During the measurement, at the beam energies mentioned above, altogether 318 $\alpha$ decays of $^{246}$Fm were detected. Beside this 41 spontaneous fission events of $^{246}$Fm were registered[2]. The obtained value for the spontaneous fission branch of $^{246}$Fm was evaluated to $b_{sf} = 6.1^{+1.9}_{-1.6}$ %. This value is in agreement with the older result obtained at SHIP in the $b_{sf} = 4.5 \pm 1.3$ % and also with the results obtained by of *Nurmia et al.* $b_{sf} = 8$ % [Nur67].

But these results are in disagreement with branching ratio for the spontaneous

[2] In this analysis only the data acquired in measurement with pure lead target were considered. The backward detectors were not included into an analysis.

fission branch of indirectly - via EC decay of $^{246}$Md - produced $^{246}$Fm. In the indirect production the values of $b_{sf} = 0.15 \pm 0.05$ % (the results of SHIP experiment in the year 1993 [Nin96]) and $b_{sf} = 0.145^{+0.030}_{-0.025}$ % (the results of SHIP experiments in the 2001) were obtained. This discrepancy was explained in this Thesis work in the chapter 6.1 by the existence of branch of $^{246}$Md isomeric state and its spontaneous fission branch.

# Zhrnutie

Predkladaná práca bola motivovaná poslednými experimentami v oblasti ťažkých a superťažkých prvkov. Po úspešnej syntéze prvkov s protónovými číslami od 107 do 112 v GSI Darmstadt (Nemecko) na konci minulého storočia boli postupne v JINR Dubna (Rusko) a v Rikene (Japonsko) syntetizované nové prvky od 113 do 116. Popri tom, postupný vývoj experimentálnej techniky umožnil spektroskopickú štúdiu izotopov s protónovým číslom do Z = 108.

Mnohé fyzikálne veličiny, nevyhnutné pri realizácii experimentov, musia byť v súčastnosti získavané pomocou semiempirických a empirických modelov. Väčšina týhto modelov vyžaduje nastavenie mnohých empirických parametrov, ktoré sa získavajú fitovaním experimentálnych údajov. Cieľom práce bolo získanie nových informácií, ktoré doplnenia databázu týhto experimentálnych údajov. Nové údaje naviac umožňujú priamu konfrontáciu s výsledkami teoretických modelov a ich postupné vylepšenie.

Experimenty opísané v tejto práci boli realizované v rámci dlhodobého projektu štúdia spektroskopických vlastností transuránov a superťažkých prvkov. Všetky študované izotopy - $^{246}$Md, $^{247}$Md, $^{254}$Lr a $^{255}$Lr - boli po prvý krát syntetizované pred dlhším časom, avšak doposiaľ nebolo uskutočnené detailné meranie zamerané na štúdium ich rozpadových charakteristík. Z pohľadu spektroskopických dát boli preto tieto izotopy bielymi miestami v tabuľke izotopov.

Pri analýze dát boli využité metódy $\alpha$ a $\alpha$ - $\gamma$ koincidenčnej spektroskopie kombinovanej s $\alpha$ - $\alpha$ a recoil - $\alpha$ korelačnou metódou. Výsledky ukázali, že použité metódy v kombinácii s účinným separátorom produktov ťažkoiónových reakcií, sú silným nástrojom na štúdium rozpadových vlastností izotopov s krátkym polčasom rozpadu (dolný limit je $\approx 10$ $\mu$s) a malým účiným prierezom reakcie potrebnej na ich produkciu (dolný limit je $\approx 1$ nb).

Ako už bolo spomenuté, experimenty boli realizované na rýchlostnom filtri SHIP v GSI Darmstadt v rámci dlhodobej kolaborácie s tamojšou experimentálnou skupinou. Pri analýze dát bol využitý analyzačný software GO4 s analytickou nadstavbou GO4SHIP umožňujúcou analyzovať experimentálne dáta získané na spomínanom experimentálnom zariadení. Táto analyzačná časť bola vyvinutá a spravovaná skupinou na katedre jadrovej fyziky FMFI UK v Bratislave. Správnosť výsledkov bola overená vo viacerých experimentoch, pri ktorých bola vykonávaná paralelná analýza s programovým balíkom GOOSY.

Výsledky opísané v tejto práci je možné rozdeliť na 4 časti:

a. *Rozpadový reťazec $^{247}$Md.* Známe dáta pre $\alpha$ rozpad izotopu $^{247}$Md boli potvrdené výsledkami so zlepšenou presnosťou. $\alpha$ rozpad s energiou $E_\alpha = 8416 \pm 10$ keV bol priradený rozpadu zo základného stavu $7/2^-[514]$ Nilssonovho levelu izotopu $^{247}$Md. Taktiež bol po prvý krát nameraný $\alpha$ prechod s energiou $E_\alpha = 8660 \pm 20$ keV ktorý bol predbežne priradený prechodu medzi základnými stavmi $^{247}$Md a $^{243}$Es.

   Po prvý krát bol registrovaný aj $\alpha$ rozpad z izomerického stavu $^{247m}$Md s polčasom rozpadu $T_{1/2} = 0.257 \pm 0.033$ s a s energiou $E_\alpha = 8783 \pm 40$ keV. Tento level bol priradený stavu $1/2^-[521]$. Doposiaľ bol tento izomerický stav predpokladaný iba na základe dvoch štiepení registrovaných pri produkcii tohto izotopu s polčasom $T_{SF} = 0.23^{+0.19}_{-0.12}$ s [Hof94].

   Po prvý krát boli registrované gamma prechody s energiami $E_\gamma = 209.6 \pm 0.5$ keV a $E_\gamma = 157.5 \pm 0.5$ keV v koincidencii s $\alpha$ rozpadom $^{247}$Md. Tieto prechody boli priradené prechodom z nízko ležiacich vzbudených hladín izotopu $^{243}$Es, ktorých spiny a parity boli určené: $7/2^-[514]$ pre hladinu s excitačnou energiou $E_{exc} = 209.6$ keV a $9/2^+[624]$ pre hladinu s excitačnou energiou $E_{exc} = 52.1$ keV. Taktiež je $\alpha$ rozpadom $^{247m}$Md obsadzovaný stav $1/2^-[521]$. Základnému stavu a/alebo nízkoležiacemu vzbudenému stavu izotopu $^{243}$Es môže byť priradený stav $7/2^+[633]$ a/alebo $3/2^-[521]$ (viď diskusia v časti 6.1.1).

   V prípade $\alpha$ rozpadu izotopu $^{243}$Es bola potvrdená iba jedna (z dvoch) publikovaných energií rozpadu [Hat89] $E_\alpha = 7893 \pm 10$ keV. Očakávaný $\alpha$ rozpad s energiou 7939 keV nebol sledovaný, avšak bol registrovaný prechod s energiou $E_\alpha = 7860 \pm 20$ keV.

   Všetky získané dáta sú sumarizované v tabuľke 6.3. Návrh rozpadovej schémy je na obrázku 6.5).

b. *Rozpadový reťazec izotopu $^{246}$Md.* Pre tento izotop je typický silný vplyv sumovania energie $\alpha$ rozpadu s energiou elektrónu vznikajúceho pri vnútornej konverzi. Energetické spektrum $\alpha$ rozpadu $^{246}$Md možno rozdeliť na tri oblasti. Prvou je oblasť od 8250 keV do 8690 keV s polčasom $T_{1/2} = 1.3 \pm 0.4$ s. Druhou oblasťou je okolie čiary s energiou $8744 \pm 10$ keV a s polčasom $T_{1/2} = 0.75 \pm 0.18$ s. Obe oblasti sú priradené rozpadu zo základnej hladiny $^{246}$Md.

   Ďalej bol po prvý krát sledovaný $\alpha$ rozpad s energiou $E_\alpha = 8178 \pm 10$ keV a polčasom $T_{1/2} = 4.4 \pm 0.8$ s. Tento $\alpha$ rozpad bol priradený rozpadu z izomerického stavu $^{246m}$Md.

   Podobne, ako v prípade $\alpha$ rozpadu $^{246}$Md, taktiež pre $\alpha$ rozpad izotopu $^{242}$Es je evidentný silný vplyv sumovania energie s konverznými elektrónmi. Oblasť $\alpha$ rozpadu pre tento izotop leží od 7780 keV do 7960 keV. Pre vetviaci pomer EC rozpadu bola získaná hotnota $b_{EC} = 54.4 \pm 2.6$ %.

V koincidencii s $\alpha$ rozpadom izotopov $^{246}$Md a $^{242}$Es boli pozorované viaceré $\gamma$ prechody (viď obrázky 6.11 a 6.12). Všetky získané výsledky sú sumarizované v tabuľke 6.4. Návrh rozpadovej schémy pre $^{246}$Md a $^{242}$Es je zobrazený na obrázku 6.13). V dôsledky komplikovanej energetickej štruktury $\alpha$ rozpadu oboch izotopov a nemožnosti merať energie konverzných elektrónov ako aj nedostatku záchytných bodov potrebných pri zostavovaní rozpadovej schémy však nebolo možné priradiť spin a paritu jednotlivým stavom a je potrebné brať danú rozpadovú schému len ako predbežný návrh.

c. *Rozpadový reťazec $^{255}Lr$.* Spin a parita základného stavu $^{255}$Lr bola priradená stavu $7/2^-[514]$. Taktiež bol po prvý krat registrovaný $\alpha$ rozpad s energiou $E_\alpha = 8310 \pm 10$ keV priradený, na základe jeho polčasu rozpadu, $\alpha$ prechodu zo základného stavu $^{255}$Lr na vzbudený stav $^{251}$Md s energiou $E^* \approx 60$ keV. Bolo zistené, že oba doposiaľ známe $\alpha$ rozpady smerujú z rôznych energetických hladín. Rozpad s energiou $E_\alpha = 8462 \pm 10$ keV bol priradený rozpadu z izomerického stavu $1/2^-[521]$ s polčasom rozpadu $T_{1/2} = 2.56 \pm 0.25$ s. Pre rozpad s energiou $E_\alpha = 8369 \pm 10$ keV bol nameraný polčas $T_{1/2} = 19.9 \pm 5.3$ s a bol prisúdený rozpadu základného stavu tohto izotopu.

   Pre izotop $^{251}$Md bol po prvý krát detekovaný $\gamma$ prechod s energiou 294 keV a s charakterom E1 príp. E2 prechodu, v koincidencii s $\alpha$ rozpadom s energiou $E_\alpha = 7535 \pm 10$ keV. Level v izotope $^{247}$Es produkovaný týmto $\alpha$ rozpadom bol priradený stavu $7/2^-[514]$.

d. *Rozpadový reťazec $^{254}Lr$.* V koincidencii s $\alpha$ rozpadom izotopu $^{254}$Lr boli po prvý krát registrované $\gamma$ prechody s energiami $E_\gamma = 42.3$ keV, $E_\gamma = 209.2$ keV a $E_\gamma = 305.1$ keV. V dôsledku malej získanej štatistiky a kvôli komplikovanej rozpadovej štruktúre nebolo možné zostaviť rozpadovú schému ani získať ďalšie údaje o tomto izotope. Predbežný návrch rozpadovej schémy možno zostavit pre izotop $^{250}$Md (viď obrázok 6.23). Pre tento izotop bol zaregistrovaný prechod $E_\gamma = 152$ keV ako časť reťazca Re-$\alpha$-$\alpha$-$\gamma$. Pre tento izotop boli potvrdené obidve, doposiaľ známe energie $\alpha$ rozpadu [FiS96].

# Bibliography


[Ahm00] I. Ahmad, R.R. Chasman, P.S. Fields, Phys. Rev. C**61** (2000) 044301

[Ant04] S. Antalic, P. Cagarda, D. Ackermann, H.-G. Burkhard, F.-P. Heßberger, S. Hofmann, B. Kindler, J. Kojouharova, B. Lommel, R. Mann, S. Saro, H.-J. Schött, Nucl. Instrum. and Methods A **530** (2004) 185-193

[Ant03] S.Antalic, *Thesis work project (in slovak)*, FMFI UK, Bratislava (2003)

[Aud97] G. Audi, O. Bersilion, J. Blachot, A.H. Wapstra, Nucl. Phys. A **624**, (1997), 1 - 124

[Ben01] M. Bender, GSI Preprint 2001-03.

[Cag02] P. Cagarda *Thesis work*, FMFI UK, Bratislava (2002).

[Cag03] P. Cagarda *private communication* (2003).

[Cwi96] S. Cwiok, J. Dobaczewski, P.-H. Heenen, P. Magierski, W. Nazarewicz, Nucl. Phys. A **944**, (1996), 211-246

[Cwi94] S. Cwiok, S. Hofmann, W. Nazarewicz, Nucl. Phys. A**573**, (1994), 356-394

[Dra00] O.Dragoun, M. Ryšavý and A. Špalek, J. Phys. G26 (2000) 1461-1466

[Dru70] V.A. Druin, Yadern. Fiz. 12, (1970) 268 [transl. Soviet J. Nucl. Phys. 12, (1971) 146]

[EsK71] K. Eskola, P. Eskola, M. Nurmia, A. Ghiorso Phys. Rev. C4 (1971) 632-642

[EsP73] Eskola P., Phys. Rev. C7 (1973) 280-289

[Eva55] R.D. Evans, *The Atomic Nucleus*, (McGraw-Hill, New York, 1955)

[FiS96] R.B. Firestone and V.S. Shirley (Editors), *Table of Isotopes*, 8th edition, (John Wiley and Sons, New York, 1996).

[Fol95] H. Folger, W. Hartmann, F.P. Heßberger, S. Hofmann, J. Klemm, G. Münzenberg, V. Ninov, W. Thalheimer, P. Armbruster Nucl. Instrum. and Methods A**362** (1995) 64-69

[Gag89] H.W. Gäggeler, D.T. Jost, A. Türler, P. Armbruster, W. Brüchle, H. Folger, F.P. Heßberger, S. Hofmann, G. Münzenberg, V. Ninov, W. Reisdorf, M. Schädel, K Sümmerer, J.V. Kratz, U Scherer, M.E. Leino Nuclear Physisc A**502** (1989) 561c-570c

[Gav80] A. Gavron, Phys. Rev. **C21**, 230 (1980)

[GO4] H.G. Essel, *GSI Object Oriented On-line Off-line system*, GSI Darmstadt (2002); URL: `http://go4.gsi.de`

[GOO] H.G. Essel, *GOOSY Data Acquisition and Analysis*, GSI Darmstadt (1988); URL: `http://www-gsi-vms.gsi.de/anal/home.html`

[Hat89] Y. Hatsukawa, T. Ohtsuki, K. Sueki, H. Nakahara, I. Kohno, M. Magara, N. Shinohara, H.L. Hall, R.A. Henderson, C. M. Gannet, J.A. Leyba, R.B. Chadwick, K.E. Gregorich, D. Lee, M.J. Nurmia, D.C. Hoffman, Nucl. Physics A**500** (1985), 90-110

[Hes85] F.P.Heßberger, G. Münzenberg, S. Hofmann, Y.K. Agarwal, K. Poppensieker, W. Reisdorf, K.-H. Schmidt, J.R.H. Schneider, W.F.W. Schneider, H.J. Schött, P. Armbruster, B. Thuma, C.-C. Sahm, D. Vermeulen, Z. Phys. A **322** (1985), 557-566

[Hes01] F.P.Heßberger, S.Hofmann, D. Ackermann, V. Ninov, M. Leino, G. Münzenberg, S. Saro, A. Lavrentev, A.G. Popeko, A.V. Yeremin, Ch. Stodel, Eur. Phys. J. A **12** (2001), 57-67

[Hes04] F.P. Heßberger, *private communication* (2004).

[Hil76] M. Hillman and Y. Eyal, JULIAN, Brookhaven National Laboratory Report No. 22846 (1976)

[Hin85] R.Hingmann, W.Kuehn, V.Metag, R.Novotny, A.Ruckelshausen, H.Stroeher, F.P.Heßberger, S.Hofmann, G.Münzenberg, W.Reisdorf, GSI Scientific Report 1984, (1985), 88

[Hod97] P.E. Hodgeson, E. Gadioli and E. Gadioli Erba, *Introductory Nuclear Physics*, (Oxford University Press, 1997).

[Hof94] S. Hofmann, V. Ninov, F.P. Heßberger, H. Folger, G. Münzenberg, H.J. Schött, P. Armbruster, A.N. Andreyev, A.G. Popeko, A.V. Yeremin, M. Leino, R. Janik, S. Saro, M. Veselsky, GSI Scietific Report 1993 (1994), 64

[Hof95a] S. Hofmann, V. Ninov, F.P. Heßberger, P. Armbruster,H. Folger, G. Münzenberg, H.J. Schött, A.G. Popeko, A.V. Yeremin,A.N. Andreyev, S. Saro, R. Janik, M. Leino, Z. Phys., A**350** (1995), 277-280

[Hof95b] S. Hofmann, V. Ninov, F.P. Heßberger, P. Armbruster,H. Folger, G. Münzenberg, H.J. Schött, A.G. Popeko, A.V. Yeremin,A.N. Andreyev, S. Saro, R. Janik, M. Leino, Z. Phys., A**350** (1995), 281-282

[Hof96] S. Hofmann, V. Ninov, F.P. Heßberger, P. Armbruster, H. Folger, G. Münzenberg, H.J. Schött, A.G. Popeko, A.V. Yeremin, S. Saro, R. Janik, M. Leino, Z. Phys., A**354** (1996), 229-230

[Hof00] S. Hofmann and G. Münzenberg, Rev. Mod. Phys. **72** (2000) 733.

[Hof01] S. Hofmann, F.P. Hessberger, D. Ackermann, S. Antalic, P. Cagarda, S. Cwiok, B. Kindler, J. Kojouharova, B. Lommel, R. Mann, G. Münzenberg, A.G. Popeko, Š. Šáro, H.J. Schött, A.V. Yeremin, Eur.Phys. J. A**10** (2001) 5.

[Hof02] S. Hofmann, F.P. Hessberger, D. Ackermann, G. Münzenberg, S. Antalic, P. Cagarda, B. Kindler, J. Kojouharova, M. Leino, B. Lommel, R. Mann, A.G. Popeko, S. Reshitko, Š. Šáro, J Uusitalo, A.V. Yeremin, Eur.Phys. J. A**14** (2002) 147-157.

[Hof04] S. Hofmann, D. Ackermann, S. Antalic, H.G. Burkhard, P. Cagarda, F.P. Hessberger, B. Kindler, I. Kojouharov, M. Leino, B. Lommel, O.N. Malyshev, R. Mann, G. Münzenberg, A.G. Popeko, S. Saro, H.J. Schott, B. Streicher, B. Sulignano, J Uusitalo, A.V. Yeremin, GSI Scientific Report (2003) 1

[Kin00] B. Kindler, S. Antalic, H.G. Burkhard, P. Cagarda, D. Gembalies-Datz, W. Hartmann, S. Hofmann, J. Klemm, J. Kojouharova, B. Lommel, R. Mann, H.J. Schött, J. Steiner, *CP576, Proceedings to the 16$^{th}$ Int. Conference on Application of Accelerators in Research and Industry*, Denton, Texas, Npv. 1-5. 2000, Edited by J.L. Duggan and I.L. Morgan.

[Lei95] M. Leino, J. Äystö, T. Enqvist, P. Heikkinen, A. Jokinen, M. Nurmia, A. Ostrowski, W.H. Trzaska, J. Uusitalo, K. Eskola, P. Armbruster, V. Ninov, Nucl. Inst. and Meth. B**99** (1995) 653.

[Lom02] B. Lommel, D. Gambalies-Datz, W. Hartmann, S. Hofmann, B. Kindler, J. Klemm, J. Kojouharova, J. Steiner, Nucl. Instrum. and Methods A **480**, (2002) 16-21

[Lov00] W. Loveland, D. Morrissey, G. Seaborg, *modern nuclear Chemistry*, to be published

[Mor04] K. Morita *et al.* J. Phys. soc. Jpn **73**, (2004) 2593-2596

[Mun79] G. Münzenberg, W. Faust, S. Hofmann, P.Armbruster, Nucl. Instrum. and Methods**161**, (1979) 65-82

[Mun81a] G. Münzenberg, S. Hofmann, F. P. Heßberger, W. Reisdorf, K. H. Schmidt, J. H. R. Schneider, P. Armbruster, C. C. Sahm, and B. Thuma, Z. Phys. A **300**, (1981) 107-108

[Mun81b] G. Münzenberg, S.Hofmann, W.Faust, F.P.Hessberger, W.Reisdorf, K.-H. Schmidt, P.Armbruster, K. Güttner, B.Thuma, D. Vermeulen, Z. Phys. A **302**, (1981) 7-14

[Mun82] G. Münzenberg, P.Armbruster, *et al.*, Z. Phys. A **309**, (1982) 89

[Mun84] G. Münzenberg, P.Armbruster, *et al.*, Z. Phys. A **317**, (1984) 235

[MyS66] W.D. Myers and W.J. Swiatecki, Nucl. Phys. **81** 1-60

[Nin96] V. Ninov, F.P. Hessberger, S. Hofmann , H. Folger , G. Münzenberg, P. Armbruster, A.G. Popeko, M. Leino, S. Saro , A.V. Yeremin, Z. Phys. A **356**, (1996) 11-12

[Nur67] M. Nurmia, T. Sikkeland, R. Silva, A. Ghiorso, Phys. Lett. **26**B (1967) 78-80

[Oga99a] Yu.Ts. Oganessian, V.K. Utyonkov, Yu.V. Lobanov, F.Sh. Abdulin, A.N. Polyakov, I.V. Shirokovsky, Yu.S. Tsyganov, G.G. Gulbekian, S.L. Bogomolov, B.N. Gikal, A.N. Mezentsev, S. Iliev, V.G. Subbotin, A.M. Sukhov, O.V. Ivanov, G.V. Buklanov, K. Subotic, M.G. Itkis, Nature **600**, (1999), 242

[Oga99b] Yu.Ts. Oganessian, V.K. Utyonkov, Yu.V. Lobanov, F.Sh. Abdulin, A.N. Polyakov, I.V. Shirokovsky, Yu.S. Tsyganov, G.G. Gulbekian, S.L. Bogomolov, B.N. Gikal, A.N. Mezentsev, S. Iliev, V.G. Subbotin, A.M. Sukhov, G.V. Buklanov, K. Subotic, M.G. Itkis, Phys. Rev. Lett. **83**, (1999), 3154-3157

[Oga99c] Yu.Ts. Oganessian, A.V. Yeremin, G.G. Gulbekian, S.L. Bogomolov, V.I. Chepigin, B.N. Gikal, V.A. Gorshkov, M.G. Itkis, A.P. Kabachenko, V.B. Kutner, A.Yu. Lavrentev, O.N. Malyshev, A.G. Popeko, J Roháč, R.N. Sagaidak, S. Hofmann, G. Munzenberg, M. Veselský, S. Saro, N. Iwasa, K. Morita Eur. Phys. J. A**5**, (1999), 63-68

[Oga00a] Yu.Ts. Oganessian, V.K. Utyonkov, Yu.V. Lobanov, F.Sh. Abdulin, A.N. Polyakov, I.V. Shirokovsky, Yu.S. Tsyganov, G.G. Gulbekian, S.L. Bogomolov, B.N. Gikal, A.N. Mezentsev, S. Iliev, V.G. Subbotin, A.M. Sukhov, O.V. Ivanov, G.V. Buklanov, K. Subotic, M.G. Itkis, Phys. Rev. C**62** (2000) 041604(R).

[Oga00b] Yu.Ts. Oganessian, V.K. Utyonkov, Yu.V. Lobanov, F.Sh. Abdulin, A.N. Polyakov, I.V. Shirokovsky, Yu.S. Tsyganov, G.G. Gulbekian, S.L. Bogomolov, B.N. Gikal, A.N. Mezentsev, S. Iliev, V.G. Subbotin, A.M. Sukhov, O.V. Ivanov, G.V. Buklanov, K. Subotic, M.G. Itkis, K.J. Moody, J.F. Wild, N.J. Stoyer, M.A. Stoyer, R.W. Lougheed, C.A. Laue, Ye.A. Karelin, A.N. Tatarinov, Phys. Rev. C**63** (2000) 011301(R).

[Oga01a] Yu. Ts. Oganessian, M.G. Itkis, A.G. Popeko, V.K. Utyonkov, A.V. Yeremin, Nucl. Phys A**682** (2001) 108c-113c.

[Oga01b] Yu.Ts. Oganessian, Nucl. Phys. A**685** (2001) 17c.

[Oga02] Yu.Ts. Oganessian, Eur. Phys. J. A**13** (2002) 135.

[Oga04] Yu.Ts. Oganessian, V.K. Utyonkov, Yu.V. Lobanov, F.Sh. Abdulin, A.N. Polyakov, I.V. Shirokovsky, Yu.S. Tsyganov, G.G. Gulbekian, S.L. Bogomolov, A.N. Mezentsev, S. Iliev, V.G. Subbotin, A.M. Sukhov, A.A. Voinov, G.V. Buklanov, K. Subotic, V.I. Zagrabaev, M.G. Itkis, J.B. Patin, K.J. Moody, J.F. Wild, M.A. Stoyer, N.J. Stoyer, D.A. Shaughnessy, J.M. Kenneally, R.W. Lougheed Phys. Rev. C**69** (2004) 021601(R)

[Pla77] F. Plasil, 'ORNL ALICE', Report ORNL-TM-6054, (1977)

[Pla78] F. Plasil, Phys. Rev. C, **17** (1978), 823

[Poe80] D.N. Poenaru, M. Ivascu and D. Mazilu, J. Phys. Lett. **41** (1980) L-589.

[ReS81] W. Reisdorf, Z. Phys. A**300** (1981) 227.

[ReS92] W. Reisdorf and M. Schädel, Z. Phys. A**343** (1992) 47.

[ROOT] Rene Brun and Fons Rademakers, *ROOT - An Object Oriented Data Analysis Framework*, Proceedings AIHENP'96 Workshop, Lausanne, Sep. 1996, Nucl. Inst. & Meth. in Phys. Res. A 389 (1997) 81-86. See also http://root.cern.ch/.

[Rös78] F. Rössel, H.M. Fries, K. Alder and H.C. Pauli, At. Data and Nucl. Data Tables **21**, 91 (1978); 291 (1978)

[Rur83] E. Rurarz, Acta Physica Polonica B**14** (1983) 917.

[Rut97] K. Rutz, M. Bender, T. Bürvenich, T. Schilling, P.G. Reinhard, J.A. Maruhn, and W. Greiner, Phys. Rev. C**56** (1997) 238.

[Sar96] Š. Šáro, R. Janík, S. Hofmann, H. Folger, F.P. Heßberger, V. Ninov, H.J. Schött, A.N. Andreyev, A.P. Kabachenko, A.V. Yeremin, Nucl. Inst. and Meth. A**381** (1996) 520.

[Sch84] K.-H, Schmidt, C.-C. Sahm, K. Pielenz, H.-G. Clerc, Z. Phys. A **316** (1984) 19 - 26

[Smo97] R. Smolanczuk, Phys. Rev. C**56** (1997) 812.

[Str67] V.M. Strutinsky, Nucl. Phys. A**95** (1967) 420.

[Str68] V.M. Strutinsky, Nucl. Phys. A**122** (1968) 1. 82

[Web] WEBELEMENTS$^{TM}$, the periodic table on the WWW, URL: `http://www.webelements.com/`, copyright 1993-2002 Mark Winter (The University of Sheffield and WebElements Ltd, UK).

[Wil71] B.D. Wilkins, M.J. Fluss, S.B. Kaufman, C.E. Gross, E.P. Steinberg, Nucl. Inst. and Meth. **92** (1971) 381.

[Yer97] A.V. Yeremin, D.D. Bogdanov, V.I. Chepigin, V.A. Gorshkov, A.P. Kabachenko, O.N. Malyshev, A.G. Popeko, R.N. Sagaidak, G.M. Ter-Akopi0an, A.Yu. Lavrentjev, Nucl. Inst. and Meth. B**126** (1997) 329.

[Zho03] Zhongzhou Ren, Ding-Han Chen, Fei Tai, H.Y. Zhang, W.Q. Shen, Phys. Rew. C**67** (2003), 064302

[ZiB03] J.F. Ziegler and J.P. Biersack, *SRIM-2003, Stopping and Range of Ions in Matter*, URL: `http://www.srim.org`, (2003).